Technical Reports

CENTRO EURO-MEDITERRANEO
PER I CAMBIAMENTI CLIMATICI

ISC – Impacts on ground and coast

Terra-LM sensitivity tests: Falkenberg 2005

Guido Rianna
Centro Euro-Mediterraneo per i Cambiamenti Climatici(CMCC)

Centro Euro-Mediterraneo
per i Cambiamenti Climatici
www.cmcc.it

January 2008 ■ TR16

Terra-LM sensitivity tests: Falkenberg 2005

Summary

In this work, are showed the results of sensitivity tests carried out on 1D version of TERRA-LM code (for further details about physical parameterization and code of TERRA-LM, see Technical Reports “Descrizione del soil-module TERRA-LM” and “Studio e valutazione dei possibili miglioramenti apportabili a Terra-LM tramite il confronto con altri modelli SVAT”).

Keywords: SVAT, water content, soil temperature

.

Address for correspondence:
Guido Rianna
E-mail: guido.rianna@unina.it

1.1 Introduction

In this work, are showed the results of sensitivity tests carried out on 1D version of TERRA-LM code (for further details about physical parameterization and code of TERRA-LM, see Technical Reports "Descrizione del soil-module TERRA-LM" and "Studio e valutazione dei possibili miglioramenti apportabili a Terra-LM tramite il confronto con altri modelli SVAT").
This version allows simulating hydric and thermal balance of a soil column for long periods, using as boundary conditions, hourly data of:

- precipitation;
- global radiation;
- counter radiation;
- relative humidity at $2m$;
- dew temperature;
- wind velocity;
- temperature at $2m$;
- cloudiness;

and for site characterization:

- thermal and hydric soil parameters
- vegetation parameters (roughness length, LAI, plant cover and root depth)[1]

The dominant soil type data set is taken from the Digital Soil Map of the World (DSMW) which is based on the FAO/UNESCO Soil Map of the World (FAO-Unesco (1974).; in this classification, the classes are marked according to relative proportions of *clay*, *silt* and *sand*; besides for ice-covered land and rocky terrain are considered other two classes: ICE and ROCK.
In Table 1 are reported the correspondence between number, accompanying soil characteristics and short name:

No.	soil characteristic	name
1	Glacier/Ice	'ice'
2	Lithosols	'rock'
3	Coarse textured	'sand'
4	Coarse to medium textured	'sandy loam'
5	Medium textured	'loam'
6	Medium to fine textured	'loamy clay'
7	Fine textured	'clay'
8	Histosols	'peat'

Table 1

In table 2 are reported all the values of hydric and thermal parameters:

[1] Usually , for these parameters are defined maximum and minimum values and is assumed sinusoidal trend during the year

soil type	1 ice	2 rock	3 sand	4 sandy loam	5 loam	6 loamy clay	7 clay	8 peat
volume of voids w_{PV} [1]	-	-	0.364	0.445	0.455	0.475	0.507	0.863
field capacity w_{FC} [1]	-	-	0.196	0.260	0.340	0.370	0.463	0.763
permanent wilting point w_{PWP} [1]	-	-	0.042	0.100	0.110	0.185	0.257	0.265
air dryness point w_{ADP} [1]	-	-	0.012	0.030	0.035	0.060	0.065	0.098
minimum infiltration rate I_{K2} $[kg/(m^2 s)]$	-	-	0.0035	0.0023	0.0010	0.0006	0.0001	0.0002
hydraulic diffusivity parameter D_0 $[10^{-9} m^2/s]$	-	-	18400	3460	3570	1180	442	106
hydraulic diffusivity parameter D_1 [1]	-	-	-8.45	-9.47	-7.44	-7.76	-6.74	-5.97
hydraulic conductivity parameter K_0 $[10^{-9} m/s]$	-	-	47900	9430	5310	764	17	58
hydraulic conductivity parameter K_1 [1]	-	-	-19.27	-20.86	-19.66	-18.52	-16.32	-16.48
heat capacity $\rho_0 c_0$ $[10^6 J/(m^3 K)]$	1.92	2.10	1.28	1.35	1.42	1.50	1.63	0.58
heat conductivity								
λ_0 $[W/(Km)]$	2.26	2.41	0.30	0.28	0.25	0.21	0.18	0.06
$\Delta\lambda$ $[W/(Km)]$	0.0	0.0	2.40	2.40	1.58	1.55	1.50	0.50
exponent B [1]	1.0	1.0	3.5	4.8	6.1	8.6	10.0	9.0

Table 2

When the code TERRA-LM is used in coupling with Lokal Modell or in the configuration 2D, the boundary data are passed by atmospheric model (then they are forecast values) and the site values are passed by datasets (CORINE, GLCC, GLC2000).
While for run 1D it is possible simulate hydric and thermal balance in the soil for long periods (a year's or longer analysis), in the 2D version, usually the simulation, because of calculating load, are shorter (order of magnitude: few days).
Furthermore in the Figure 1, is reported the layer structure of the multi-layer model utilized in all performed runs (anyway, it is possible to vary the layer structure according to own purposes).

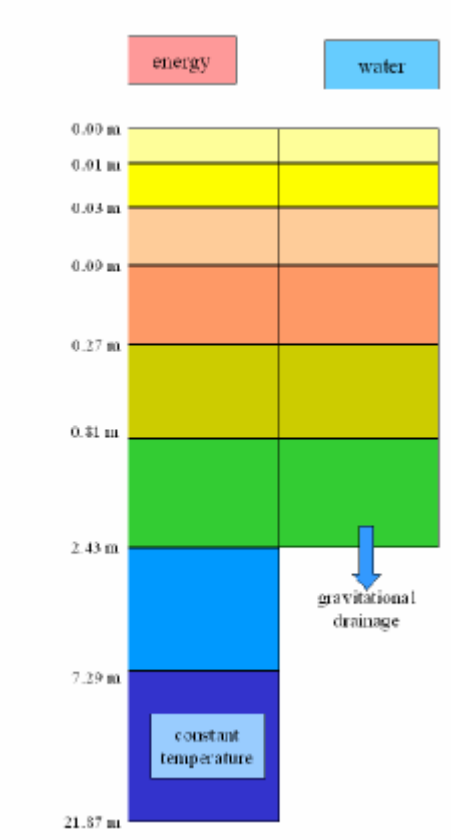

Fig. 1

In the performed simulations, atmospheric inputs are from Boundary Layer Field Site at Falkenberg near Meteorological Observatory Lindenberg (for entire year 2005[2]); by FAO MAP, for this site is considered there is soil type "sand" and vegetation parameters are:

- plant cover max[3] $=0.9$
- plant cover min $=0.52$
- root depth $=0.99m$
- LAI max $=3.31$
- LAI min $=0.73$
- roughness length $=0.1m$

As initial conditions, are required water content $(n*S_r)$ and temperature (K) for every layer; in all simulations, the following values are used:

[2] for this year, precipitation data don't distinguish between rain and snow; if the precipitation if, at the same time, precipitation and air temperature below zero is registered, snow presence is simulated

[3] **plant cover** is the fractional area covered by plants

L.A.I. (leaf area index) is a ratio in which at the numerator there is the total leaf surface of a plant (divided by two) and at denominator there is the surface area of the land on which the vegetation grows.

roughness length-the height above the displacement plane at which the mean wind becomes zero when extrapolating the logarithmic wind- speed profile downward through the surface layer (from http://amsglossary.allenpress.com/glossary/search?id=aerodynamic-roughness-length1)

Layer	***water content*** $(n * S_r)$	***temperature*** (K)
1	0.255	274
2	0.255	274
3	0.255	274
4	0.243	275
5	0.226	277
6	0.226	279
7	0.226	280
8	0.226	280

Table 3

It is important to highlight that the time step is $60s$ while in operative settlement for *Lokal Modell* (7km horizontal resolution) it is $40s$.
Hereinafter, are showed the annual trends of some outputs useful to define hydric and thermal behaviour of the soil:

- water content and temperature in every layer;
- sensible and latent heat;
- solar radiation and thermal radiation at the ground;
- surface and subsurface runoff.

First of all, for Falkenberg case-study[4]; subsequently, is tested the code sensitivity varying soil type, evaporation and transpiration model, lower boundary and treatment of drainage.
All the graphs are reported in *Appendix A*.

[4] for this case-study, usual operative settings are used

- evaporation and transpiration model: BATS
- root distribution: uniform

1.2 Falkenberg case study

From the water content graphs (**graphs1-4,** for the three upper layer and layer 7) it is possible to note that initial conditions aren't correct (probably the real water content is lower for all layers); infact in the first time, because of persistent precipitations, (except for 11 day, in the first layer) the water content values remain near the initial conditions but when the precipitations end, quickly the water content values decrease.
In the surface layers, the water content trends don't seem to be influenced by daily precipitation inputs; probably, the higher peaks correspond to higher hourly precipitation values.
As it is expected, the influence of atmospheric boundary conditions (especially rain and air temperature) on the water content and temperature profiles are gradually subsiding along the soil column

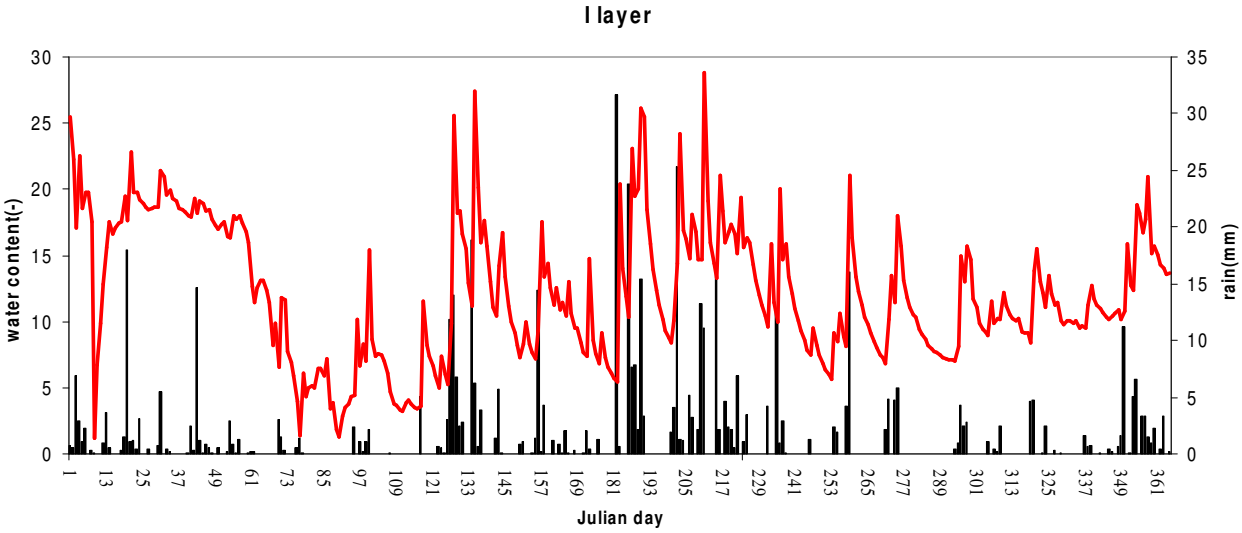

graph 1: the red line represents the water content at first level; while the black bar is the cumulated daily precipitation

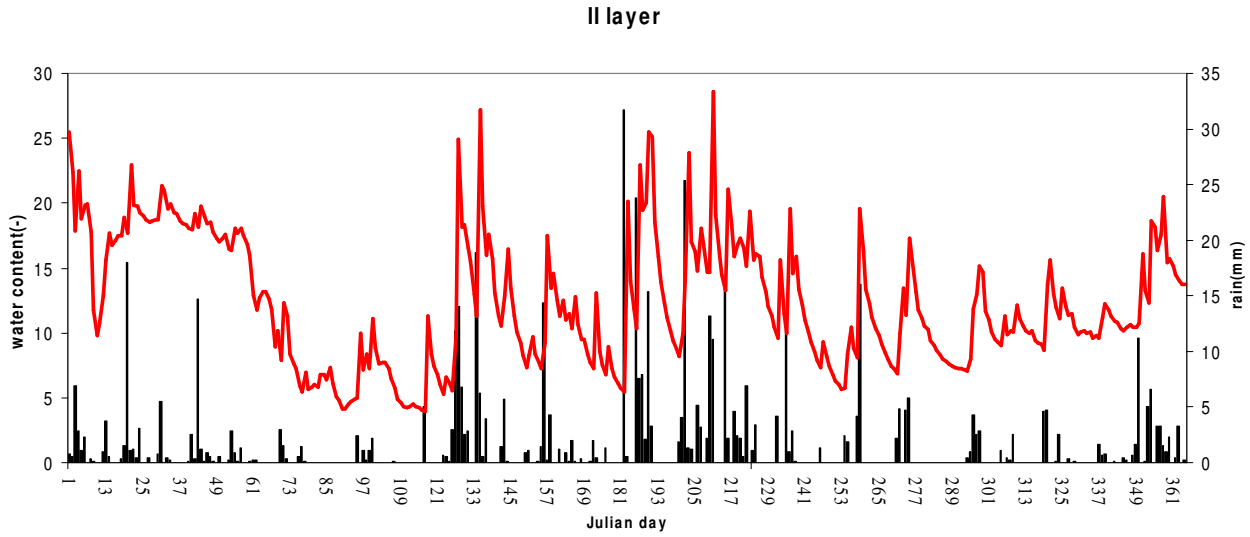

graph 2: the red line represents the water content at second level; while the black bar is the cumulated daily precipitation

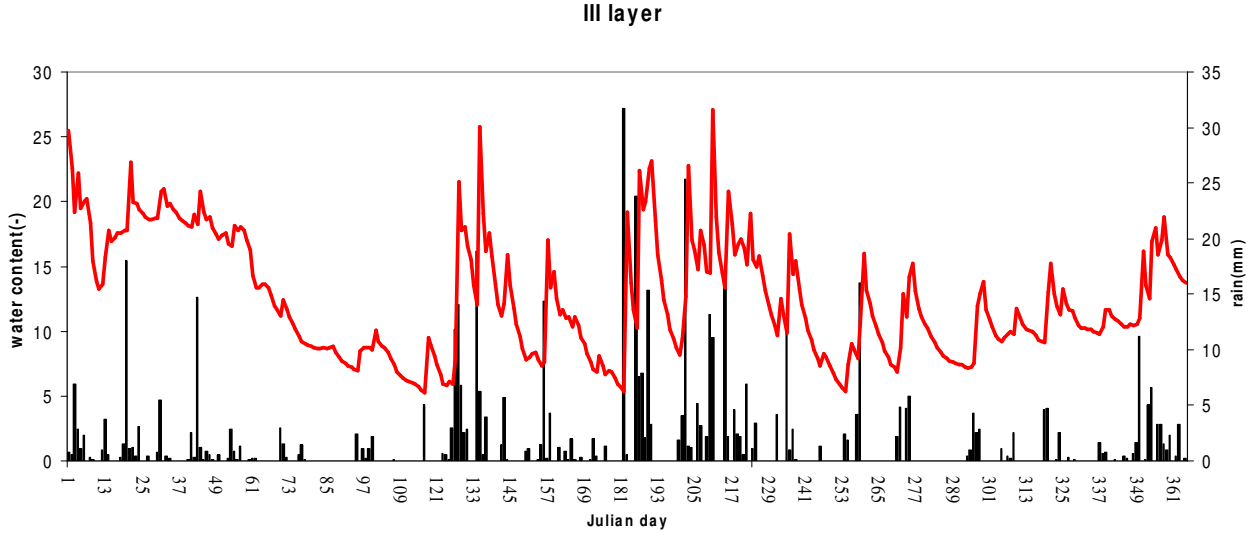

graph 3: the red line represents the water content at third level; while the black bar is the cumulated daily precipitation

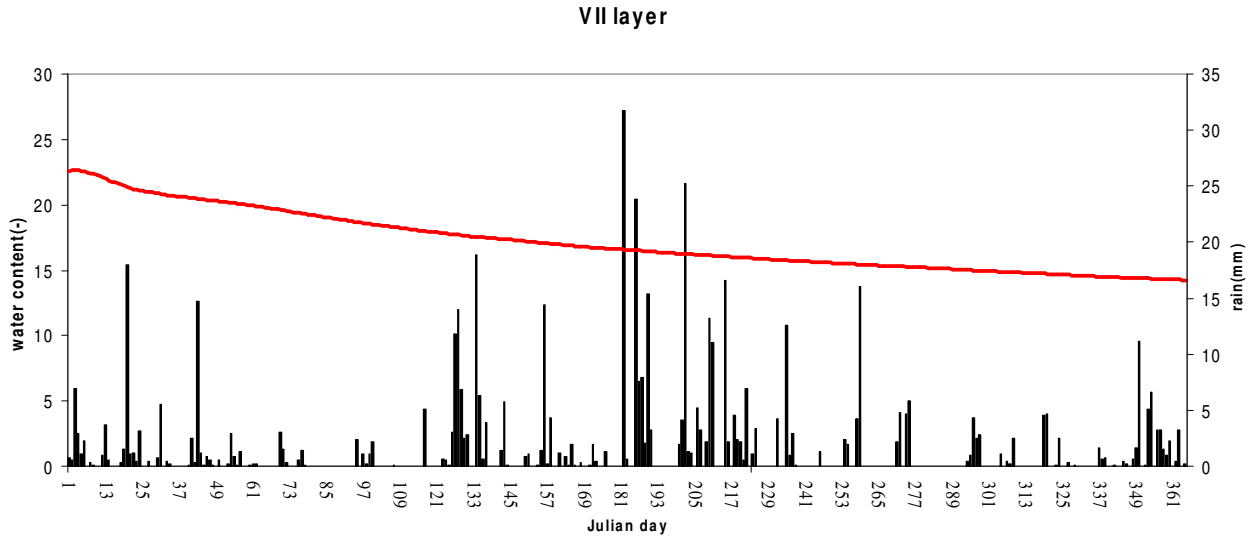

graph 4: the red line represents the water content at seventh level; while the black bar is the cumulated daily precipitation

In the lowest layers, the water content values vary only to tend to equilibrium value; then they aren't influenced by rainfall series.
Spin-off time is approximately twenty days-one month; in this period, on the 11th day, in the upper layer, a sudden decrease of water content happens; at the same time, for the latent heat and sensible heat trends (**graphs 5-6**), are observed peak values; latent heat $\left[L\left(F_{q^v}^3\right)_{sfc}\right]$ is function of L (constant) and $\left(F_{q^v}^3\right)_{sfc}$ proportional to water exchanges (evaporation, transpiration, dew); sensible heat $\left[H = \rho C_h^d |v_h| \left(\theta\pi_{sfc} - T_{sfc}\right)\right]$ is proportional to difference between air and soil temperature; any value influencing latent and sensible heat assumes abnormal value.
(In the sensible heat trend a negative value means the presence of a flux from soil, while a positive value means the presence of a flux versus soil).

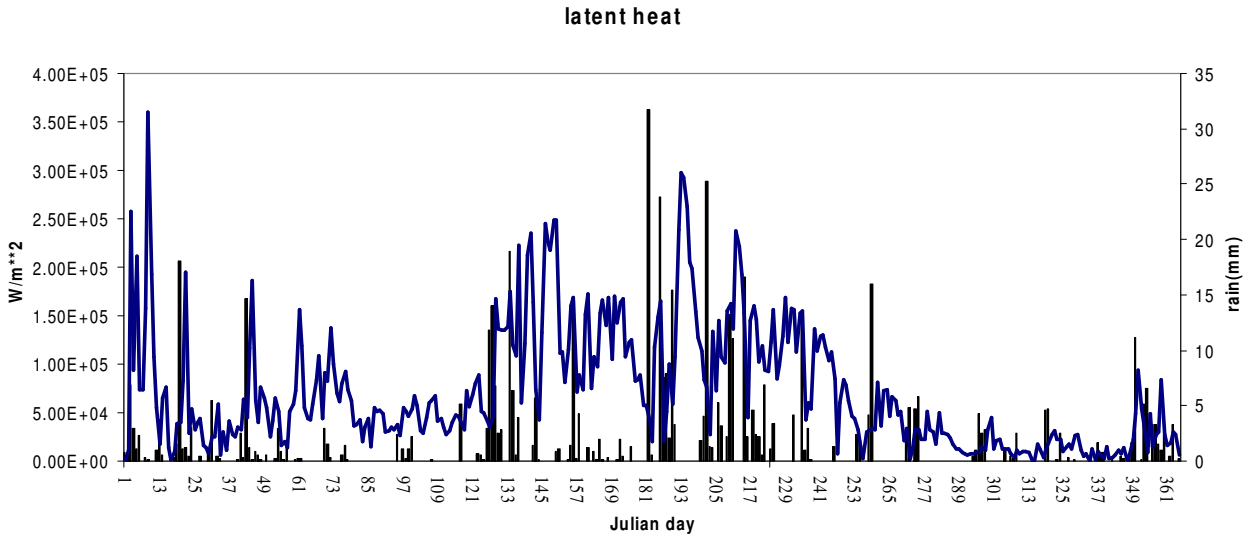

graph 5: the blue line represents the latent heat; while the black bar is the cumulated daily precipitation

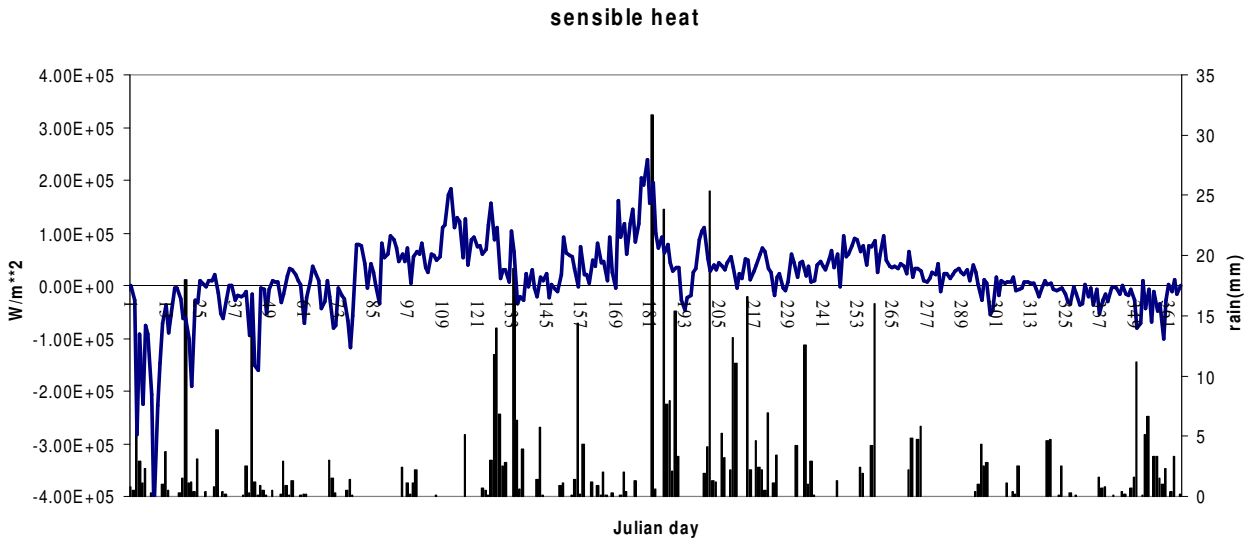

graph 6: the blue line represents the sensible heat; while the black bar is the cumulated daily precipitation

The soil temperature trends are showen in **graph 7-11**, for the three upper layers, 6th and 8th layer. In the upper layer, the soil temperature (green line) follow the air temperature values (black line); but while in the cold season, soil temperature is higher than air temperature, in the warm season the opposite happens (because of the different thermal properties between soil and atmosphere).
For the lower layers, the temperature tends to climatological value $(T = 280K)$; in the 8th layer a constant value is simulated.

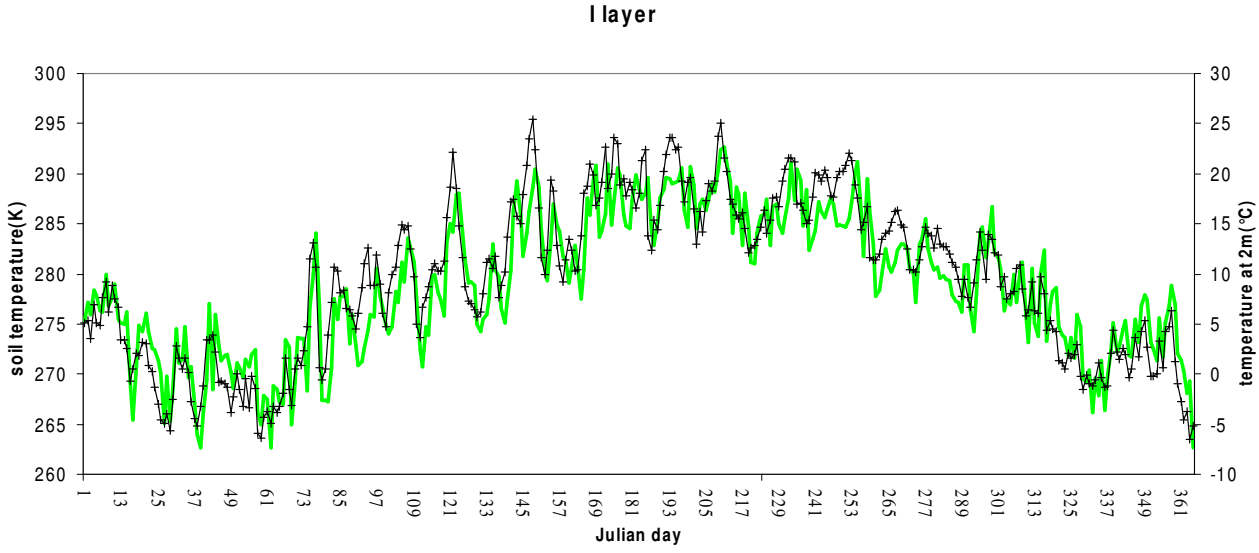

.

graph 7: the green line represents the soil temperature; while the black line is the air temperature**.**

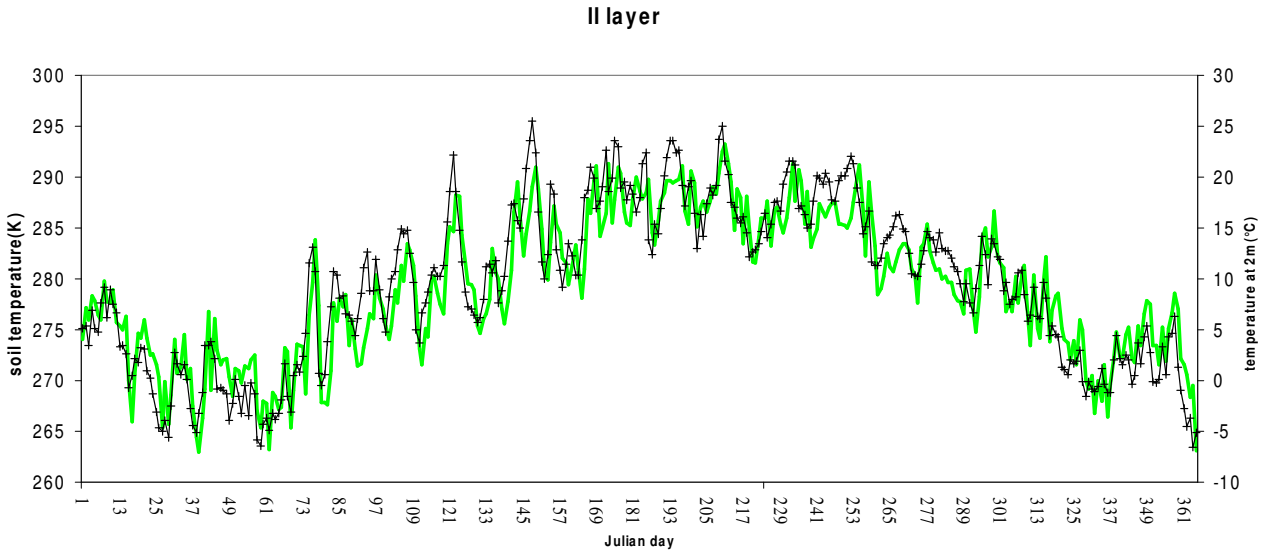

.graph 8: the green line represents the soil temperature; while the black line is the air temperature**.**

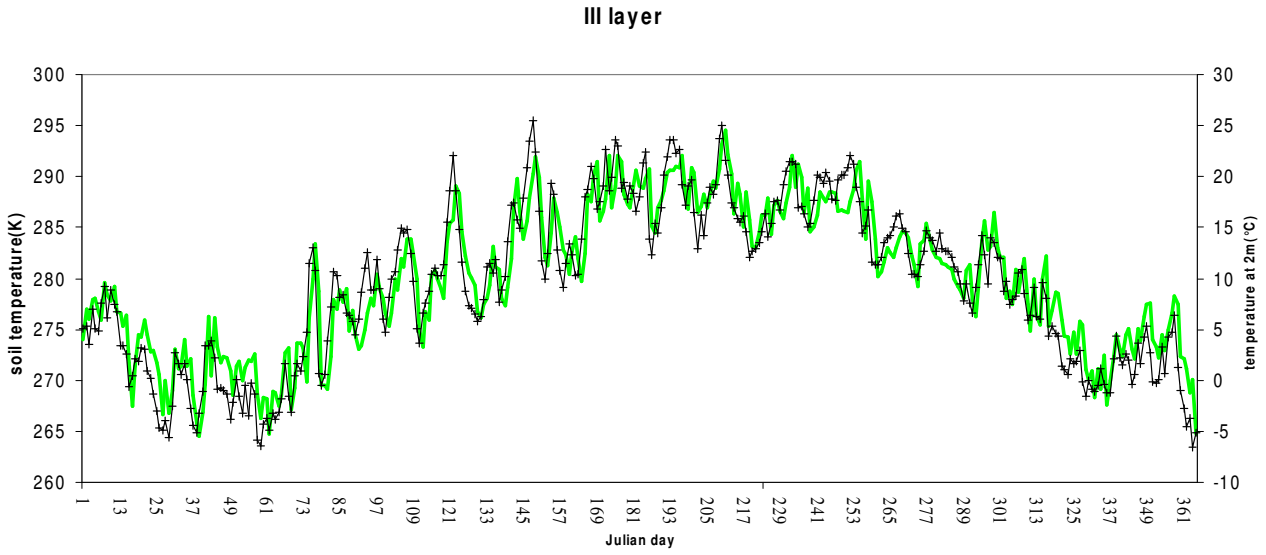

.graph 9: the green line represents the soil temperature; while the black line is the air temperature**.**

.
.

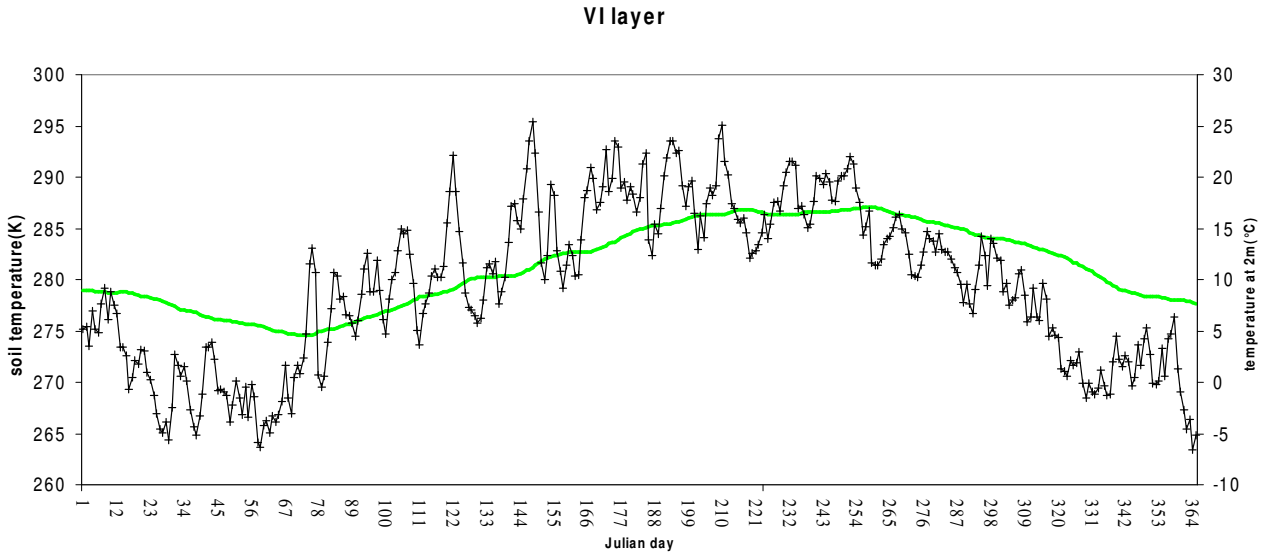

.graph 10: the green line represents the soil temperature; while the black line is the air temperature**.**

.

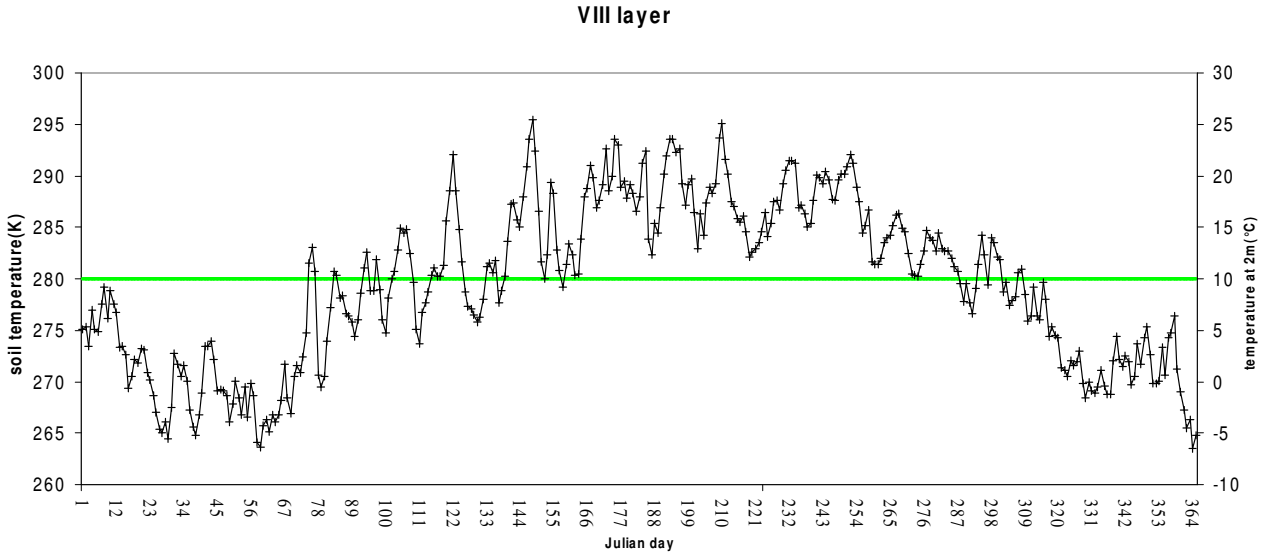

. graph 11: the green line represents the soil temperature; while the black line is the air temperature.

The surface runoff trends are showen in graph 12 and graph 13 (in this, there is a zoom about interval between 0 and $1 kg/m^2$); all the values are in this range except on on 181st day; it's not possible to verify if this value overvalues the real value.
Furthermore, for many wet days a zero surface runoff value is simulated; these values can be verisimilar if low hourly precipitation value are recorded.

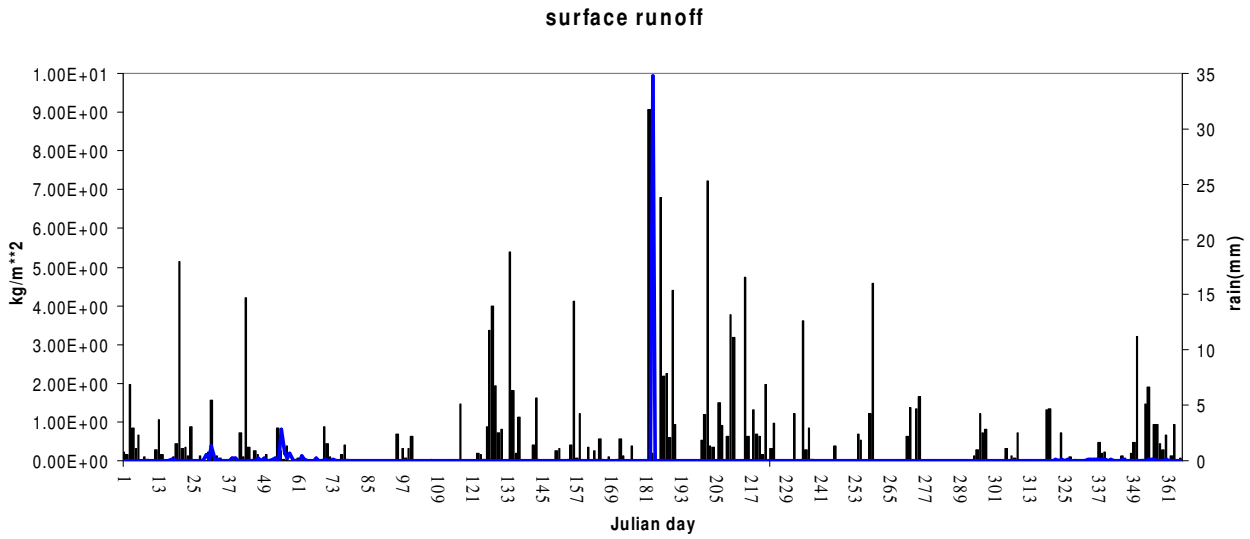

graph 12: the blue bar represents the surface runoff; while the black bar is the daily cumulated precipitation**.**

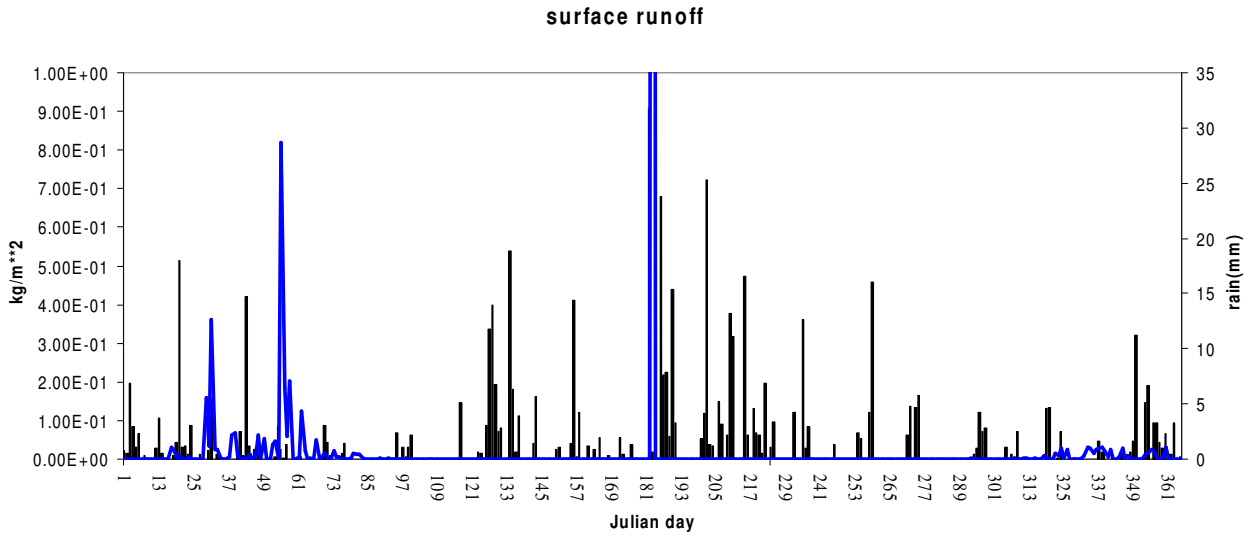

graph 13: the blue bar represents the surface runoff; while the black bar is the daily cumulated precipitation. In this graph there is a zoom about interval between 0 and $1kg/m^2$ of the surface runoff.

For a long initial time (about 50 days), the subsoil runoff trend shows anomalous values; after this time, between rainfall event and subsoil runoff peak, there is a time lag of almost one day (soil type "sand" shows high permeability values)

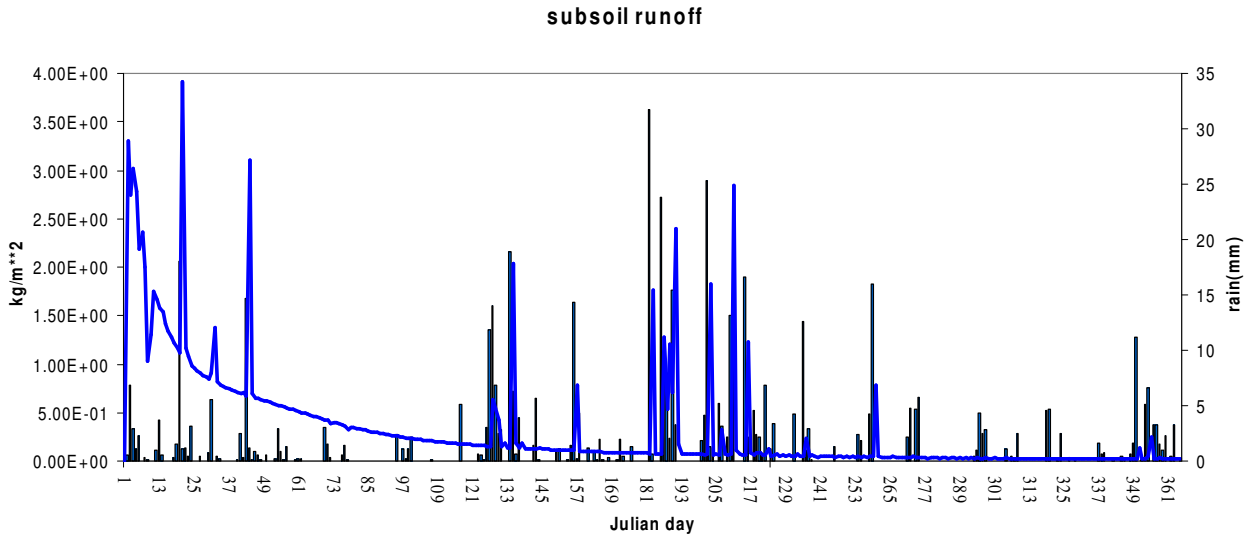

graph 14. : the blue bar represents the subsoil runoff; while the black bar is the daily cumulated precipitation**.**

1.3 Sensitivity tests

1.3.1 Different soil types

To test the code sensitivity varying soil type, are carried out some simulations; in these, all the settings are unchanged, but all different soil type are used.
Some results are showen in **graphs 15-20** (they are water content and soil temperature trends for three layers)

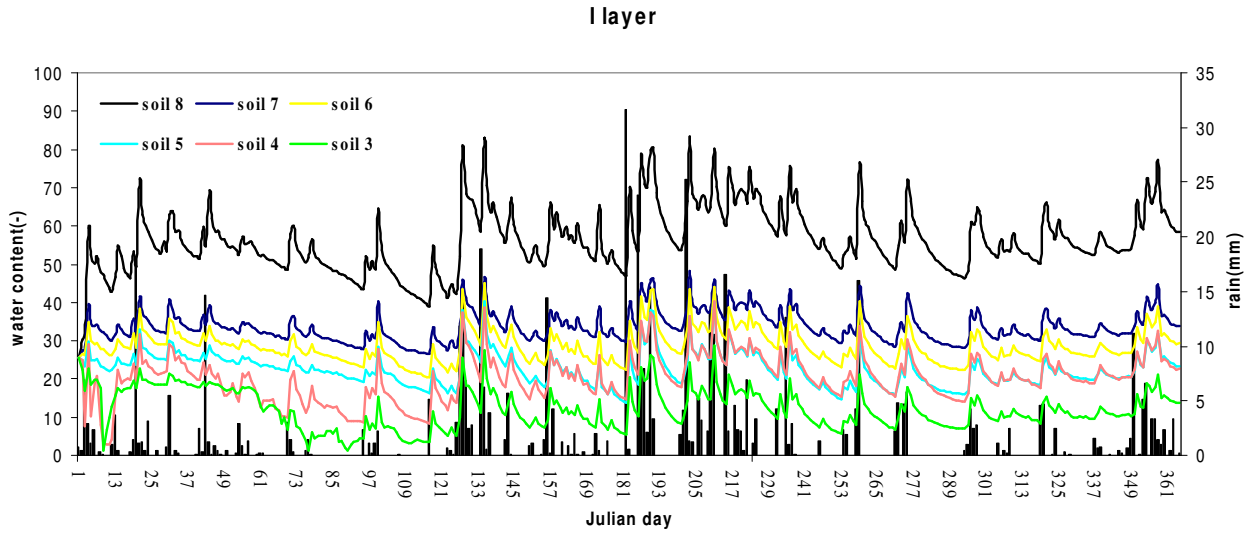

graph 15: the black bar represents the cumulated daily precipitations; the others curves are the water content curves in the first soil level varying the soil type.

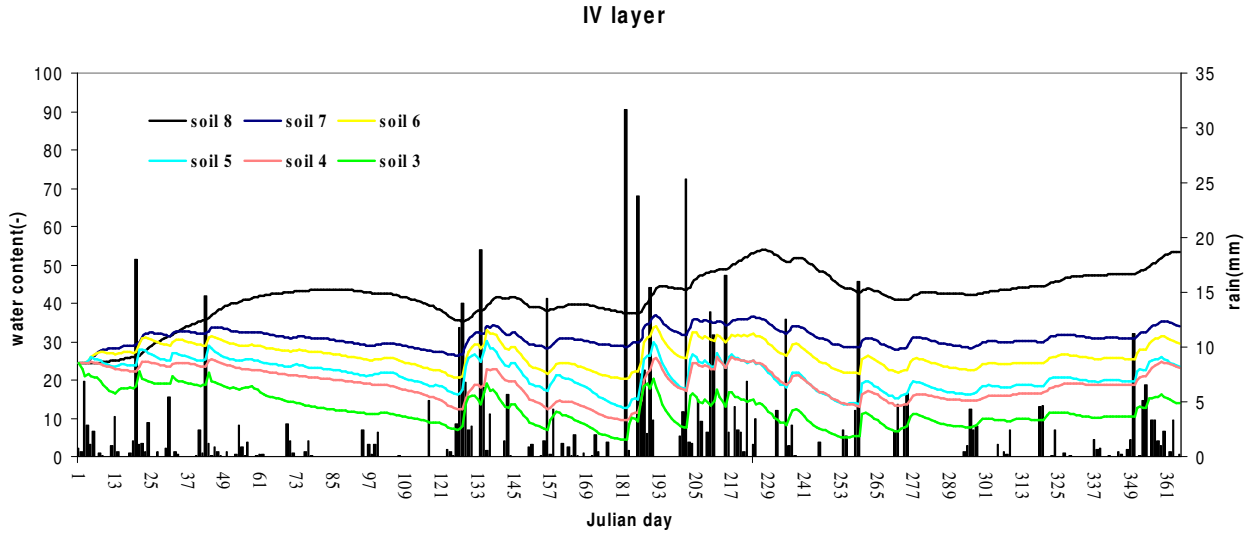

graph 16: the black bar represents the cumulated daily precipitations; the others curves are the water content curves in the second soil level varying the soil type

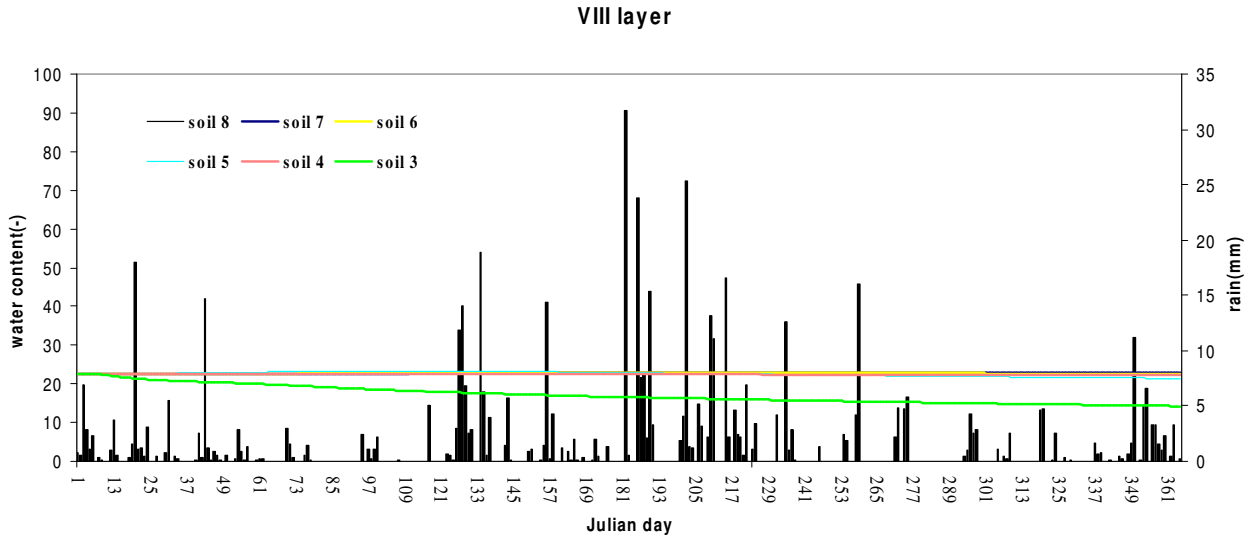

graph 17: the black bar represents the cumulated daily precipitations; the others curves are the water content curves in the seventh soil level varying the soil type

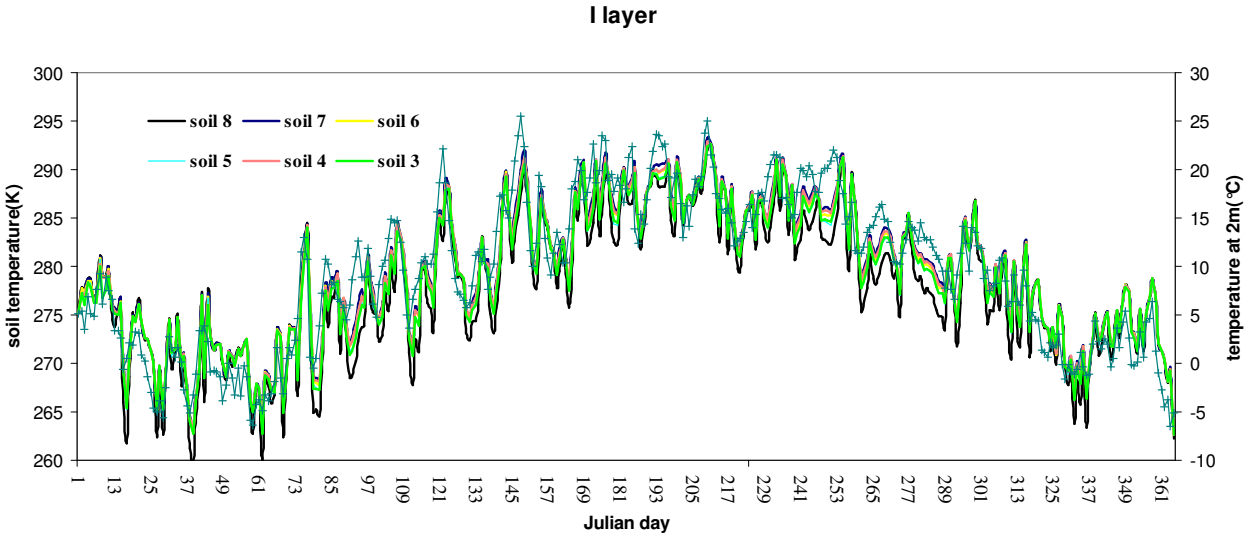

graph 18: the crossed line represents the observed temperature at 2 meters; while the others curves are the soil temperatures at the first soil level varying the soil type

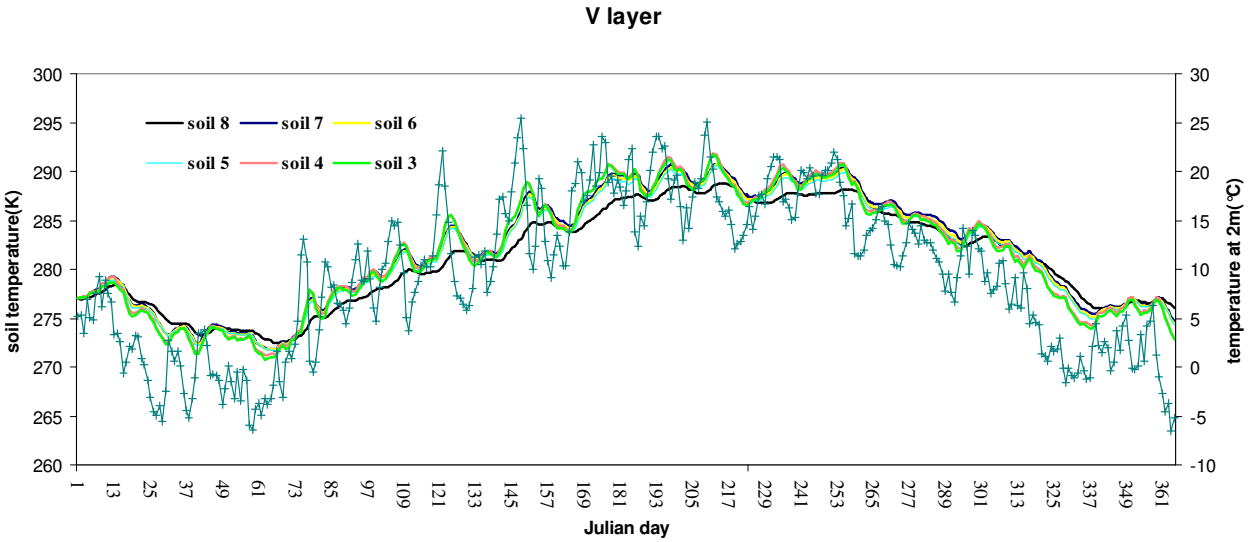

graph 19: the crossed line represents the observed temperature at 2 meters; while the others curves are the soil temperatures at the fifth soil level varying the soil type

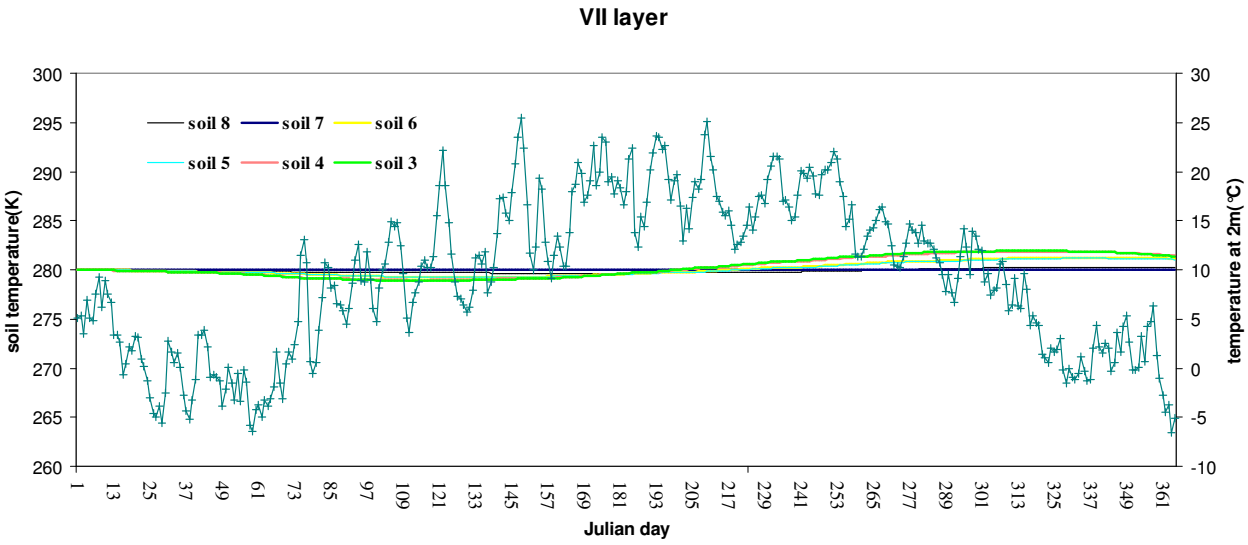

graph 20: the crossed line represents the observed temperature at 2 meters; while the others curves are the soil temperatures at the seventh soil level varying the soil type

The water content trends are heavily influenced by volume of voids and hydraulic conductivity; increasing these parameters, in the soil increases water content; if instead of water content trends, are considered saturation degree trends (for example, for two upper layers, **graph 21-22**):

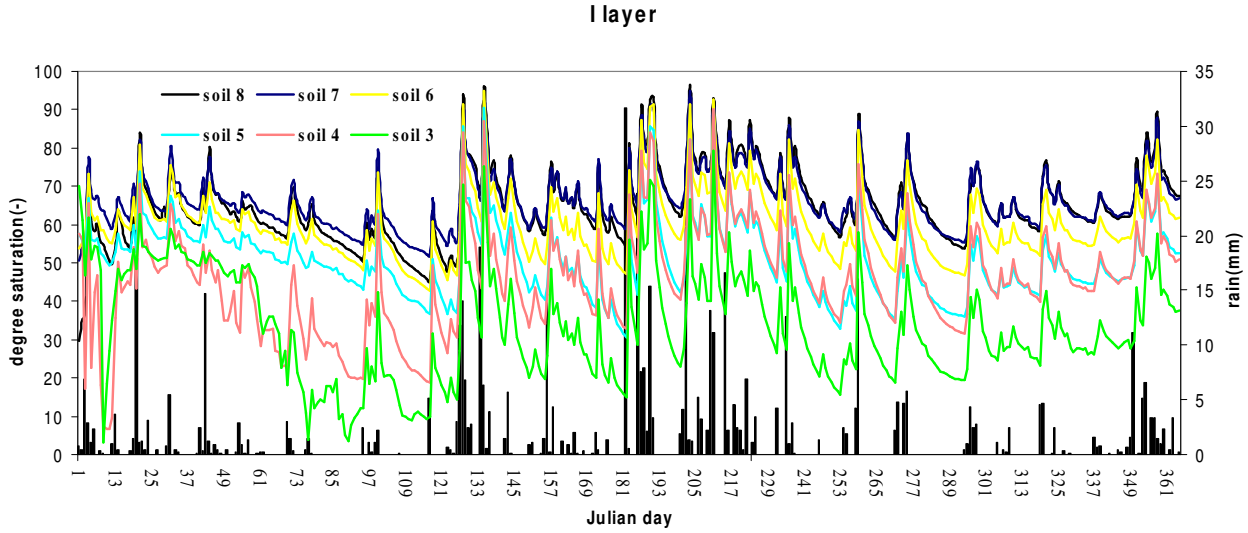

graph 21: the black bar represents the cumulated daily precipitations; the others curves are the degree saturation curves in the first soil level varying the soil type

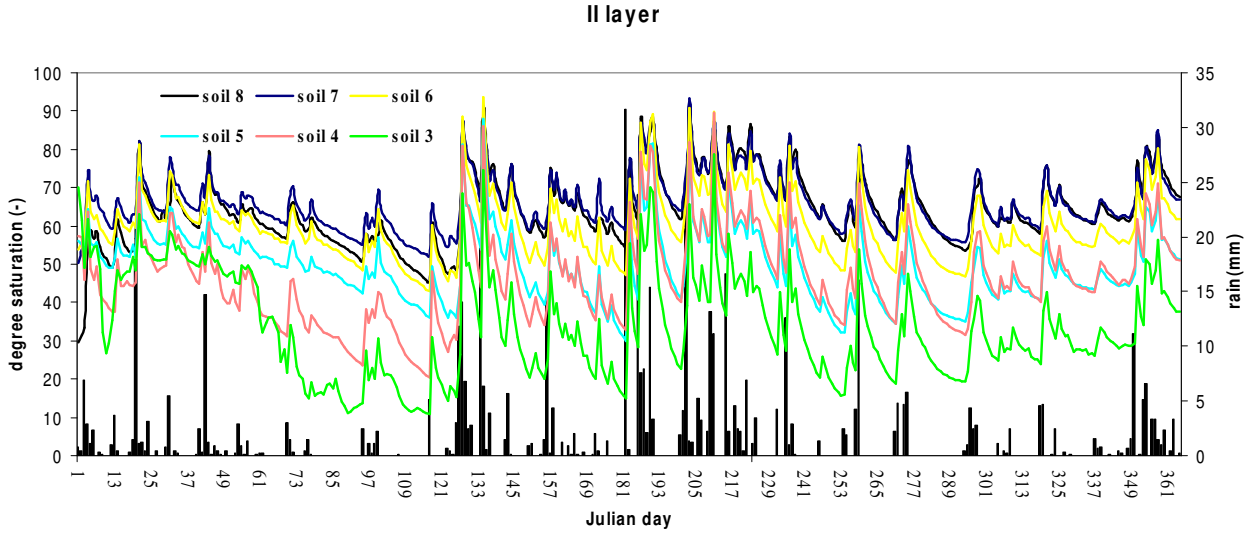

graph 22: the black bar represents the cumulated daily precipitations; the others curves are the degree saturation curves in the second soil level varying the soil type

only the "soil 8" (peat) curve exchanges its position; really, this soil type has very low permeability but very high volume of voids (see Table 2); for soil type with low permeability, on 11th day, (soil 5-8), there isn't any anomalous value, then, this anomaly, in spin-off time, is due only to soil properties.

Except for soil type "sand", in 8th layer, final water content values are almost egual.

For soil type with intermediate properties, final conditions seem to be congruent with initial conditions, while for other soil type, they aren't correct.

Because of similar thermal parameters, for all layers, soil temperature curves are superimposed; because of low conductivity properties, peat curve shows different behaviour (soil is colder than others on winter and more hot on summer).

Reducing water permeability, surface runoff increases (graph 23); in fact precipitation has more difficulties to seep into soil.

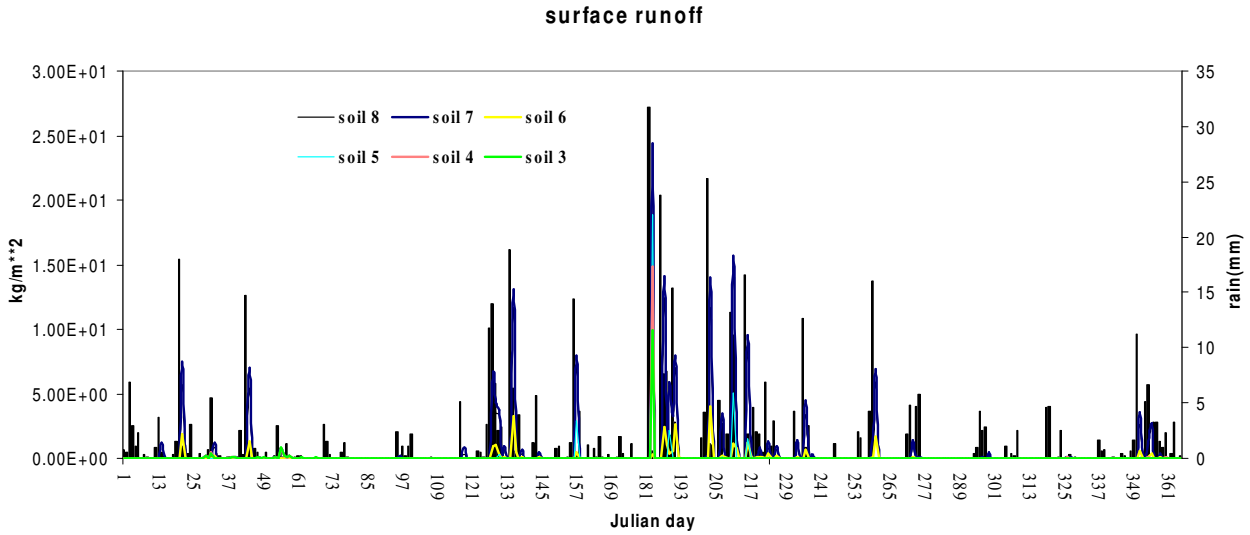

graph 23: the black bar represents the cumulated daily precipitations; the others bars are the surface runoff varying the soil type

For surface runoff, the difference between soil type are clear if there are heavy daily rainfalls. Increasing volume of voids and permeability, latent heat flux increases (**graph 24**); in fact, it is proportional to water exchanges between atmosphere and soil; then, these exchanges can happen more easily for "sand" and "sandy loam".

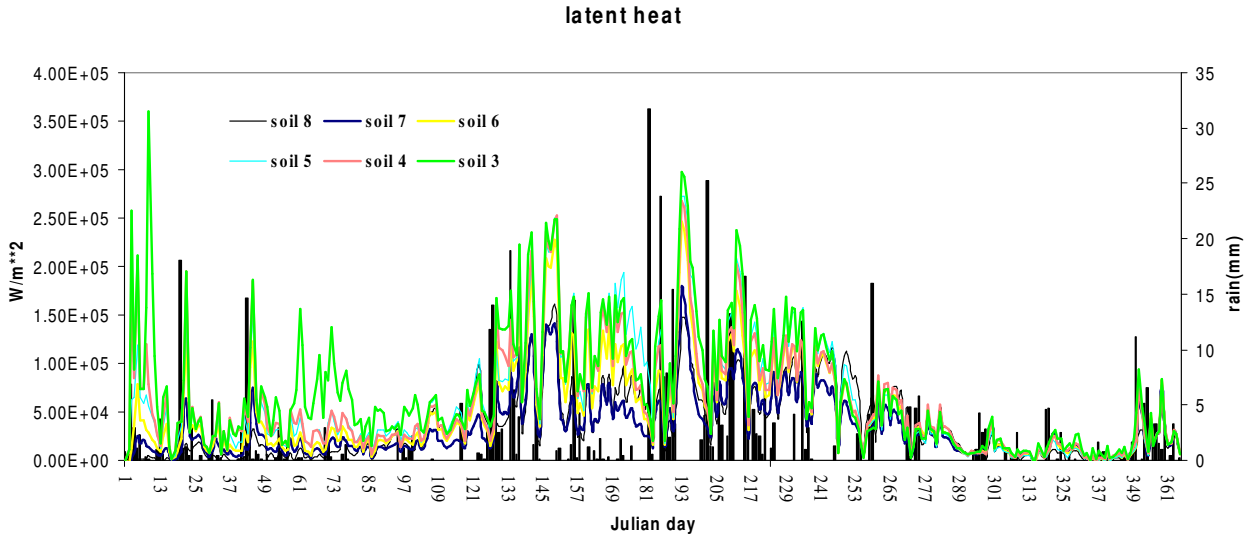

graph 24: the black bar represents the cumulated daily precipitations; the others bars are the latent heat trends varying the soil type

For subsoil runoff trends, it's the opposite in comparison with surface runoff curves; in fact; the more permeable soils show higher values of subsoil runoff; for only soil type "sand", there are, in the first time, values to check.

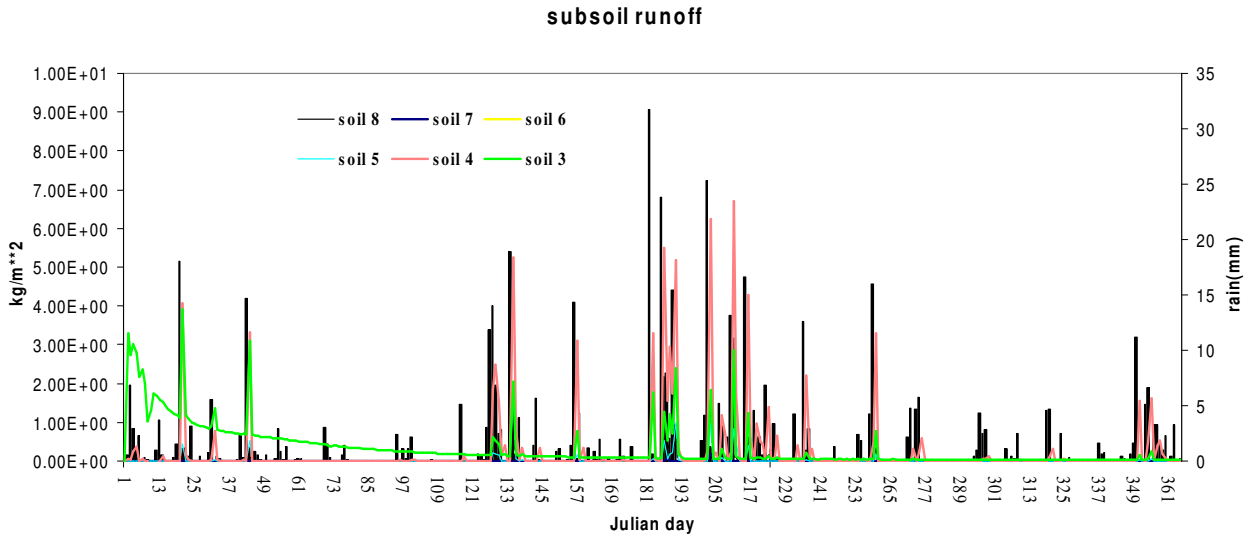

graph 25: the black bar represents the cumulated daily precipitations; the others bars are the subsoil runoff trends varying the soil type

1.3.2 Type of bare soil evaporation model

Usually, for operative purpose, to estimate evaporation flux BATS model is used.
In TERRA-LM stand alone version, it is possible to utilize other two evaporation models:

- **Bucket-Model**: a simplified experimental model; in this approach, in absence of water in the soil, potential evaporation E_p is reduced by β^2 factor:

$$E_b = (1 - f_i)(1 - f_{snow})\left(1 - f_{p\ln t}\right)\beta_{E_b}{}^2\left(- E_{pot}\left(T_{sfc}\right)\right) \quad \textbf{eq. 1}$$

with[5] β_{E_b} $\begin{cases} 0; \eta_1 < \eta_{adp} \\ \dfrac{\eta_1 - \eta_{adp}}{\eta_{fc} - \eta_{adp}}; \eta_{adp} < \eta_1 < \eta_{fc} \\ 1; \eta_1 \geq \eta_{fc} \end{cases}$ **eq. 2**

- **Noilhan-Planton:** experimental in TERRA-LM code; in this approach , reducing factor has the following form:

$\beta_{E_b} = 1$ if $\eta_1 > \eta_{fc}$ **eq. 3**

$$\beta_{E_b} = 0.5\left(1 - \cos\left(0.5\pi\left(\frac{\eta_1 - \eta_{adp}}{\eta_{fc} - \eta_{adp}}\right)\right)\right) \quad \textbf{eq. 4}$$

$$E_b = \min\left(0.0; \rho g\left(q_v - \beta_{E_b} q_{sfc}\right)\right) \quad \textbf{eq. 5}$$

Comparing the three models, some remarks are absolutely necessary (in **graph 26-29** are shown water content trends for three layers and soil temperature for upper layer).
It is necessary to underline that monitored data of water content and soil temperature are not available and then it is not possible to verify which model simulates better the real distributions of water content and temperature.
In every layer, water content curves, estimated with Noilhan-Planton method are above the others; then, it simulates lower water losses caused by evaporation. This undervaluing is higher in cold season rather than in warm season when three curves are superimposed (in the same way, it is possible to verify that latent heat curve [**graph 30**] for Noilhan-Planton approach, in the cold season, is below other curves)
Using bucket model, water content curves are above the curves obtained using BATS in cold seasons and are below these in the warm season; considering the yearly balance, the difference between two models furnish similar values of water content; then, the behaviours of three models seem not to differ particularly in the warm season when the evaporation is very important for hydric balance. Properly, in the lower layers the water content curves aren't influenced by used evaporation model.
Soil temperature trends aren't influenced by the utilized evaporation model; then, only the graph for upper layer is given. It demonstrates that, in absence of snow, hydric and thermal processes are not strictly linked in the soil.

---

[5] η_1 soil water content in upper layer

η_{adp} water content for air dryness point

η_{fc} water content for field capacity

Using Bucket or Noilhan-Planton model, on 11th day abnormal peak isn't simulated (see water content graph for first layer, latent heat); it is necessary to verify if this peak is due to the spin-off timeor, on the other hand, if it can be due to the greater complexity of the BATS model that takes in account more parameters than the others model (for instance, in the evaporation model it takes in account the soil parameters as soil permeability and porosity)

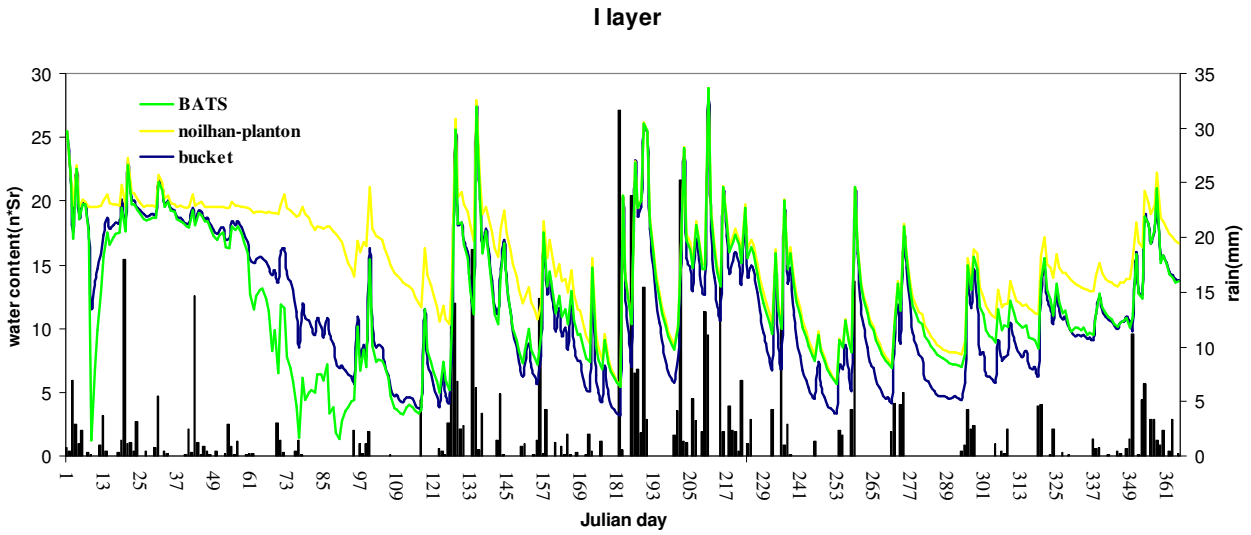

graph 26: the black bar represents the cumulated daily precipitations; the others bars are the soil moisture curves in the first layer varying the evaporation model (green line for BATS model, yellow line for Noilhan-Planton model and blue for bucket model)

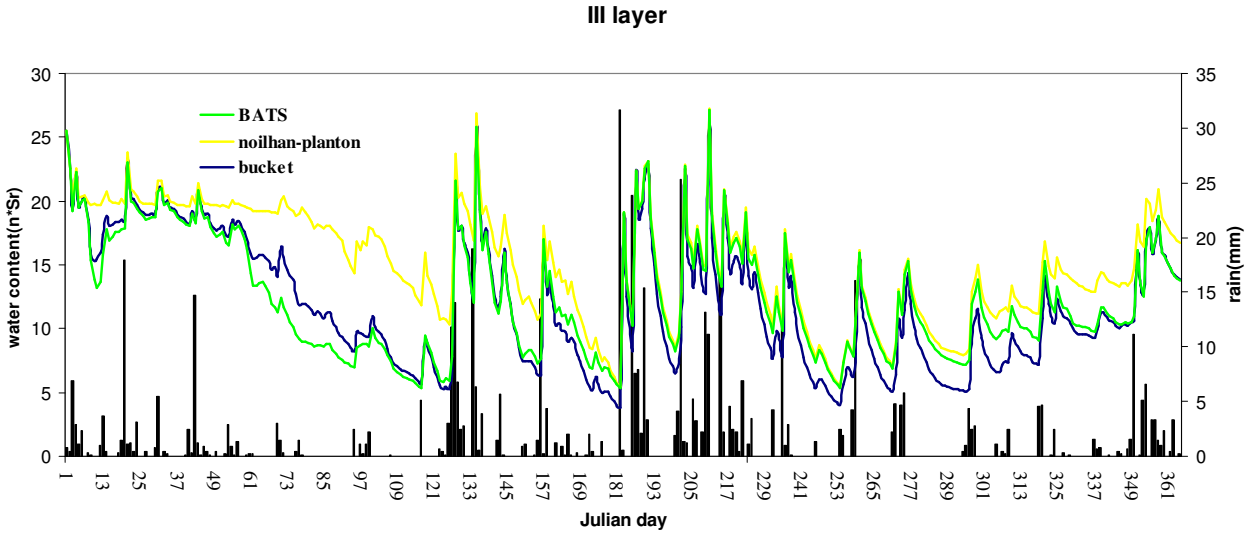

graph 27: the black bar represents the cumulated daily precipitations; the others bars are the soil moisture curves in the third layer varying the evaporation model (green line for BATS model, yellow line for Noilhan-Planton model and blue for bucket model)

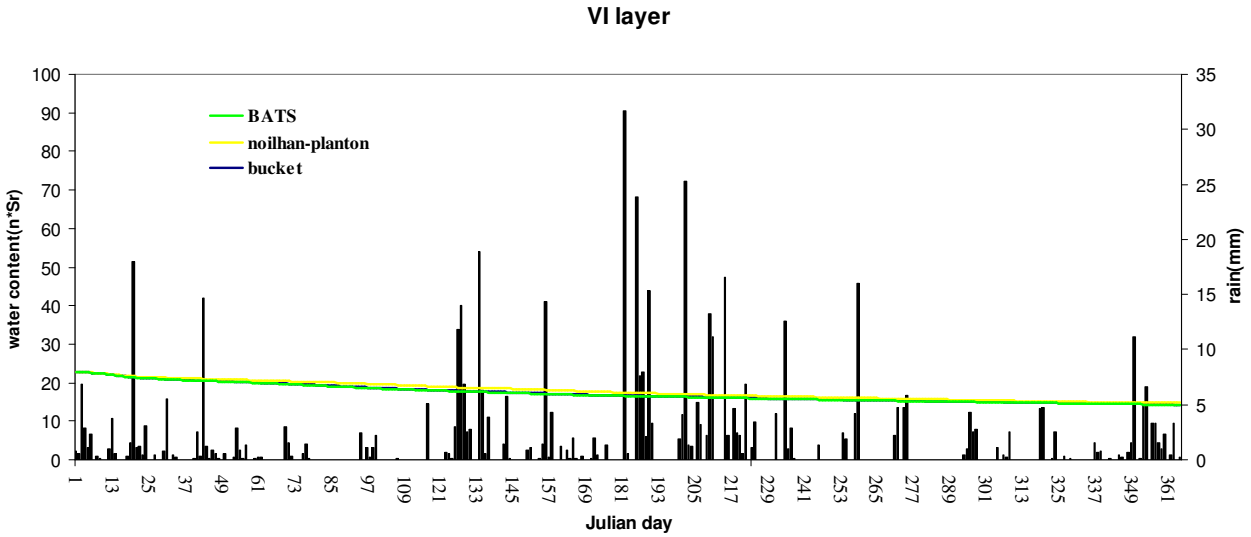

graph 28: the black bar represents the cumulated daily precipitations; the others bars are the soil moisture curves in the VI layer varying the evaporation model (green line for BATS model, yellow line for Noilhan-Planton model and blue for bucket model)

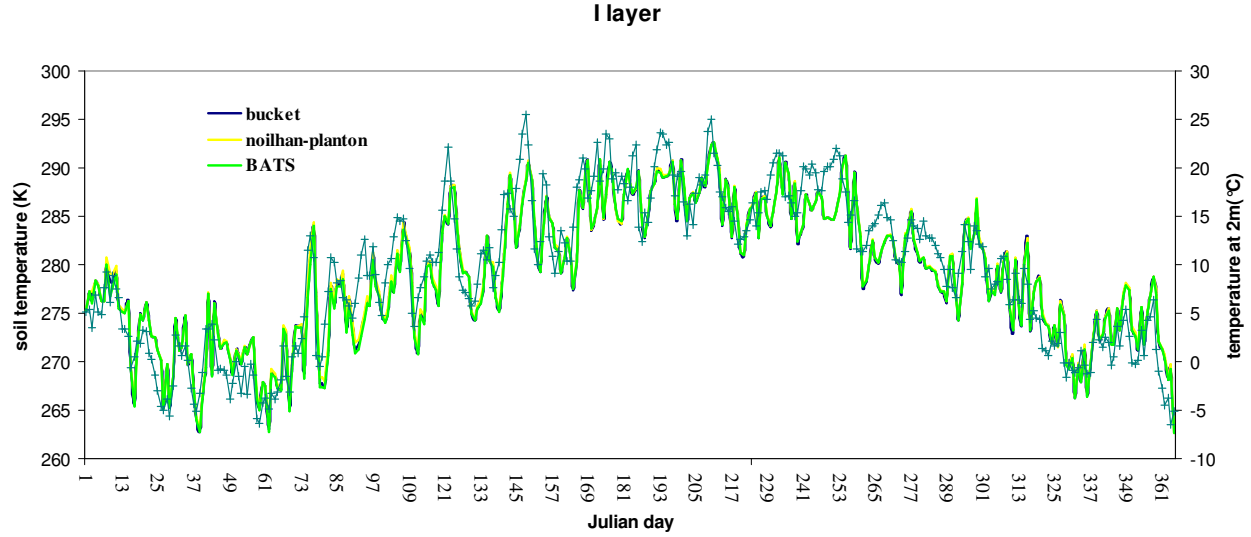

graph 29 : the grey curve with the crosses represents the air temperature the others bars are the soil temperature curves in the I layer varying the evaporation model (green line for BATS model, yellow line for Noilhan-Planton model and blue for bucket model)

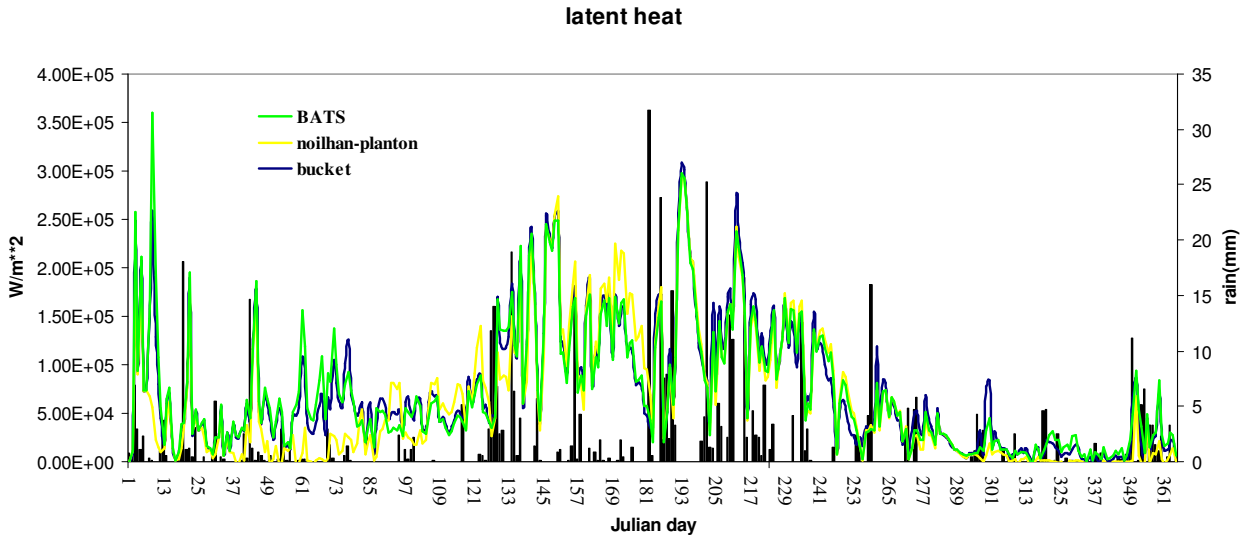

graph 30: the black bar represents the cumulated daily precipitations; the others bars are the latent heat curves varying the evaporation model (green line for BATS model, yellow line for Noilhan-Planton model and blue for bucket model)

In surface runoff graph (**graph 31**), using Noilhan-Planton approach, in the first time, very high values are simulated while blue and green curves are approximately superimposed. these values don't seem to be possible but they influence the entire trend; furthermore, yellow curve shows several peaks, according to more heavy rainfall events while the other models show an only peak on 181th day; the link between the used evaporation model and the generated surface runoff is not clear.

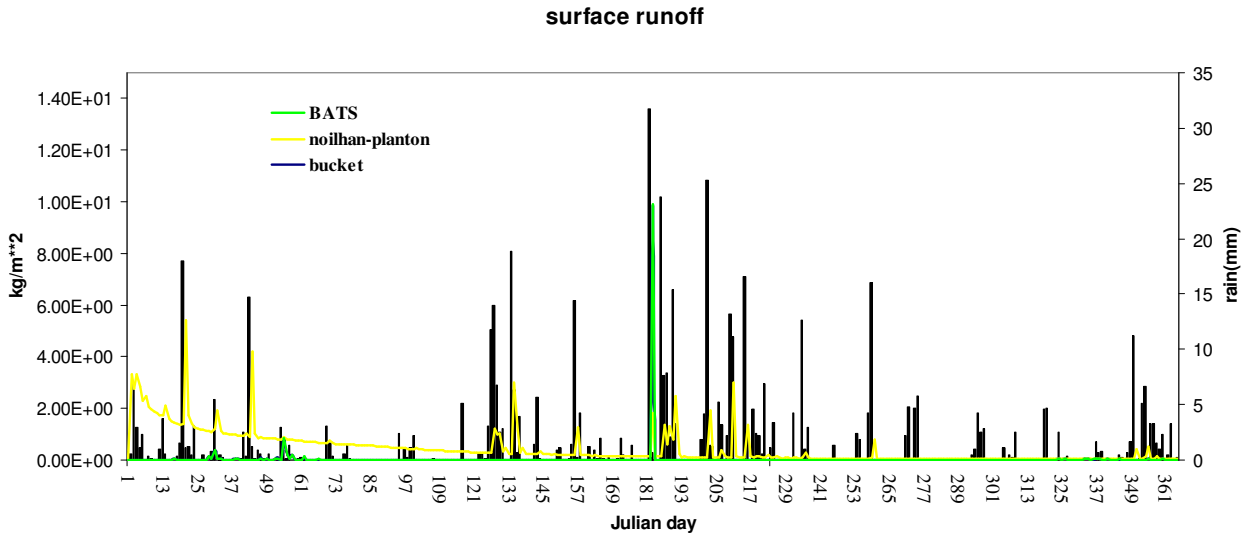

graph 31: the black bar represents the cumulated daily precipitations; the others bars are the surface runoff curves varying the evaporation model (green line for BATS model, yellow line for Noilhan-Planton model and blue for bucket model)

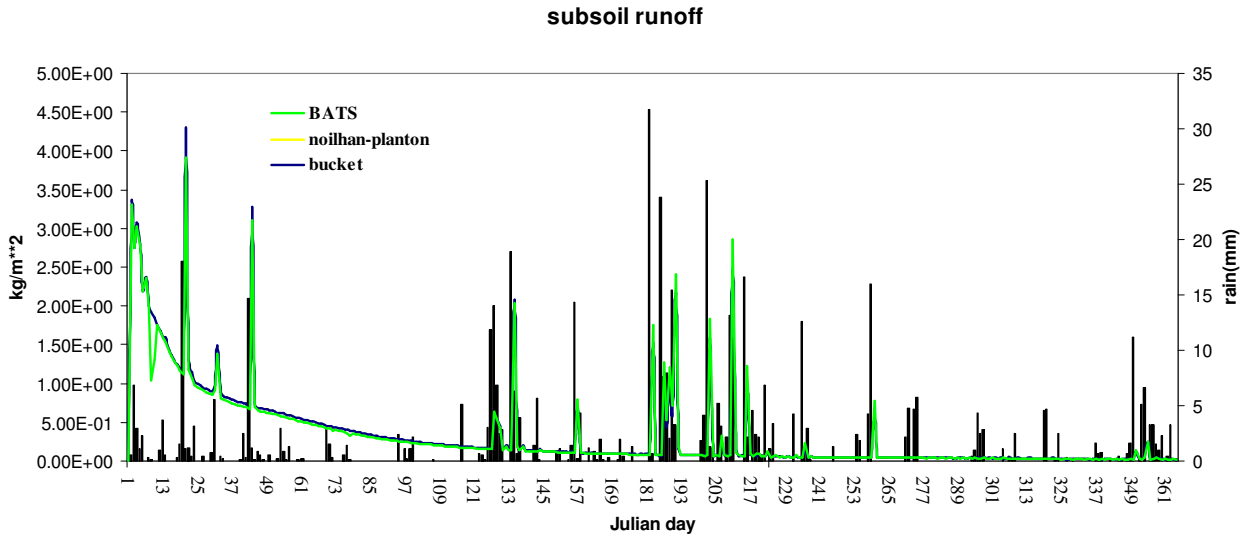

graph 32: the black bar represents the cumulated daily precipitations; the others bars are the subsoil runoff curves varying the evaporation model (green line for BATS model, yellow line for Noilhan-Planton model and blue for bucket model)

In subsoil runoff graph (**graph 33**), using all three approaches, in the first time, very high values are simulated; a large part of trends is then affected by these anomalous values.

1.3.3 Lower boundary

As lower boundary is usually utilized a flux boundary condition (in the following graphs **lb=1**); at a depth of 2.43m only the downward gravitational transport is considered (capillary transport is neglected); to test new settings, in TERRA-LM stand alone code other two experimental conditions are added:

- **Rigid lid :**impermeable bottom of soil column (at the moment, not available)
- **Constant ground water:** this condition assumes water table presence at the bottom of soil column and then ,water pressure equal to zero at this depth (now available in the following graphs **lb=3**).

In the following graphs (**graphs 33-39**) are shown the results obtained with flux boundary condition (usually used) and constant ground water condition.

For four upper layers, between two curves the differences are mainly in the first time (until 120th day); after this period, they are superimposed; on the contrary, for three lower layers, constant ground water presence influnces heavily the trends; in fact, for lower boundary 3, water content tends to porosity value while the green curve tends to an equilibrium value (probably for better initial condition, it should tend to horizontal line). Between 6th and 7th layer, the sudden variation of water content doesn't seem to be likely; the effect of constant groundwater on upper layers should be strictly marked;

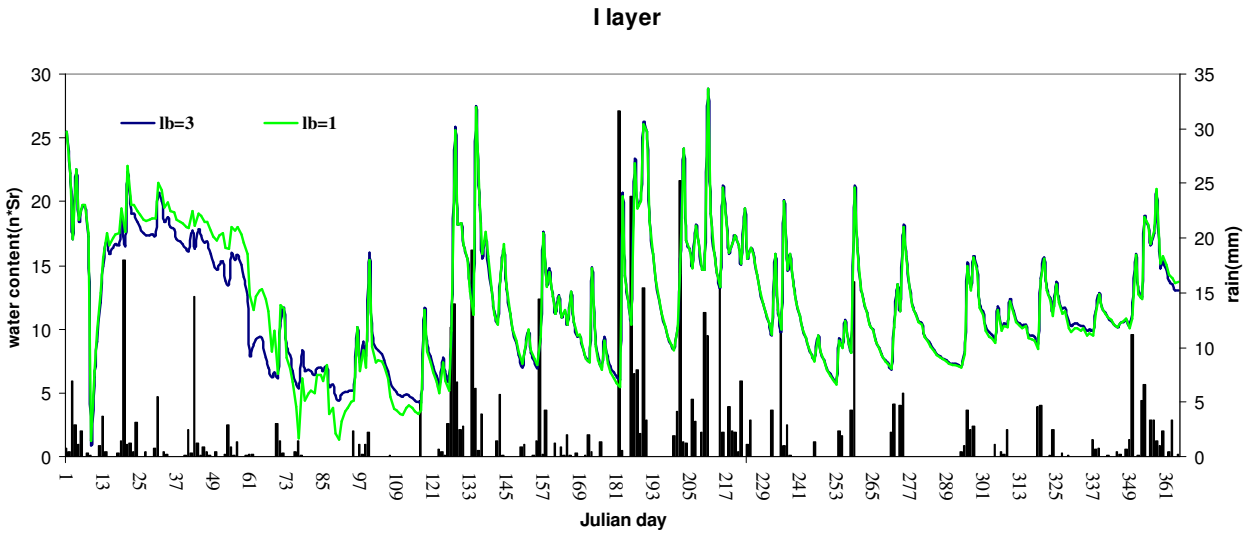

graph 33: : the black bar represents the cumulated daily precipitations; the others bars are the soil moisture curves in the first layer varying the lower boundary (green line for the unit gradient condition and blue for constant groundwater condition)

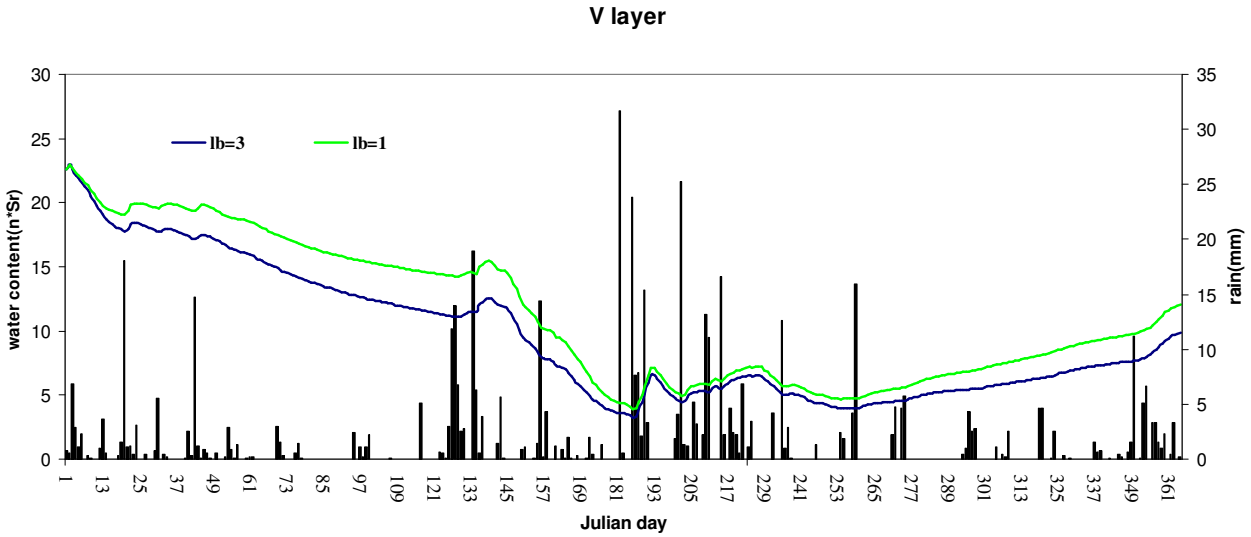

graph 34: the black bar represents the cumulated daily precipitations; the others bars are the soil moisture curves in the V layer varying the lower boundary (green line for the unit gradient condition and blue for constant groundwater condition)

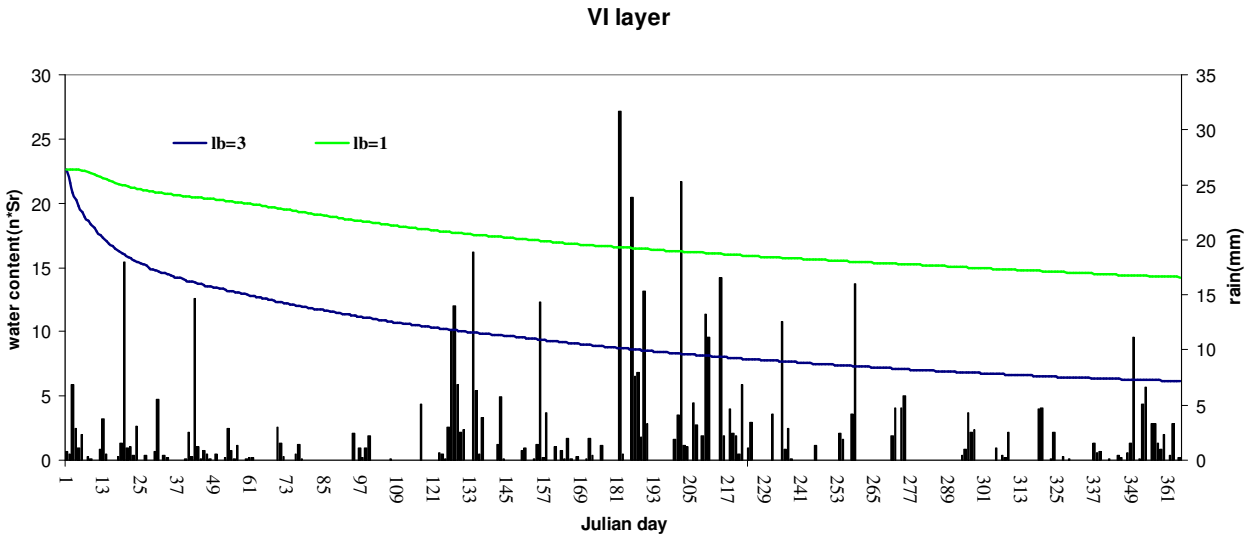

graph 35: the black bar represents the cumulated daily precipitations; the others bars are the soil moisture trends in the VI layer varying the lower boundary (green line for the unit gradient condition and blue for constant groundwater condition)

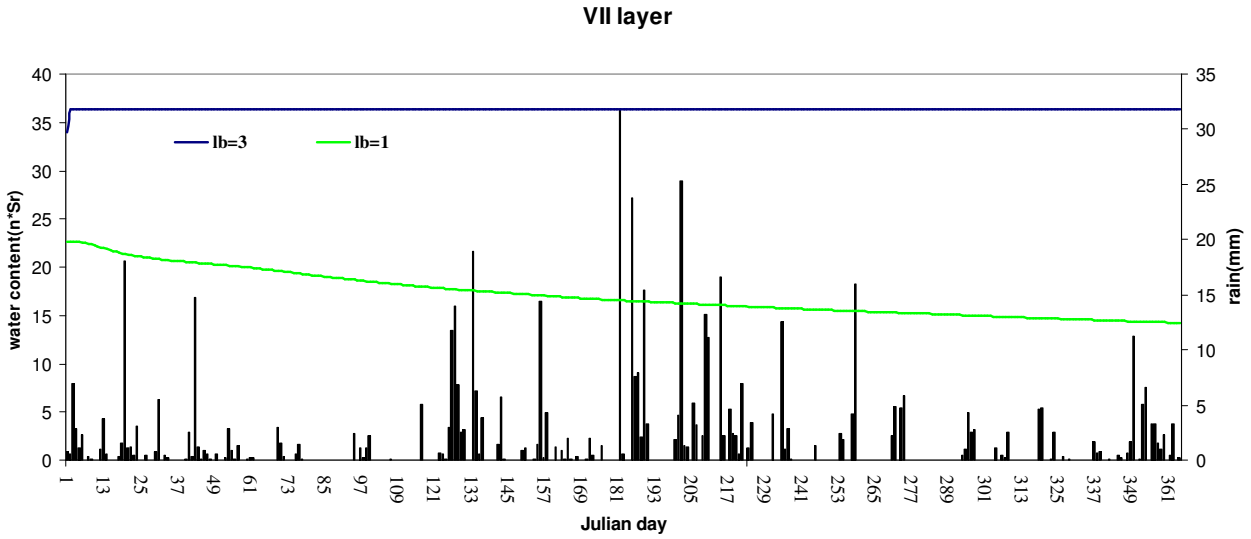

graph 36: the black bar represents the cumulated daily precipitations; the others bars are the soil moisture trends in the VII layer varying the lower boundary (green line for the unit gradient condition and blue for constant groundwater condition)

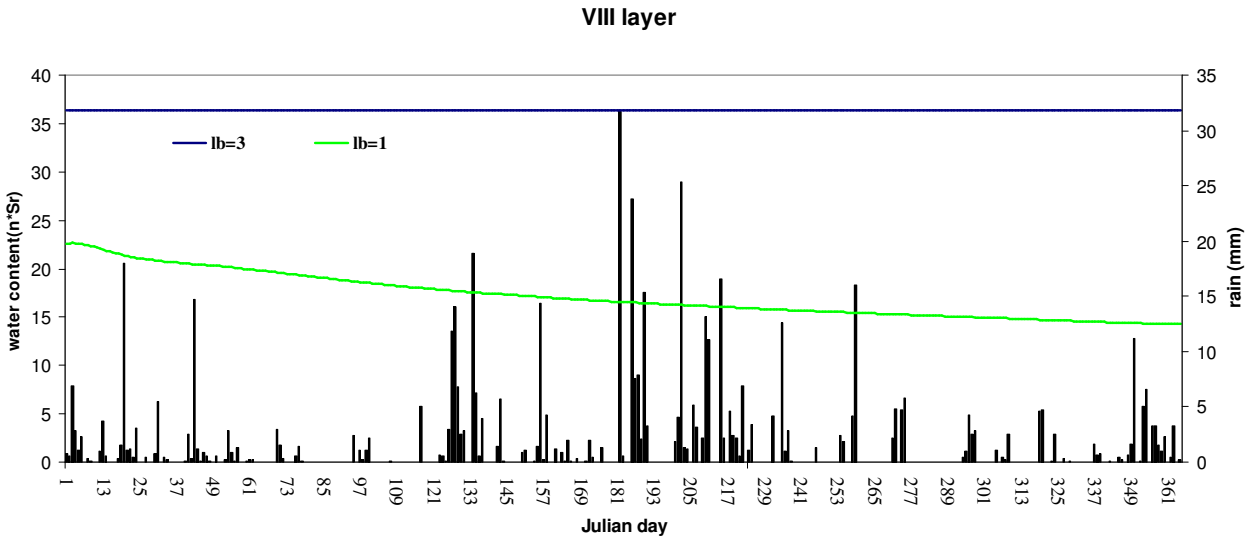

graph 37: the black bar represents the cumulated daily precipitations; the others bars are the soil moisture trends in the VIII layer varying the lower boundary (green line for the unit gradient condition and blue for constant groundwater condition)

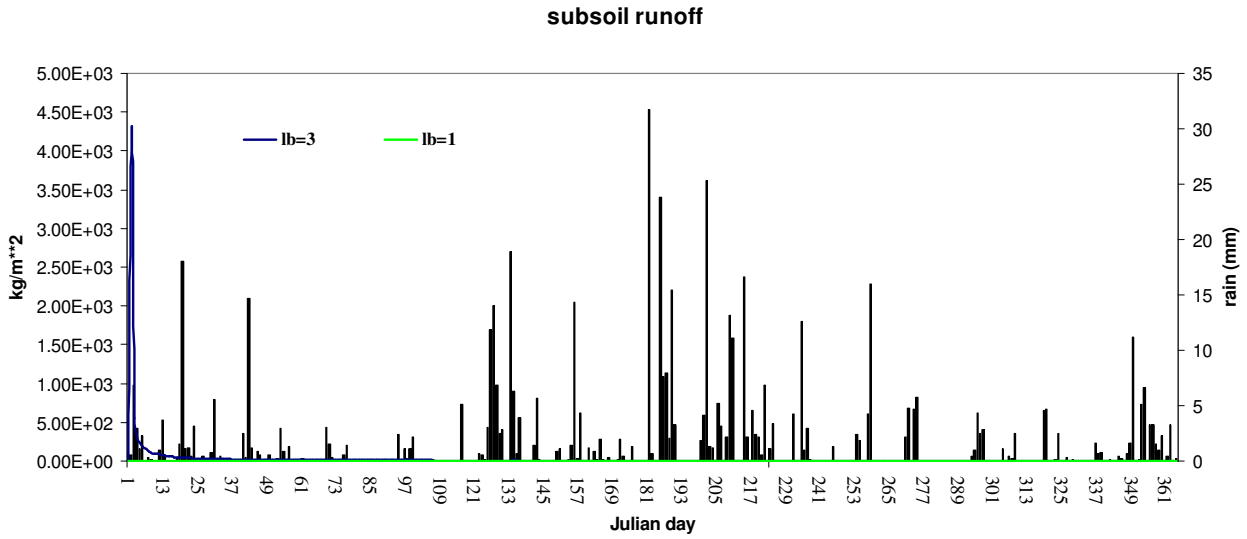

graph 38: the black bar represents the cumulated daily precipitations; the others bars are the subsoil runoff curves varying the lower boundary (green line for the unit gradient condition and blue for constant groundwater condition)

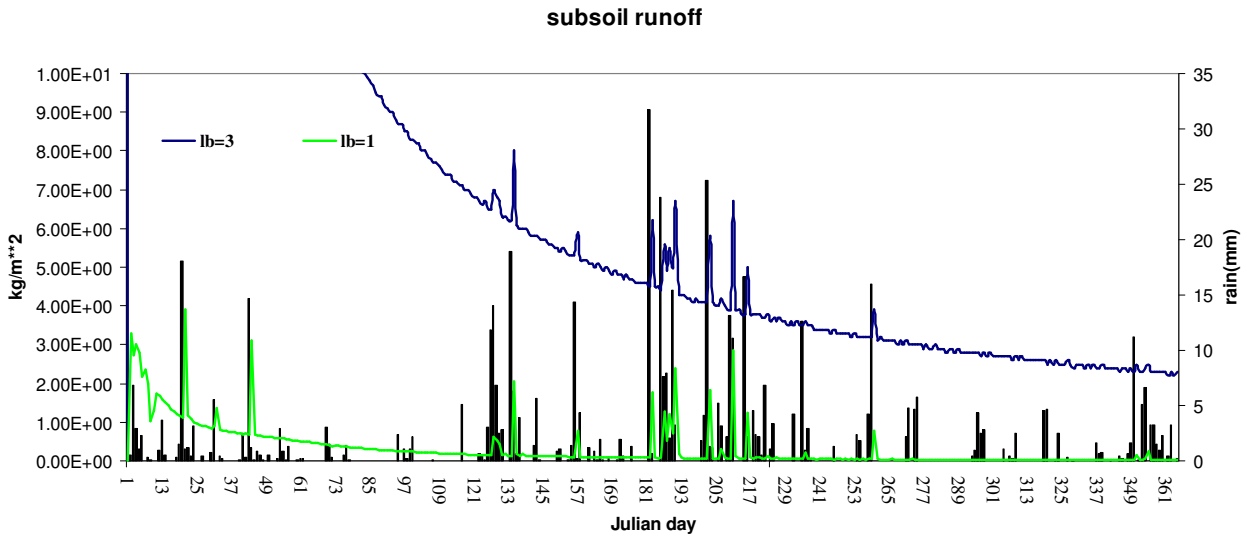

graph 39: the black bar represents the cumulated daily precipitations; the others bars are the subsoil runoff curves varying the lower boundary (green line for the unit gradient condition and blue for constant groundwater condition) –y-axis until 1kg/m^2

For subsoil runoff (**graph 38-39**), experimental lower boundary condition furnishes more higher values (about three order of magnitude); these values seem to be incorrect; furthermore after a peak in the first time, trend slopes down apart from rain history.
All other graphs aren't reported because the two curves are superimposed

1.3.4 Different numerical treatment of drainage

In TERRA-LM module, between two next layers water flux is expressed by Richards equation:

$$\frac{\partial(\eta)}{\partial t} = \frac{\partial}{\partial z}\left[D(\eta)\frac{\partial \eta}{\partial z} + k(\eta) \right] = \frac{\partial F}{\partial z} \qquad \textbf{eq. 6}$$

Permability $k(\eta)$ and hydraulic diffusivity $D(\eta)$ are expressed using *Rijtema (1969)* formulation:

$$D(\eta) = D_o e^{\frac{D_1(n-\eta_{m,l})}{n-\eta_{adp}}} \qquad \textbf{eq. 7}$$

$$k(\eta) = k_o e^{\frac{k_1(n-\eta_{m,l})}{n-\eta_{adp}}} \qquad \textbf{eq. 8}^{6}$$

the term $\eta_{m,l}$ is calculated implementing an arithmetic mean between water content of two next layers; in TERRA-LM stand alone-version is introducted an experimental value for $\eta_{m,l}$: if there is a water flux from n layer to n+1 layer, it is used , as $\eta_{m,l}$, only the water content of n+1 layer and vice versa.Implementing this variation in the simulations, for this case-study, any variation is noted.

[6] k_0, k_1, D_0, D_1 constants (see Table 1)
n volume of voids (see Table 1)

Remarks

- The stand-alone version 1D of TERRA-LM proved to be an useful tool to test the "soil module"; forcing the SVAT model via monitored atmospheric conditions, error sources are reduced.
- Calculation time are very short; in this way, it is possible to calculate a large number of sensitivity runs.
- Often the modifications have small impacts on water content and soil temperature trends.
- Some terms of hydric balance, like subsoil runoff and surface runoff, need to be verified on other case-histories.
- Because of long spin-off time, it should be better to simulate a very long time to reduce spin-off effects.
- It is not possible to verify the outputs due to lack of experimental data for the soil.
- The simulation of thermal processes shows very little sensitivity to variations of soil properties, boundary condition or evaporation models.
- It is not clear how, varying the parameterization of some processes, are induced variations on trends of other terms which are not linked to these processes (e.g. variations of runoff trends induced by different evaporation models).
- It should be very useful to carry out some tests on South Italy or Mediterranean area to understand how the model behaviour varies.
- It should be very useful to compare the outputs of other SVAT models using the same input data.

Appendix A

Falkenberg case study

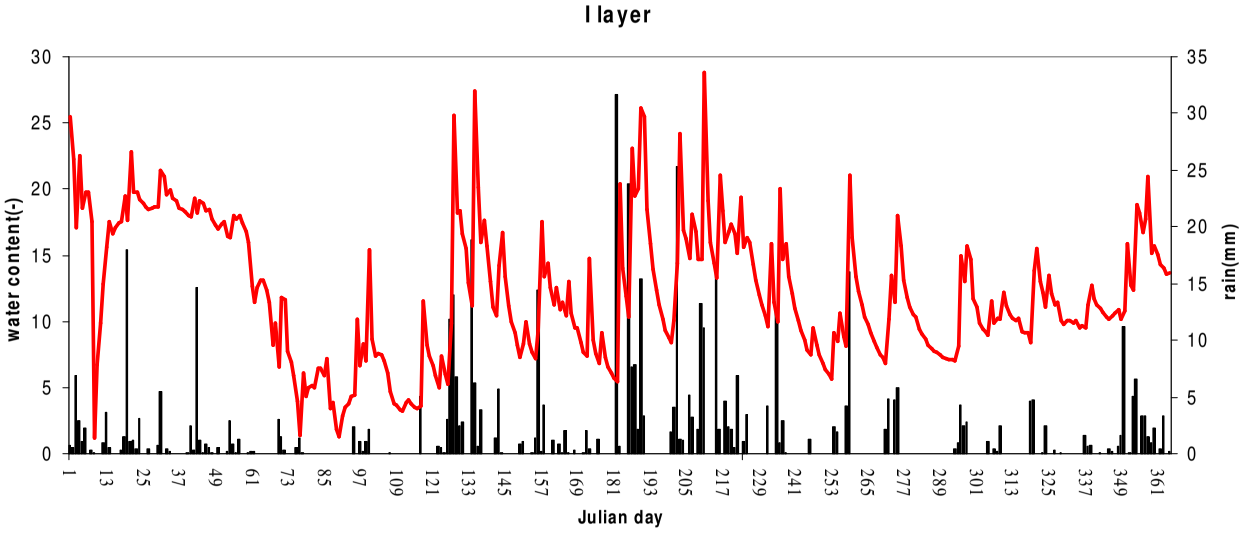

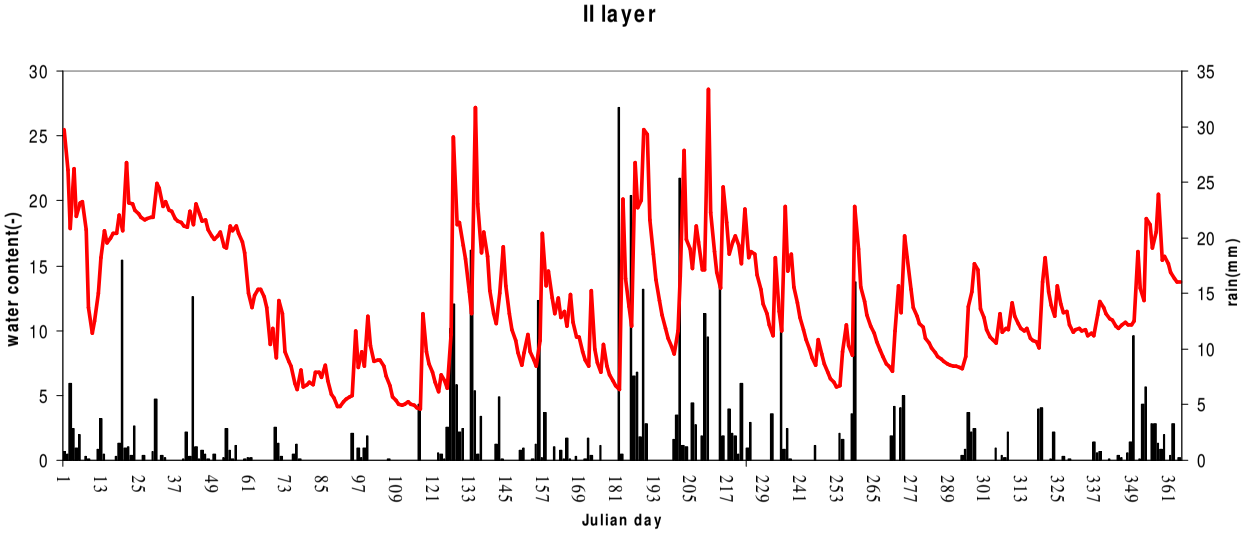

III layer

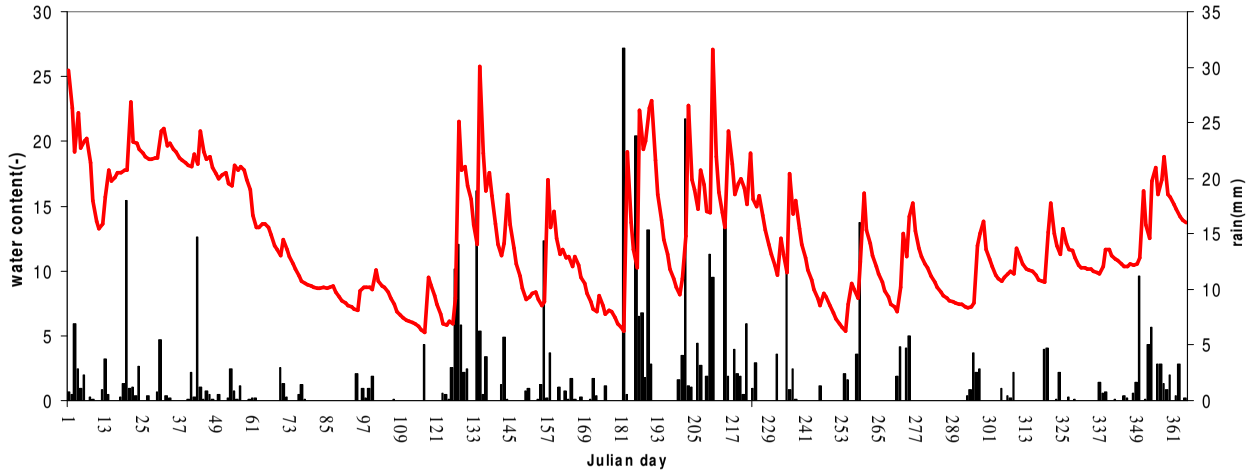

IV layer

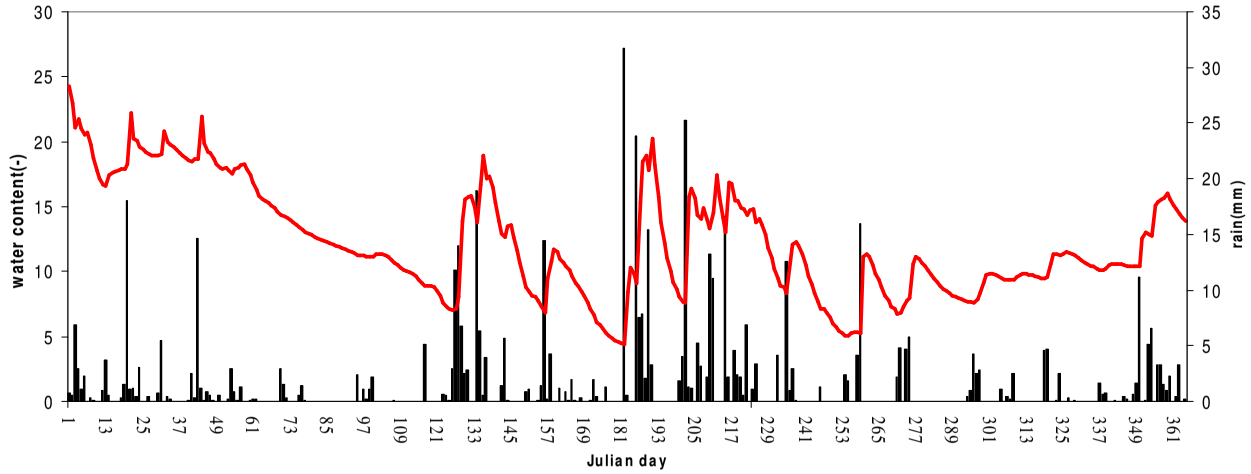

V layer

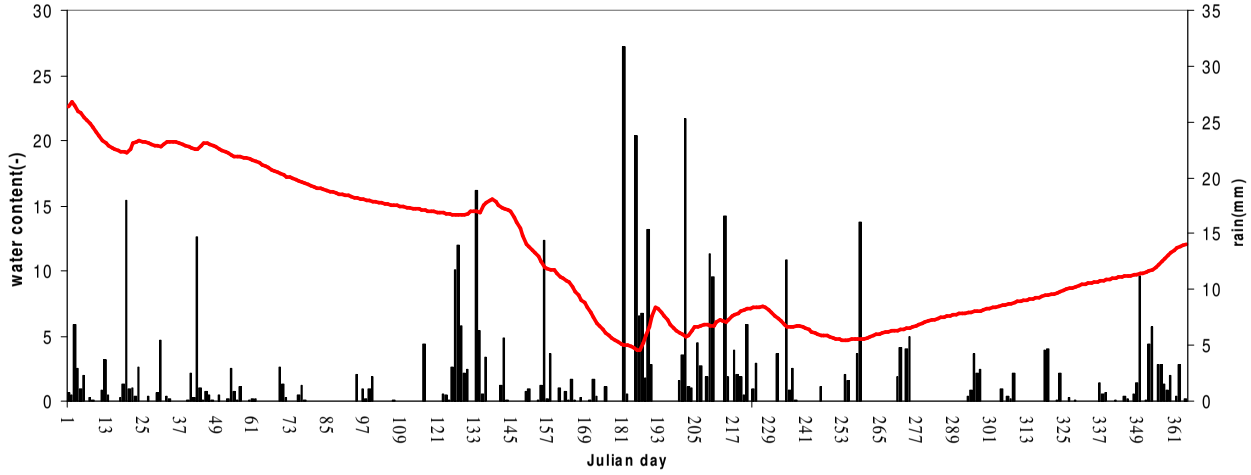

VI layer

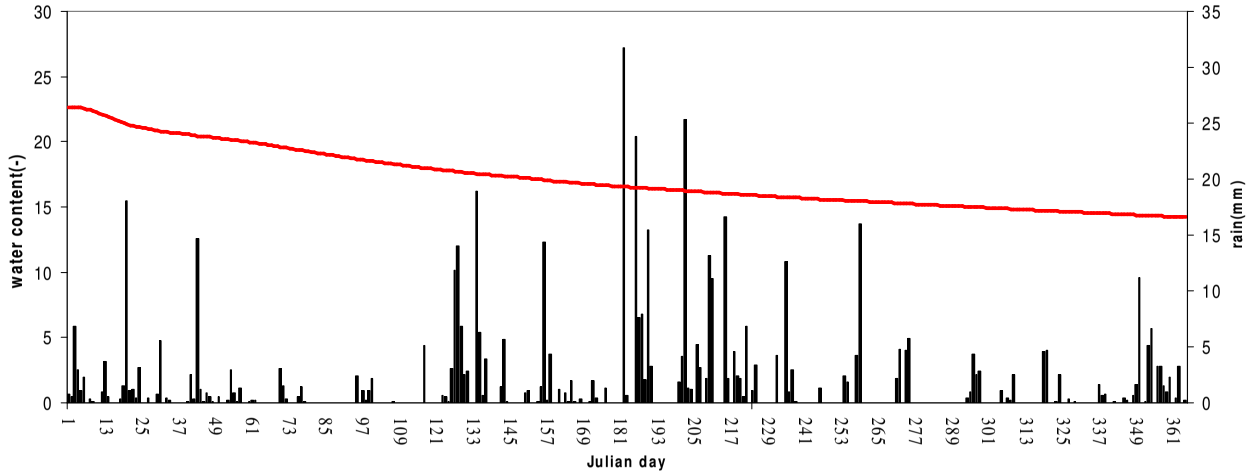

VII layer

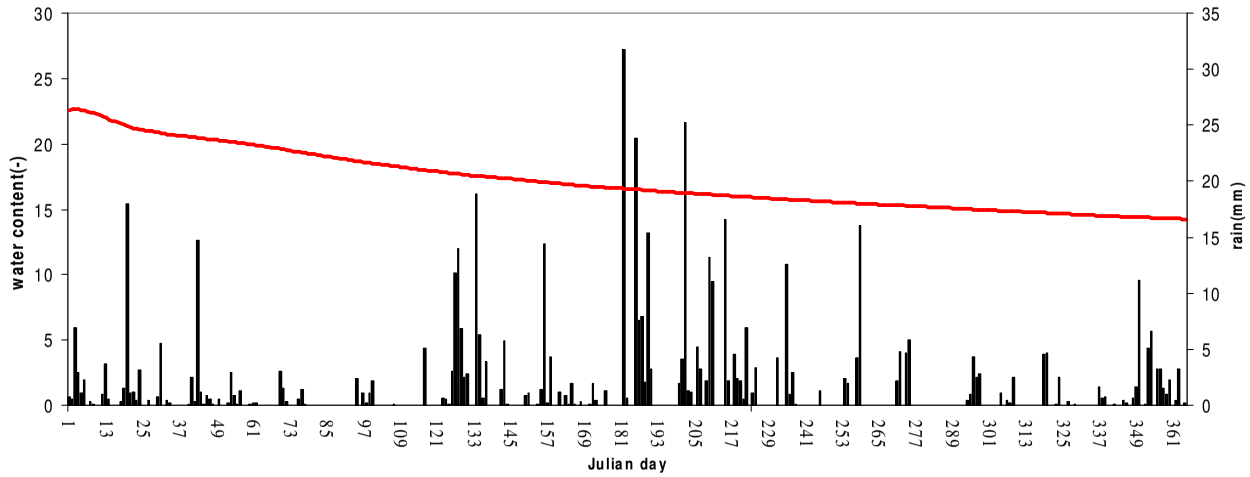

.

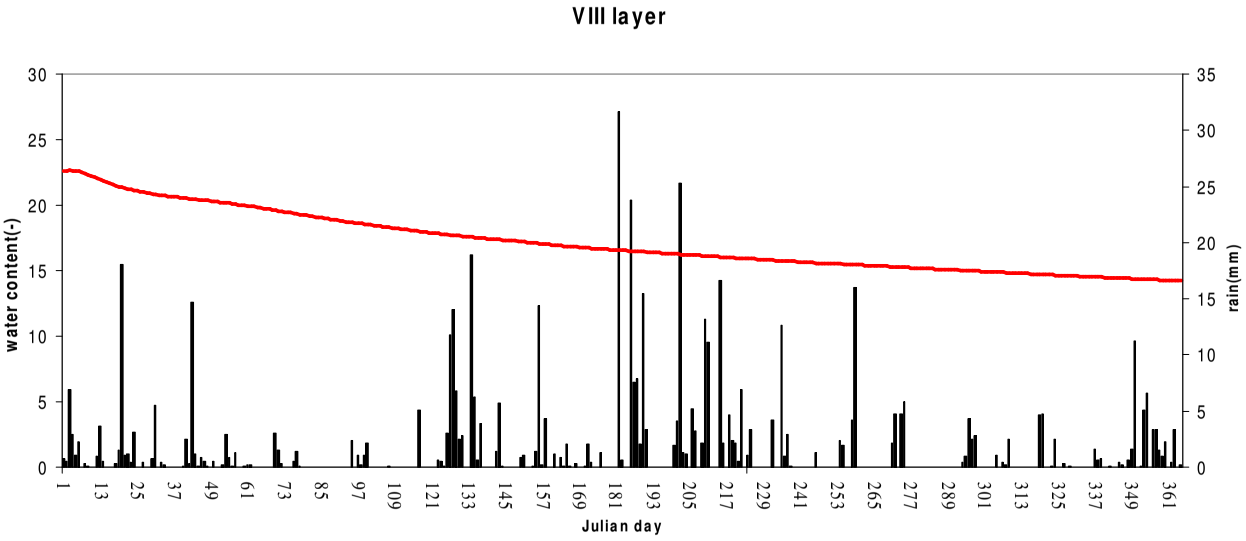
VIII layer
water content(-)
rain(mm)
Julian day
0
5
10
15
20
25
30
35
1
13
25
37
49
61
73
85
97
109
121
133
145
157
169
181
193
205
217
229
241
253
265
277
289
301
313
325
337
349
361

.

- **Soil temperature:**

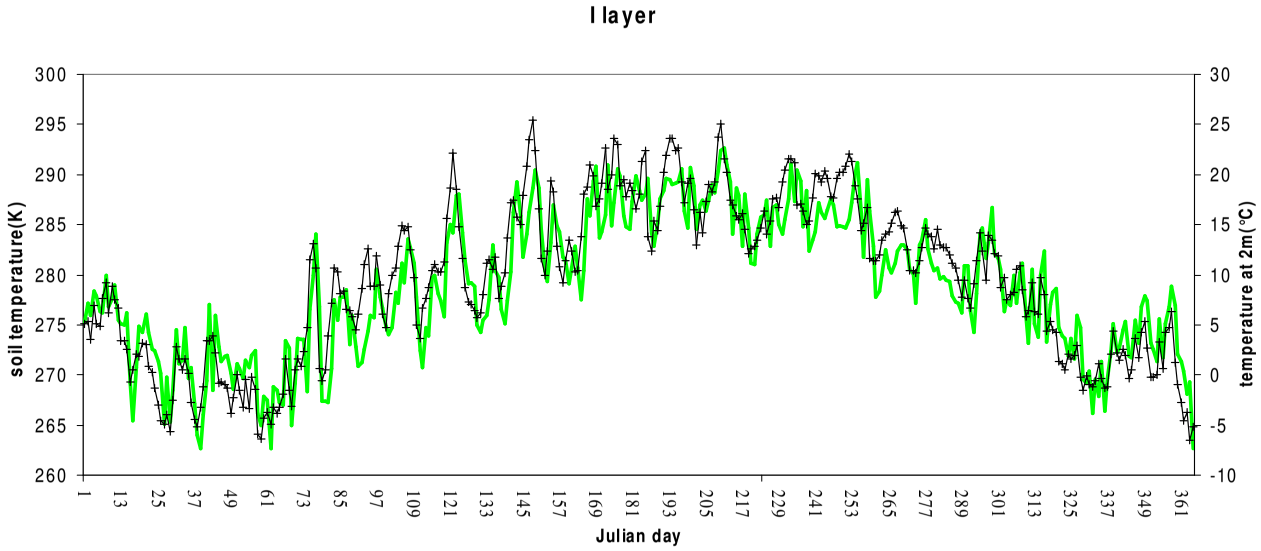

.

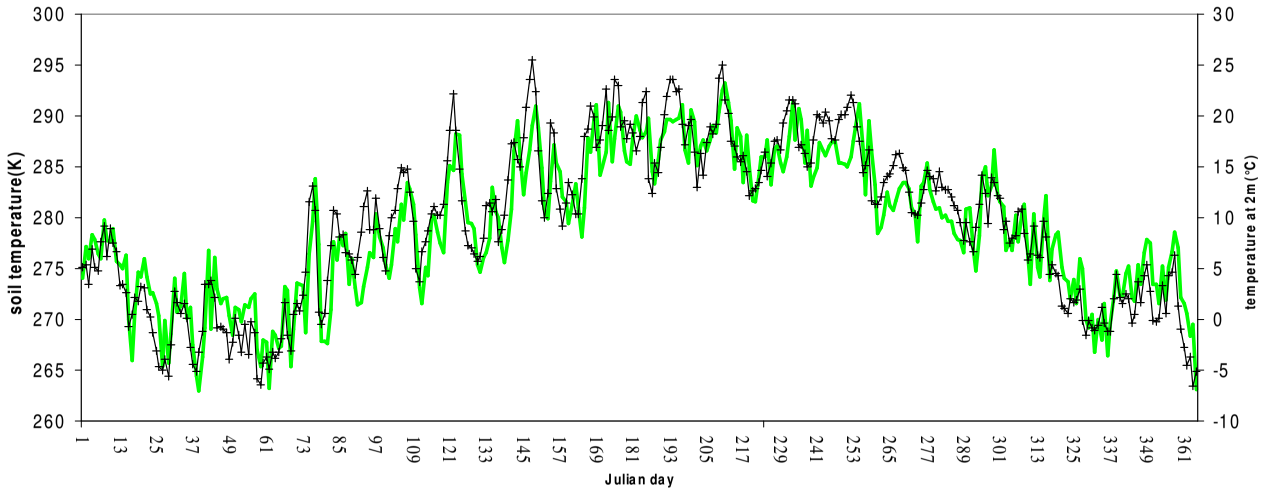

.

III layer

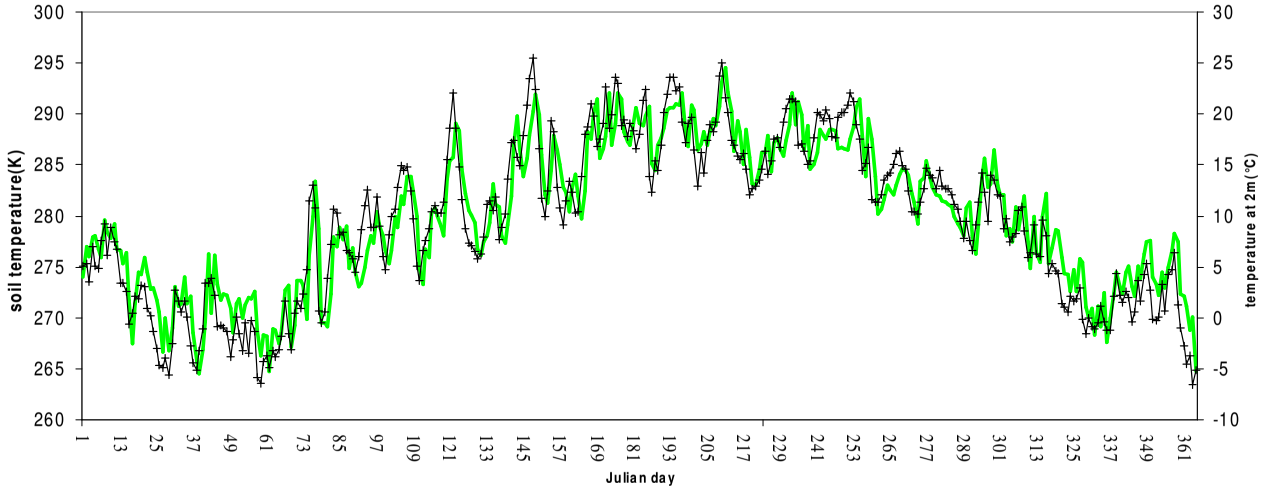

.

IV layer

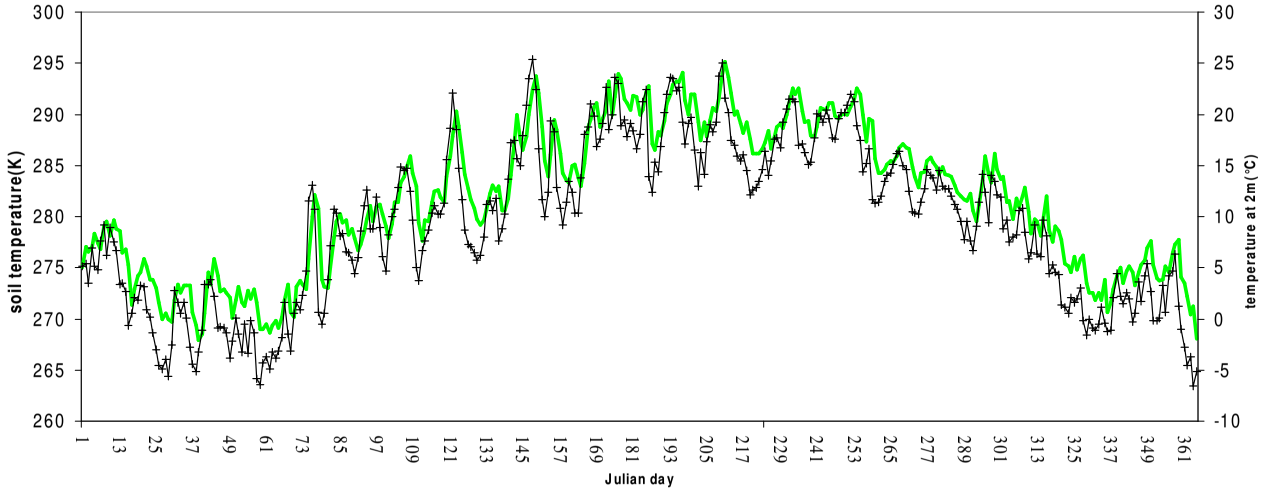

.

V layer

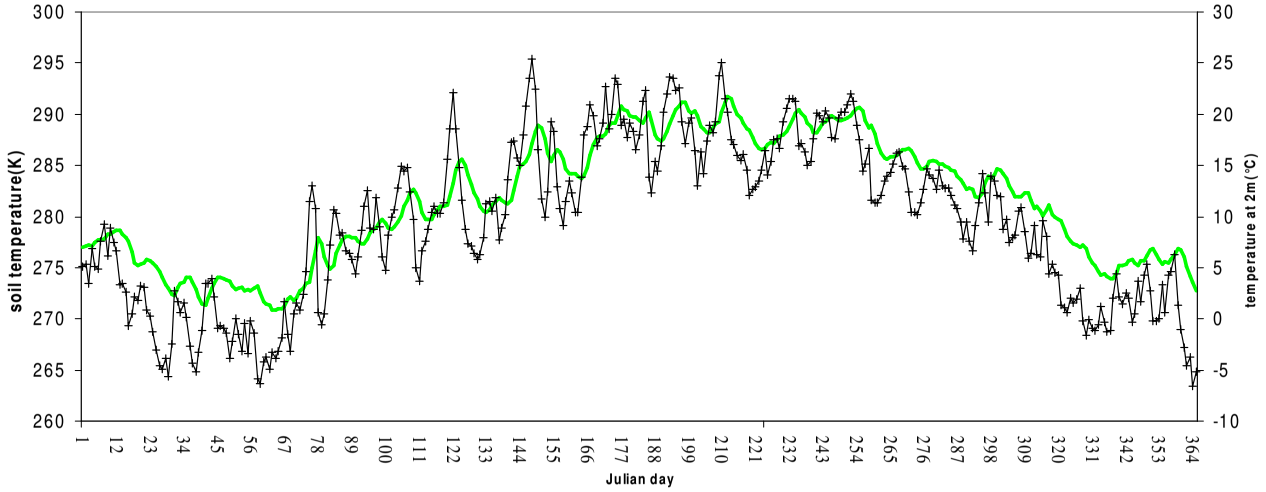

.

VI layer

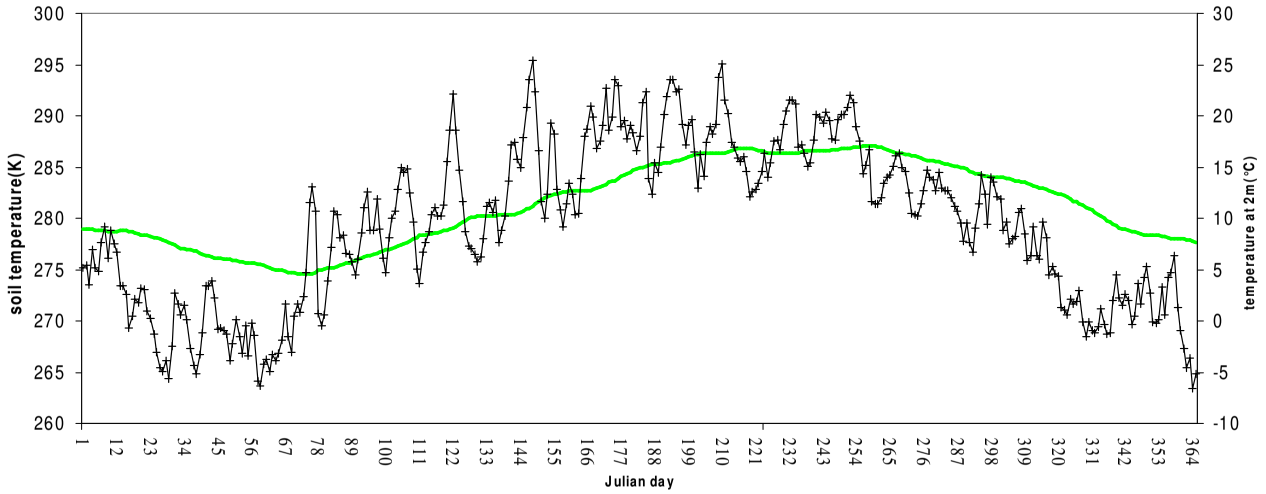

.

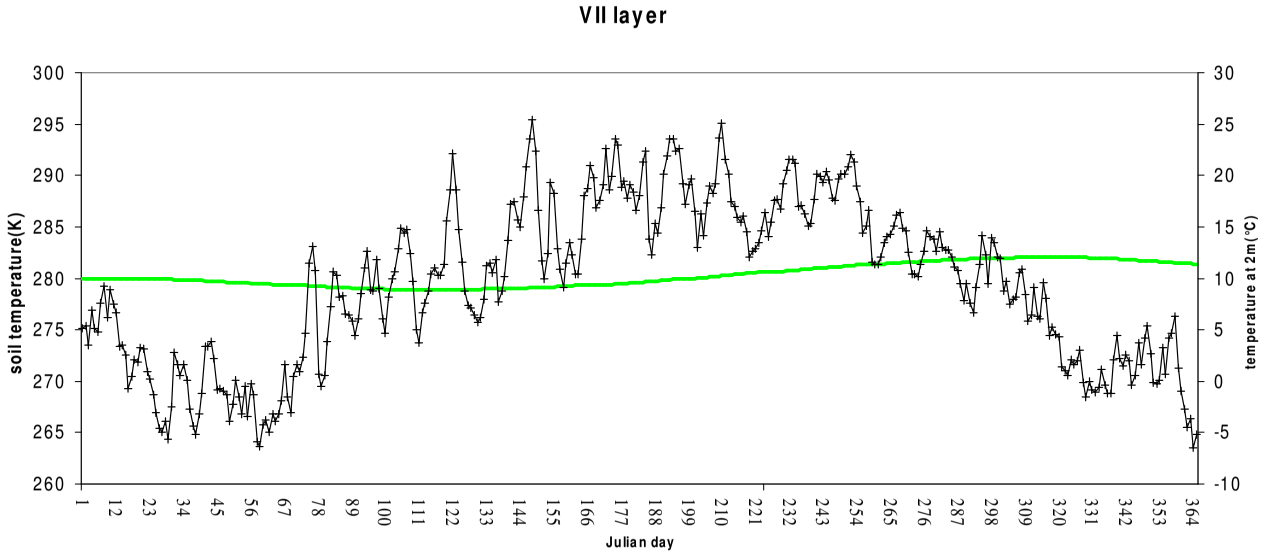

.

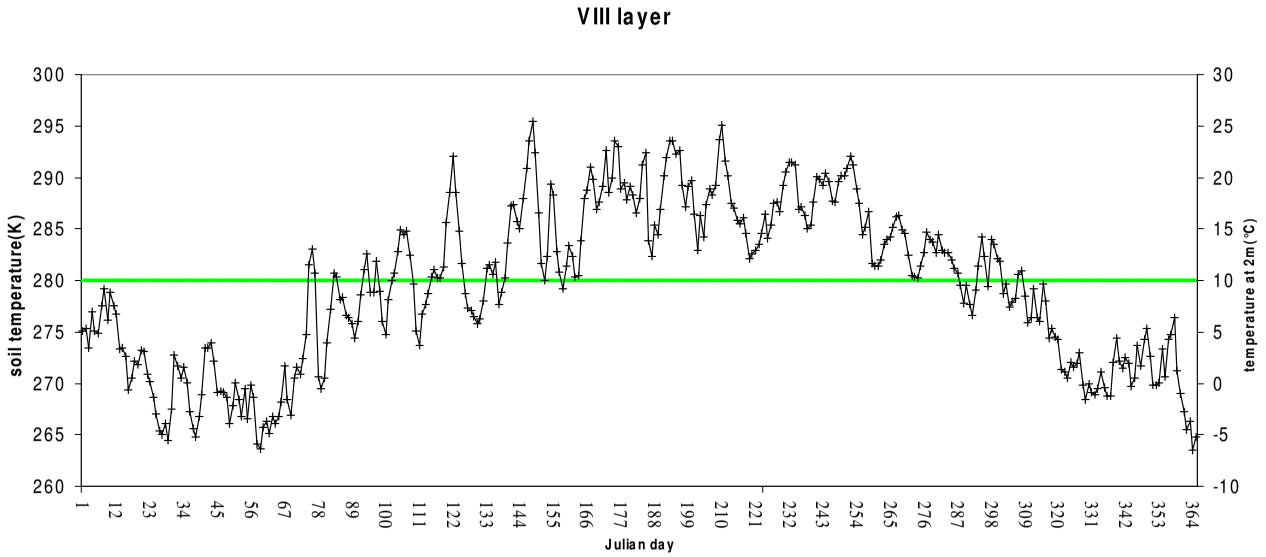

.

- **Other values:**

latent heat

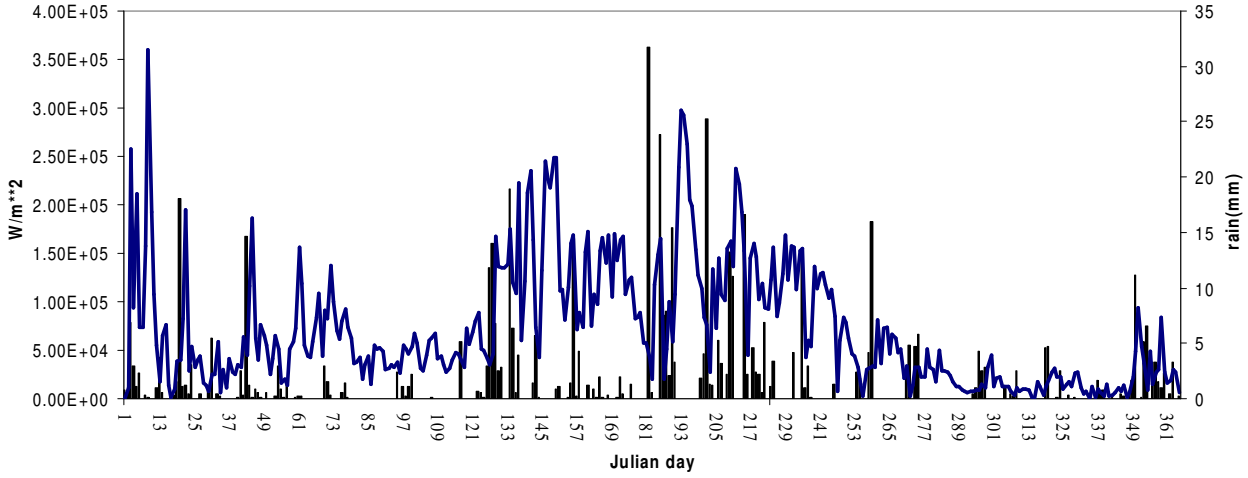

sensible heat

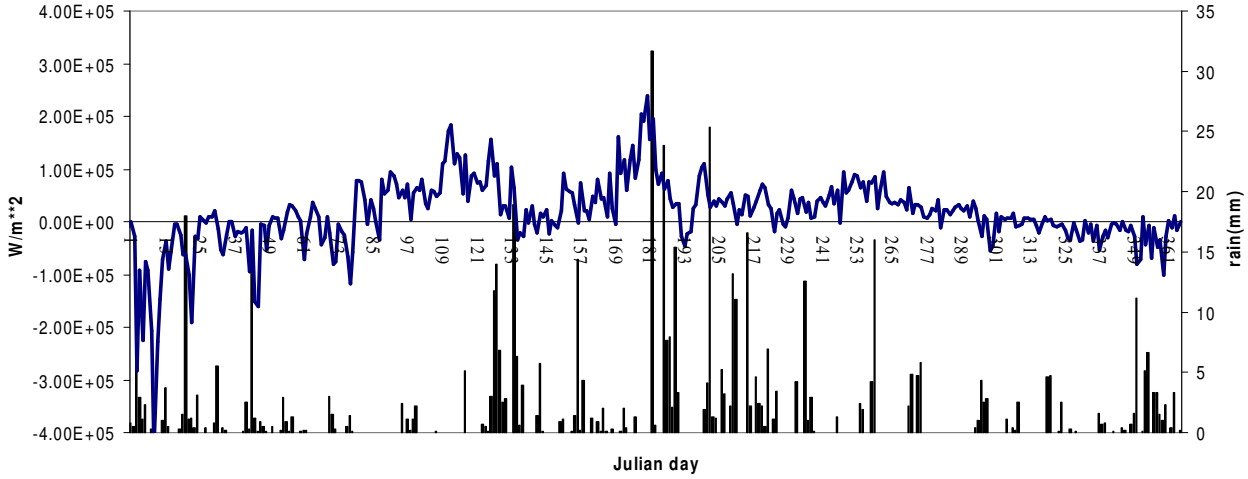

solar radiation

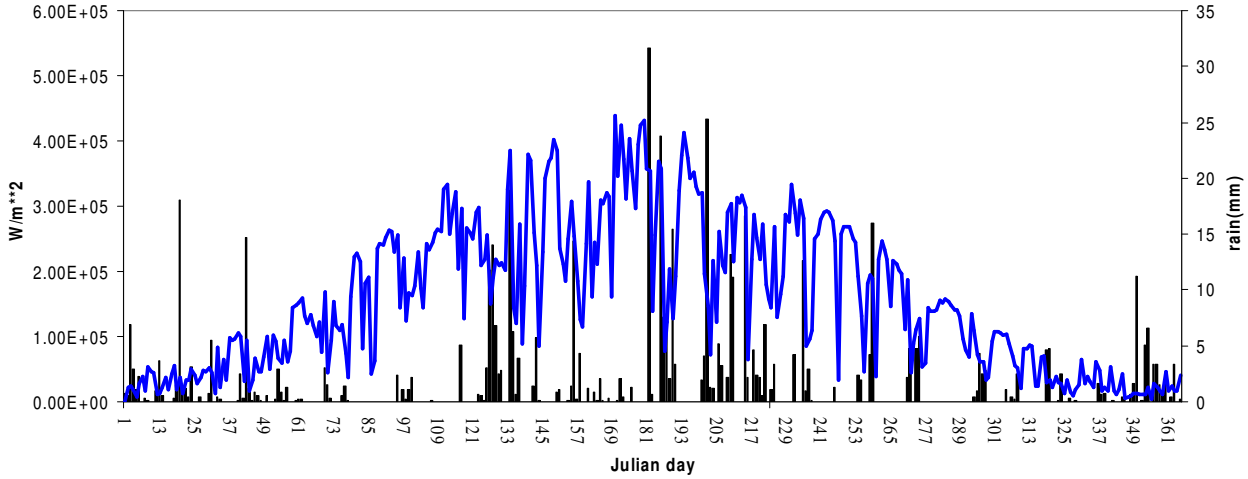

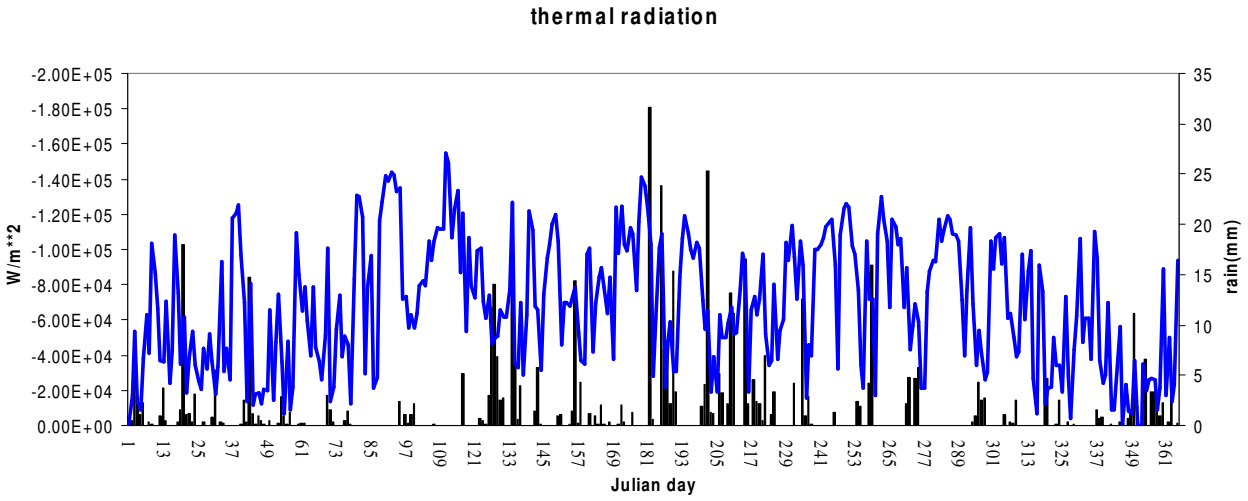
thermal radiation
W/m**2
rain(mm)
Julian day

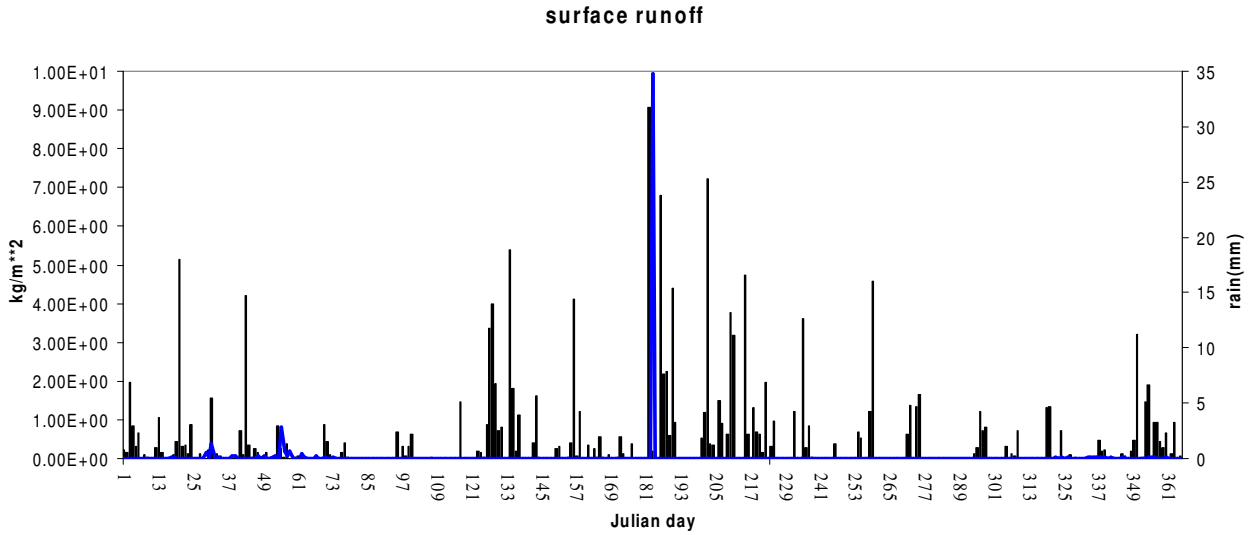
surface runoff
kg/m**2
rain(mm)
Julian day

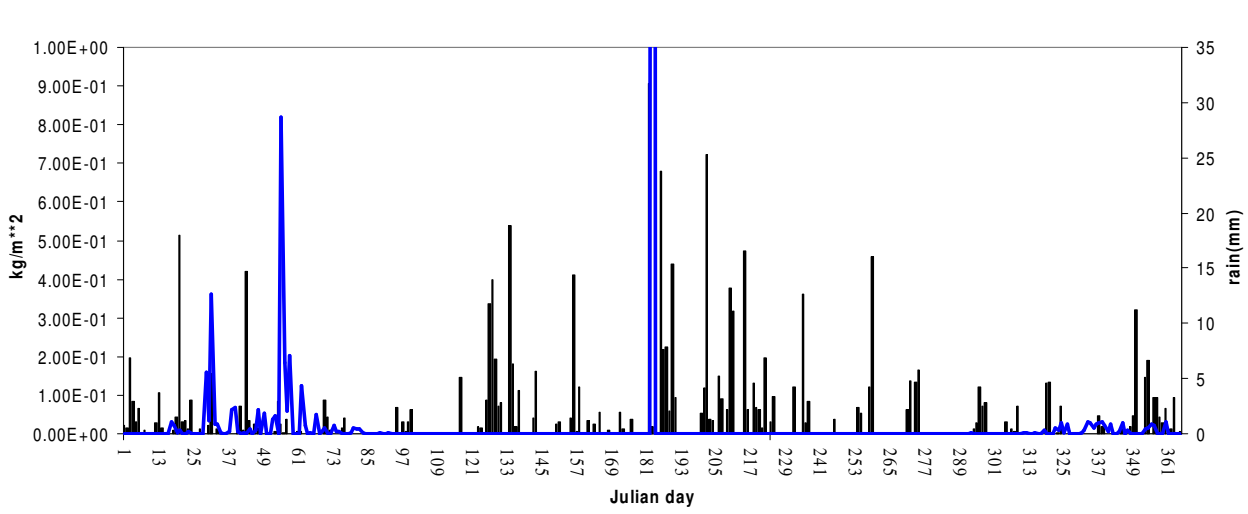
surface runoff
kg/m**2
rain(mm)
Julian day

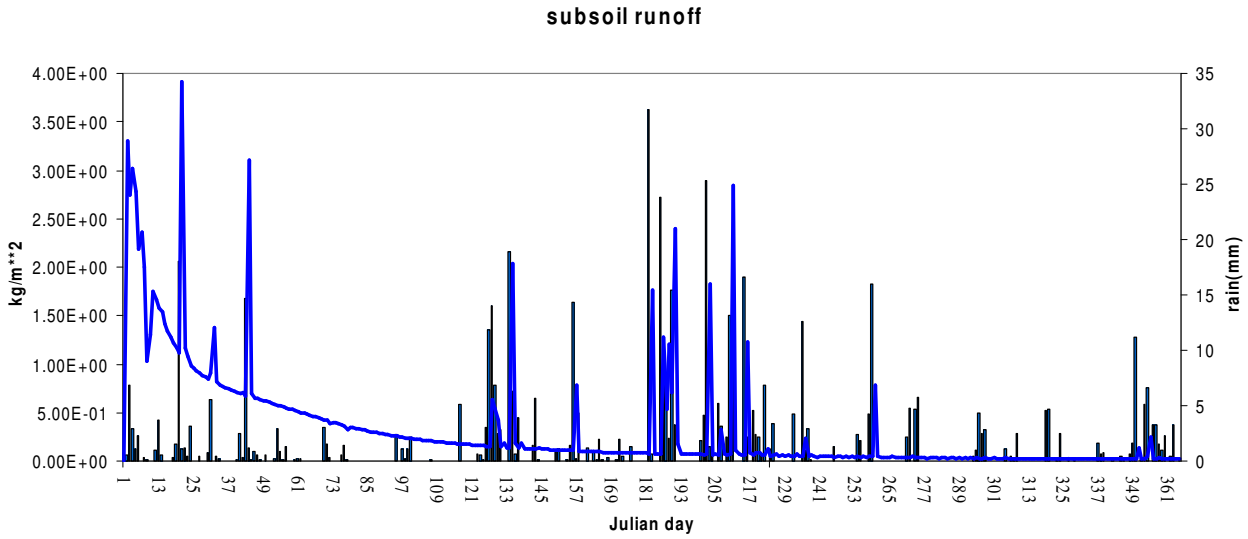
subsoil runoff
kg/m**2
rain(mm)
Julian day
4.00E+00
3.50E+00
3.00E+00
2.50E+00
2.00E+00
1.50E+00
1.00E+00
5.00E-01
0.00E+00
35
30
25
20
15
10
5
0
1
13
25
37
49
61
73
85
97
109
121
133
145
157
169
181
193
205
217
229
241
253
265
277
289
301
313
325
337
349
361

.

Different soil types

I layer

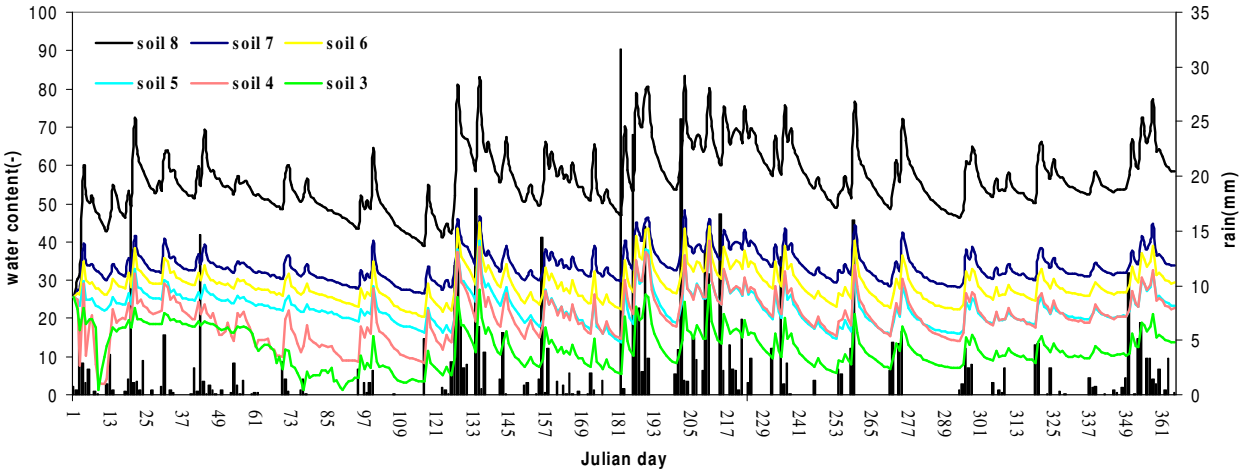

II layer

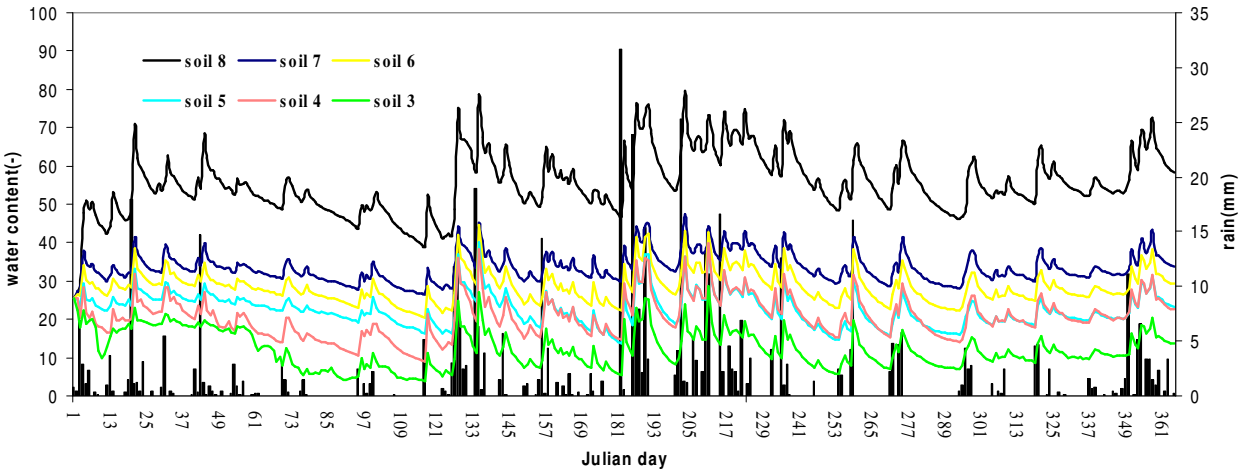

III layer

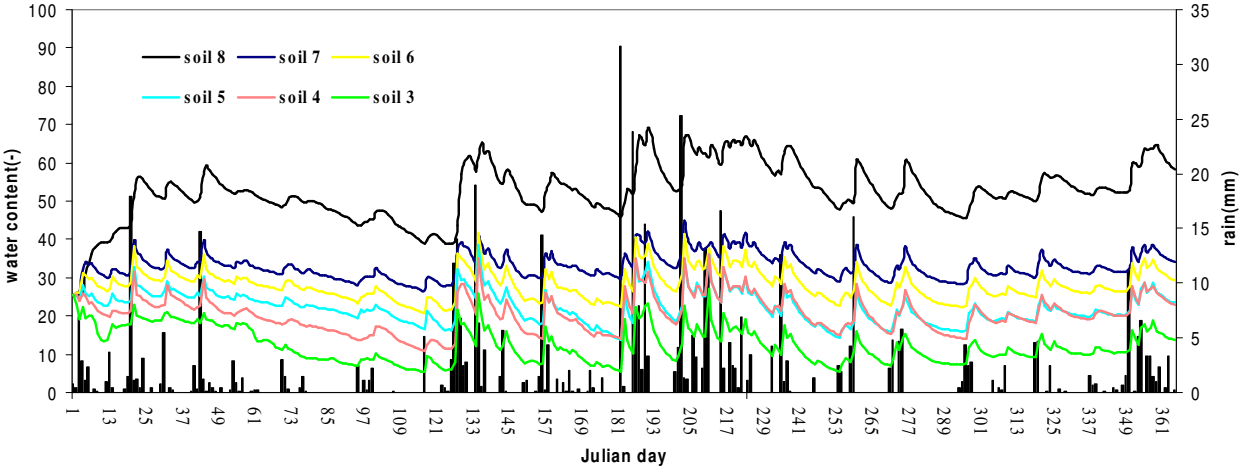

IV layer

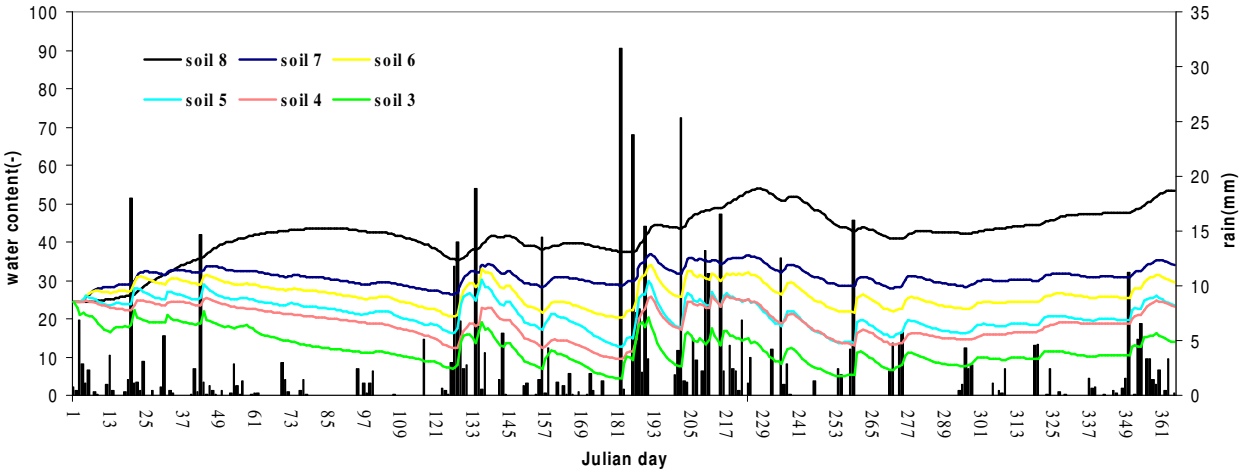

V layer

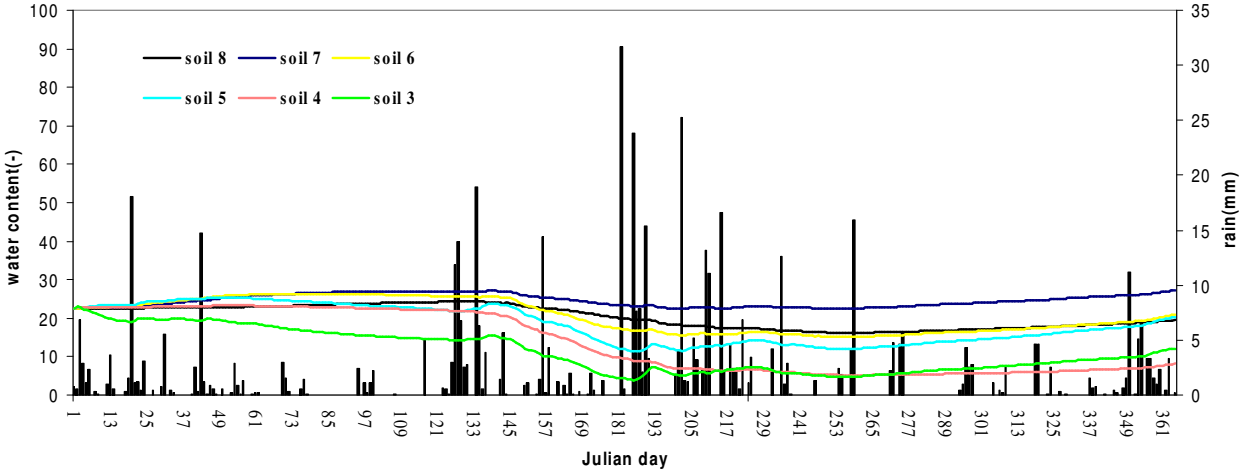

VI layer

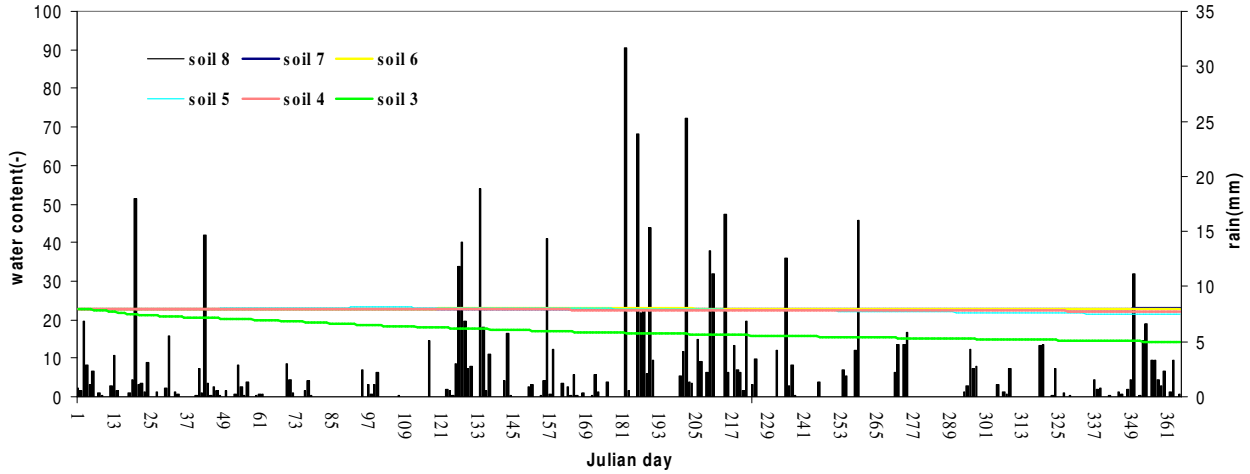

VII layer

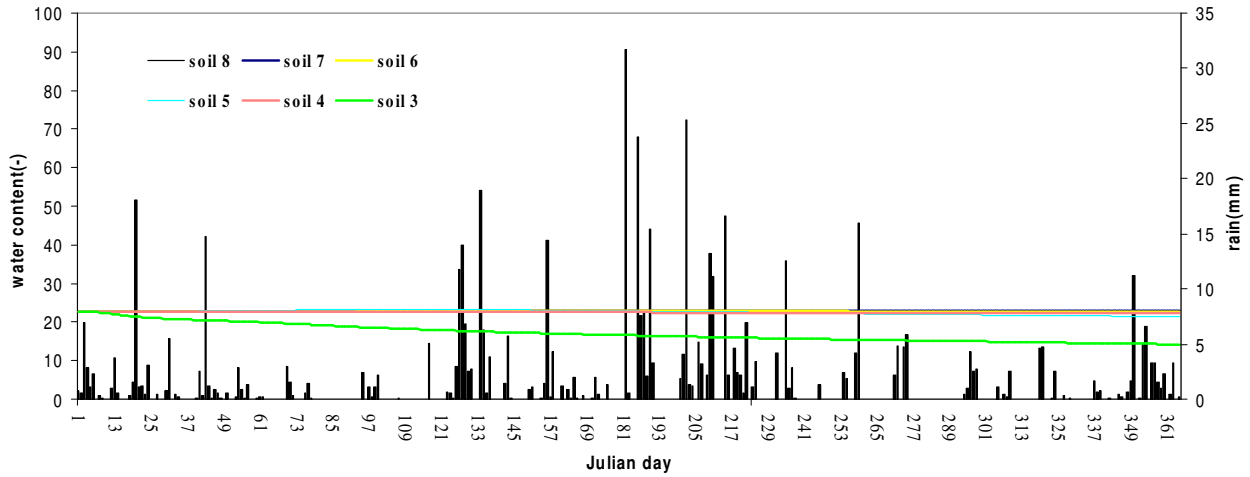

VIII layer

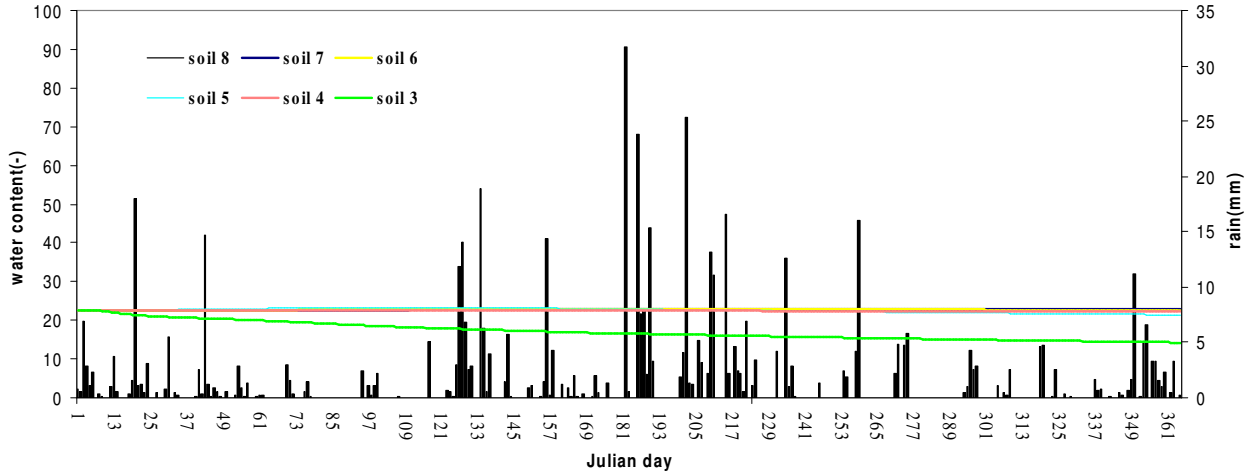

I layer

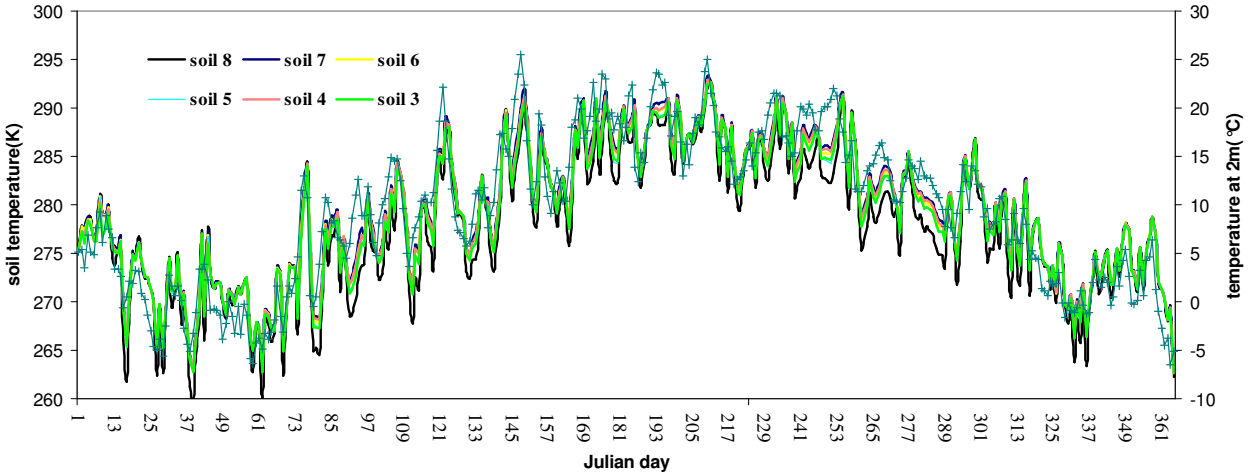

II layer

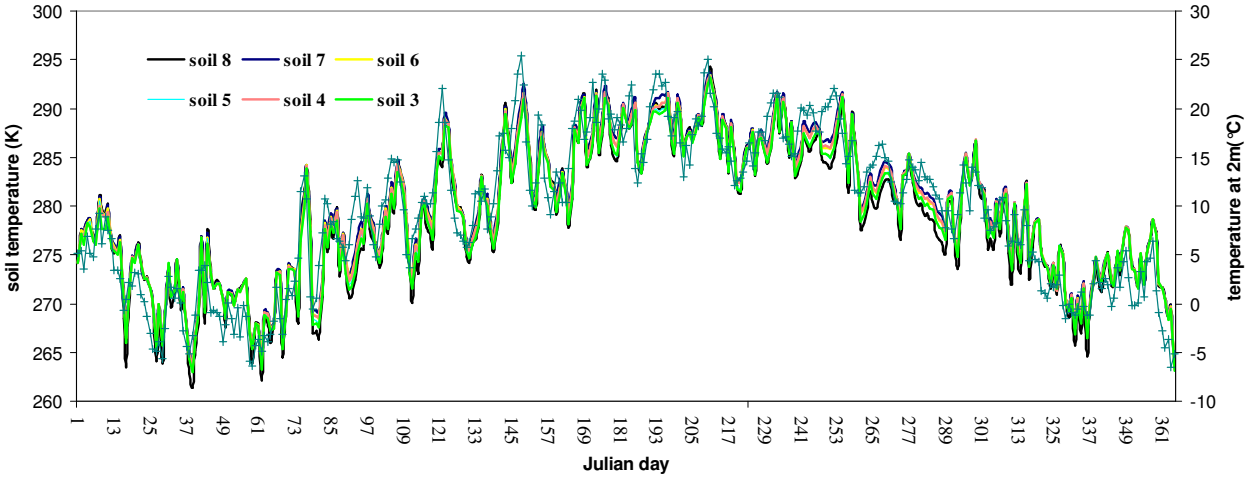

III layer

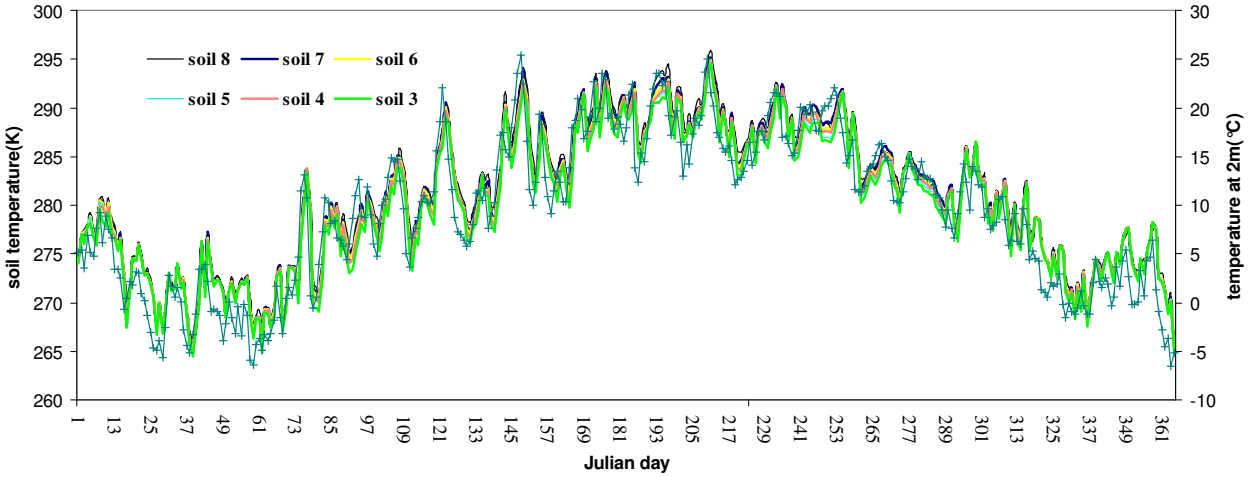

IV layer

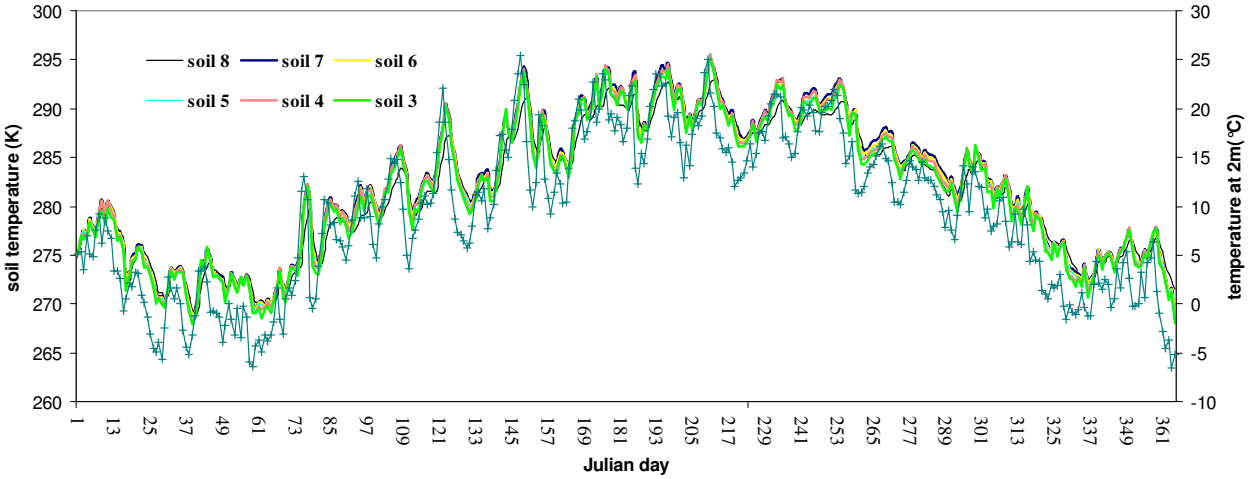

V layer

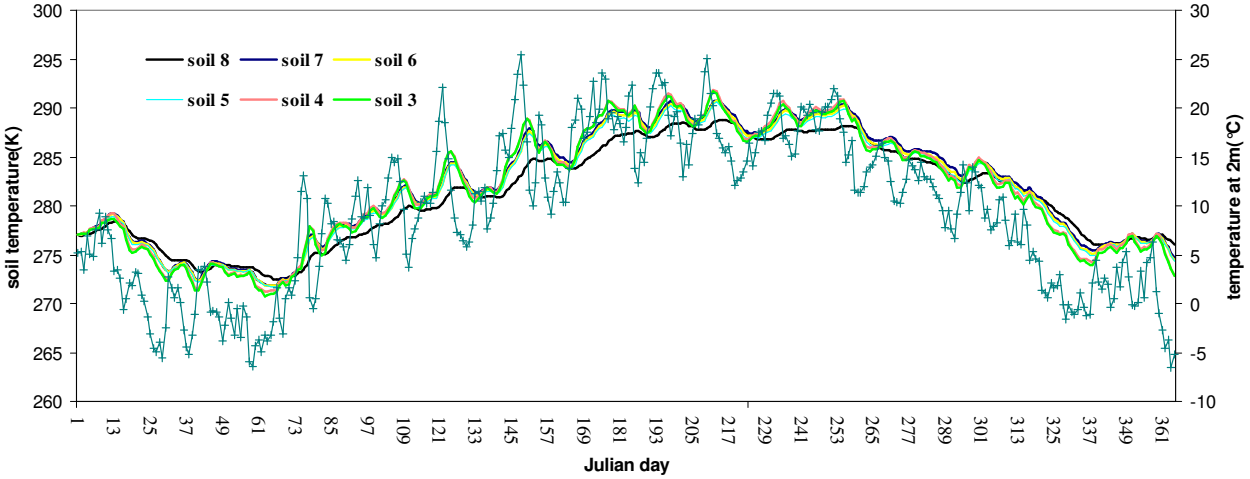

VI layer

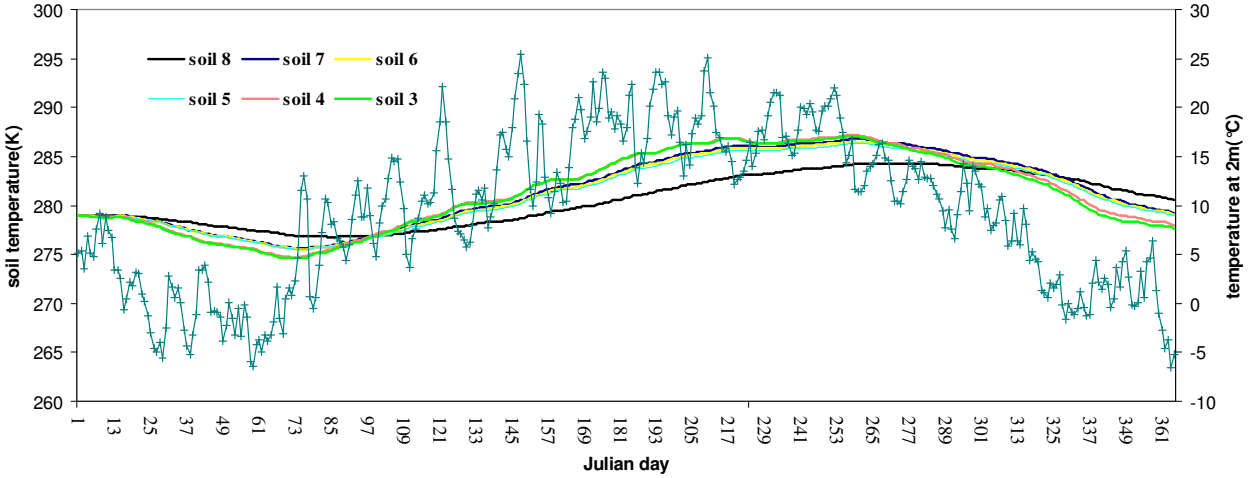

VII layer

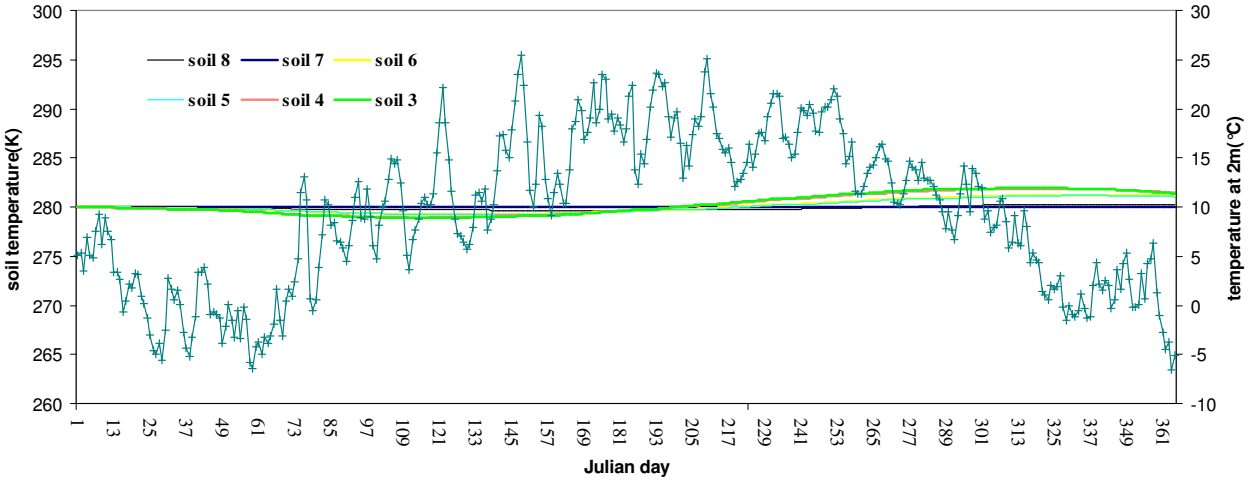

VIII layer

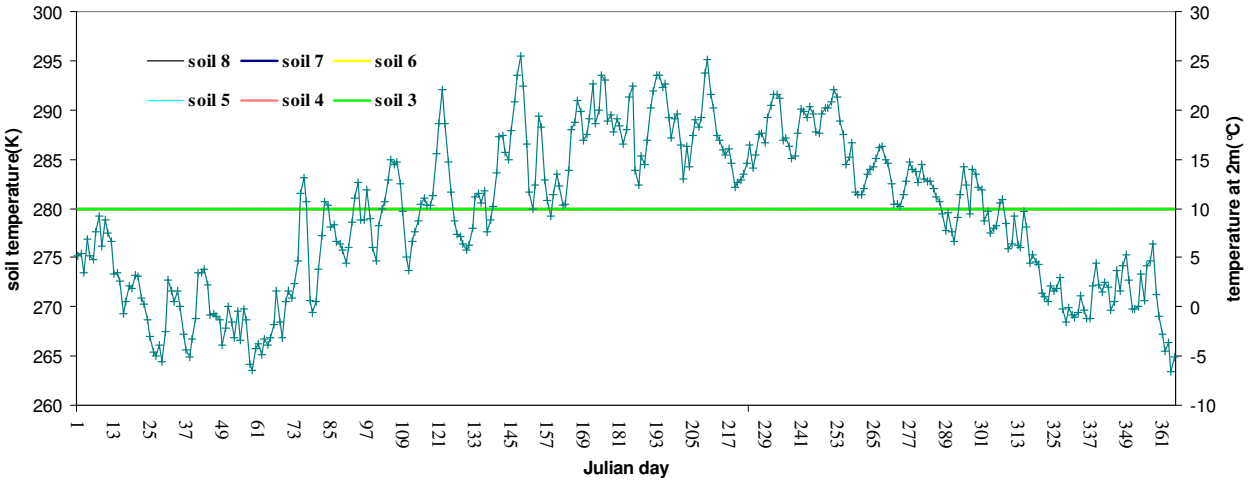

latent heat

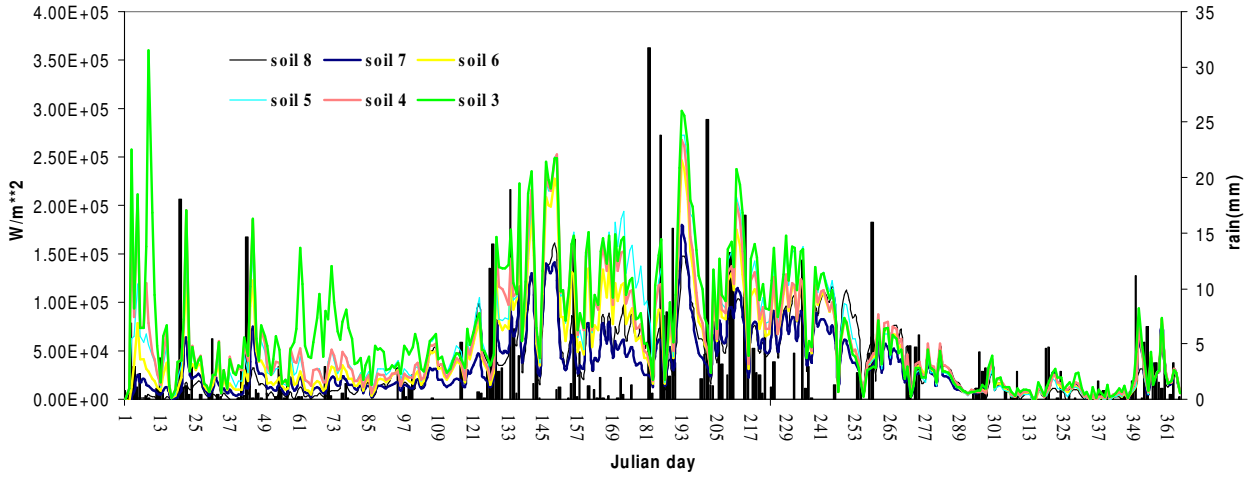

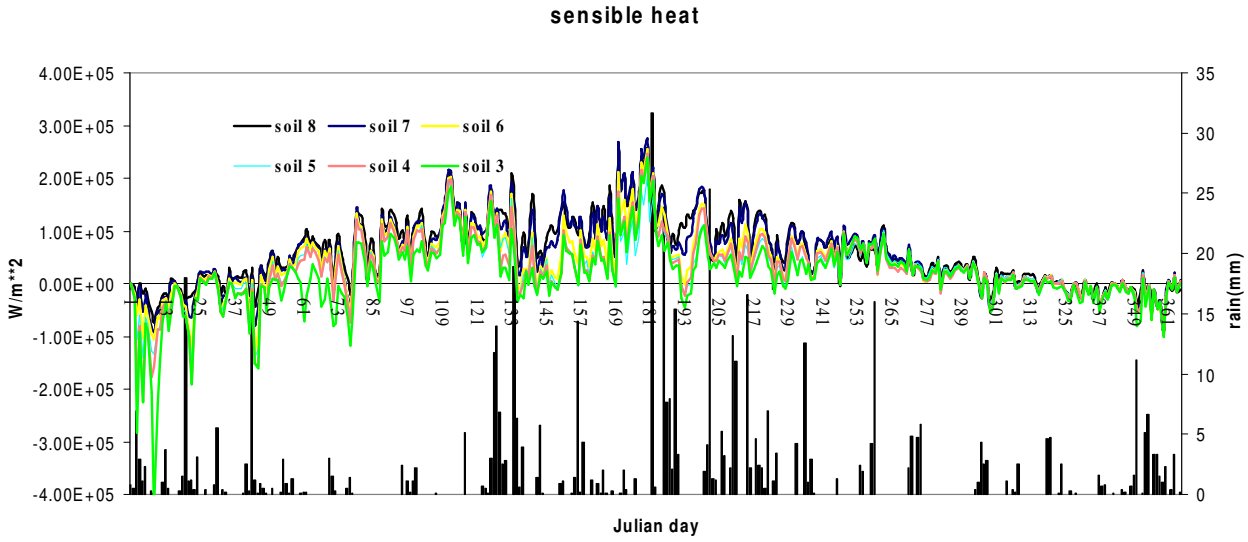
sensible heat
soil 8
soil 7
soil 6
soil 5
soil 4
soil 3
W/m**2
rain(mm)
Julian day

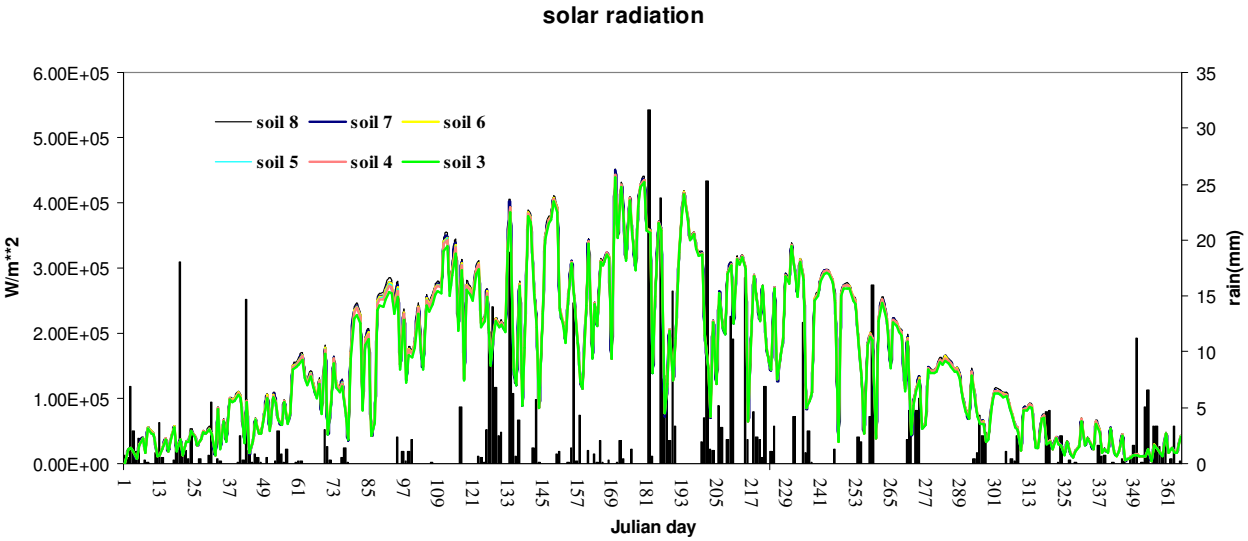
solar radiation
soil 8
soil 7
soil 6
soil 5
soil 4
soil 3
W/m**2
rain(mm)
Julian day

thermal radiation

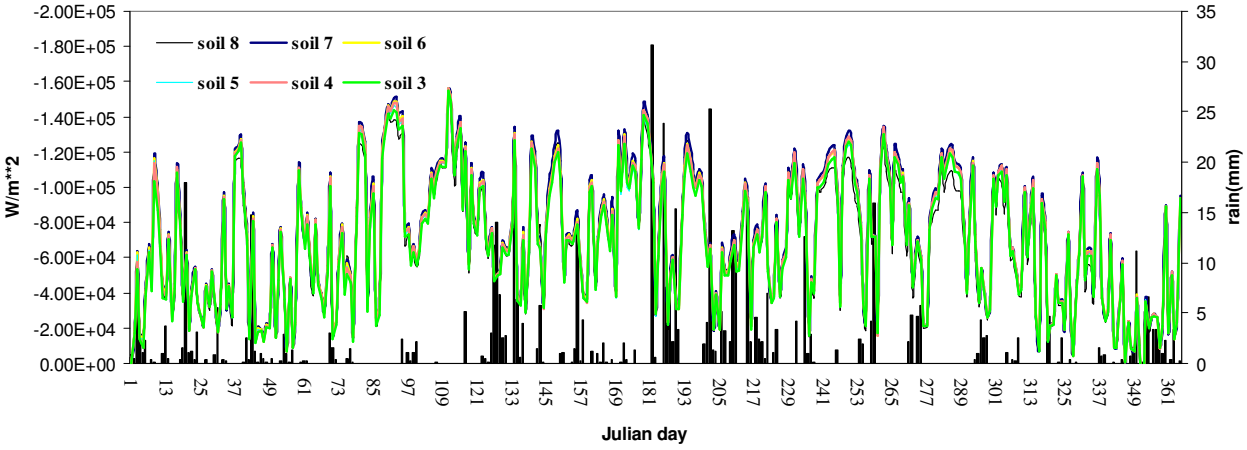

surface runoff

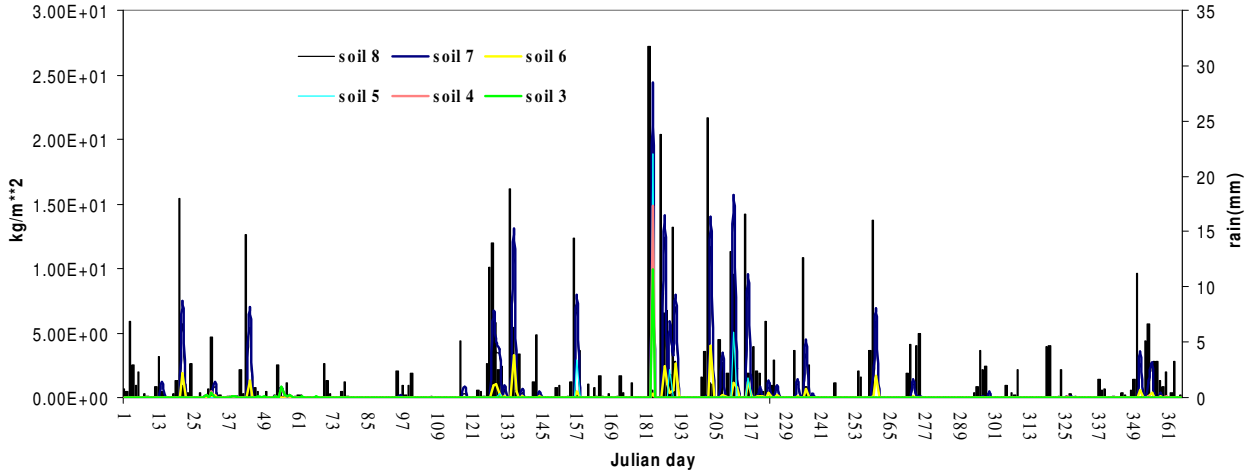

subsoil runoff

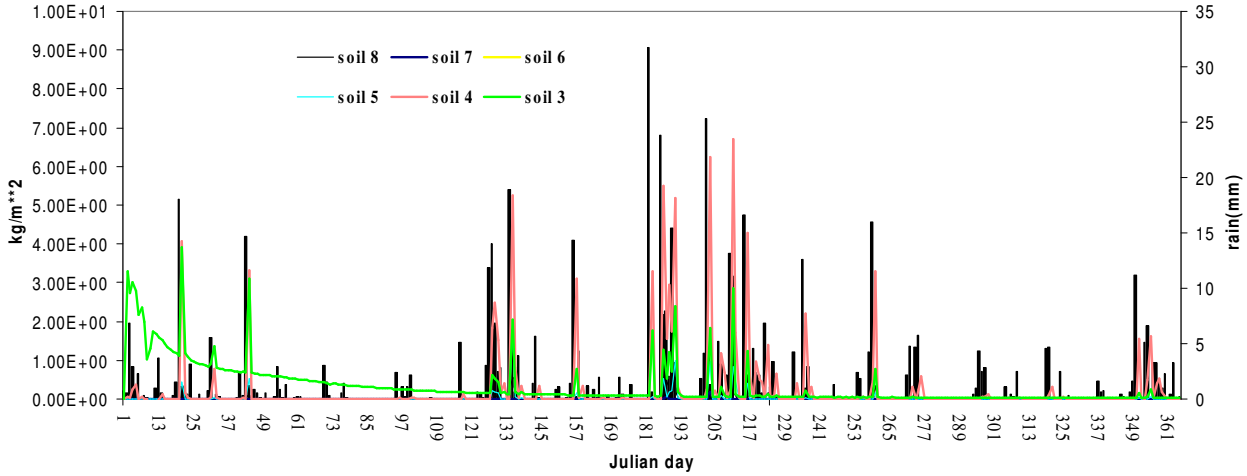

Type of bare soil evaporation models

I layer

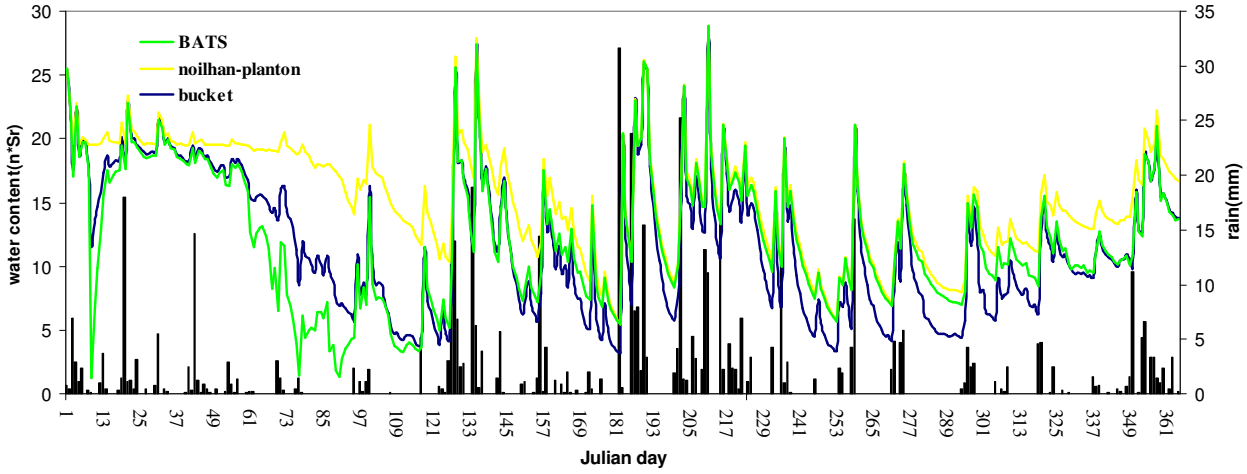

II layer

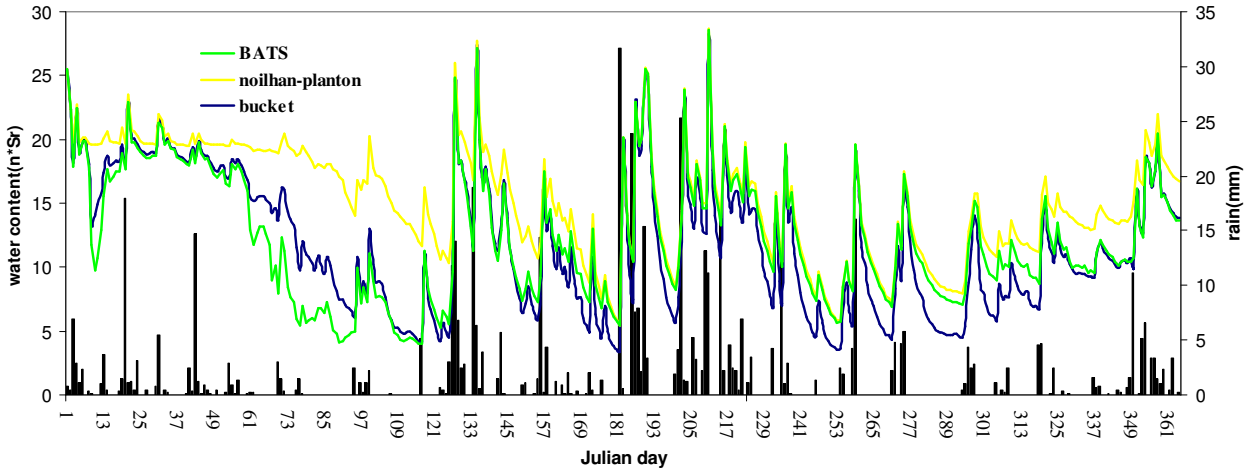

III layer

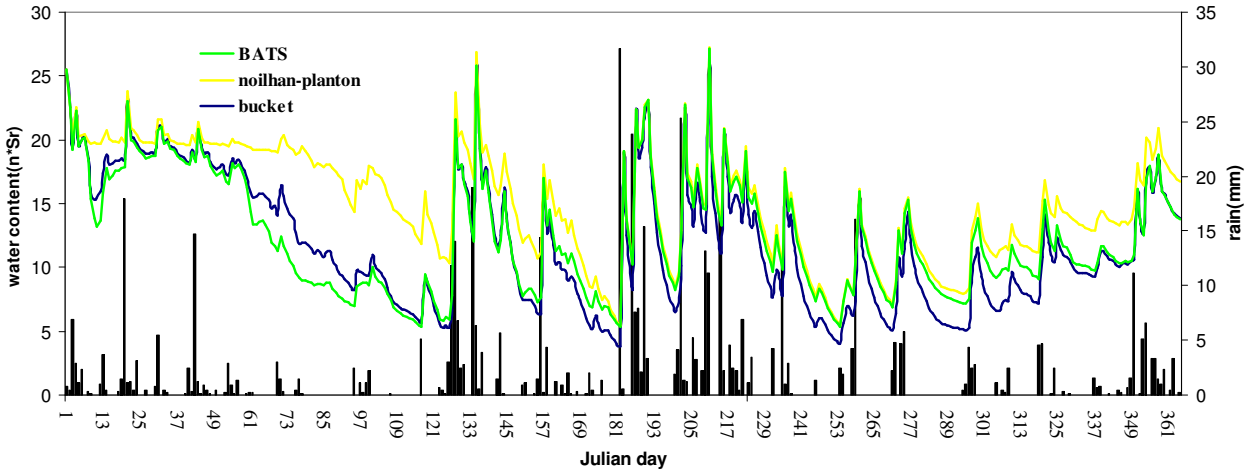

IV layer

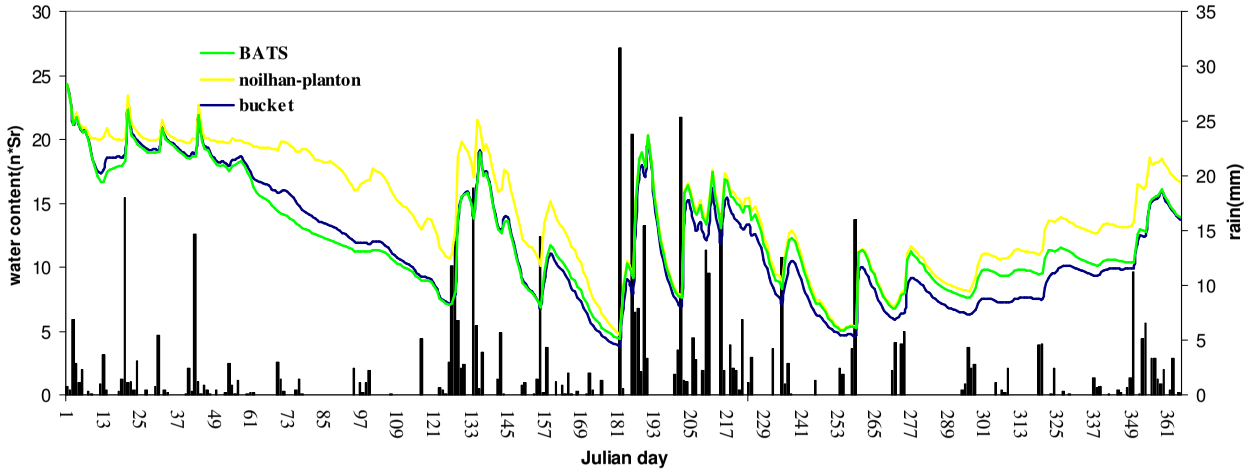

V layer

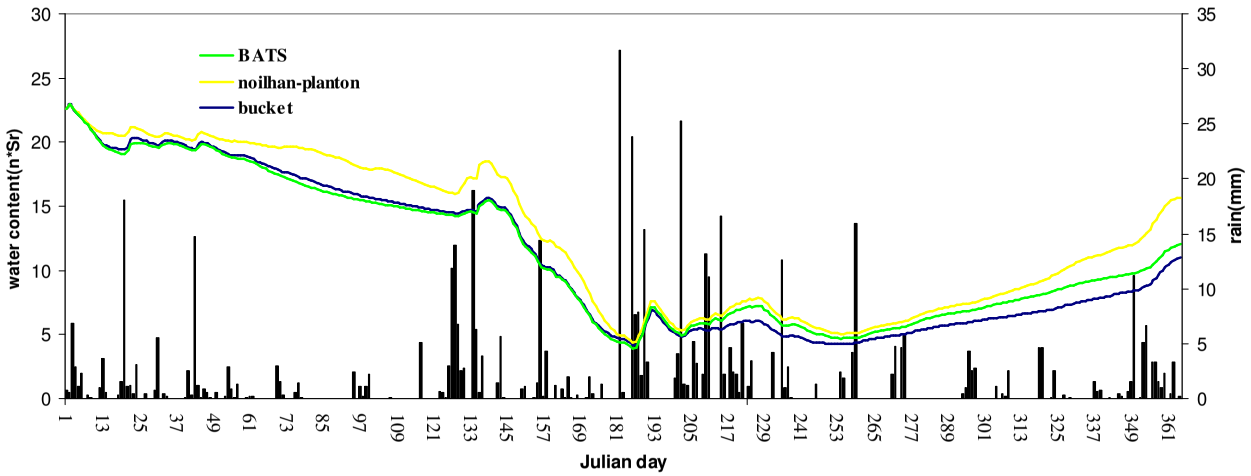

VI layer

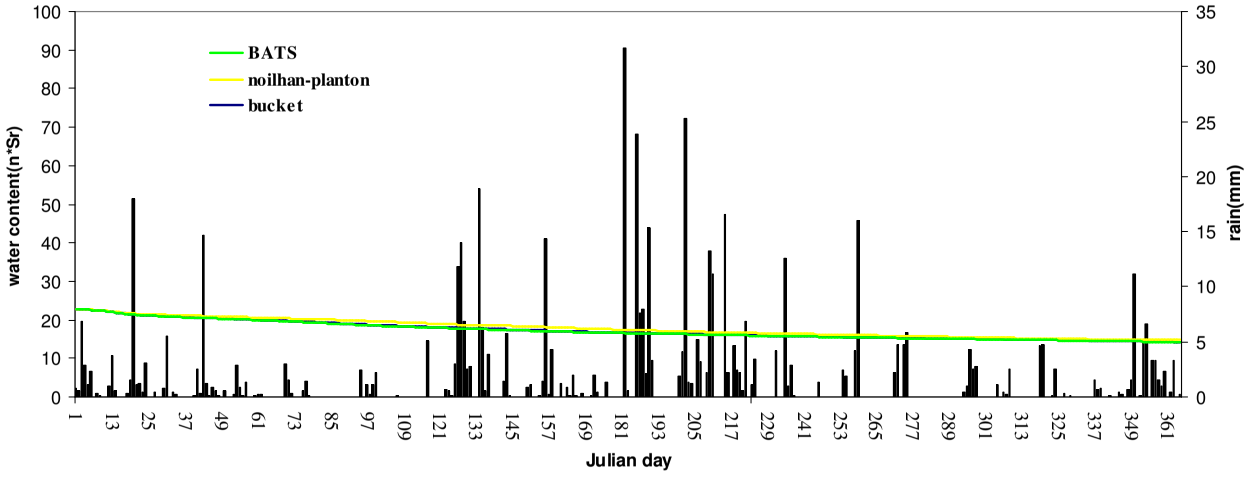

VII layer

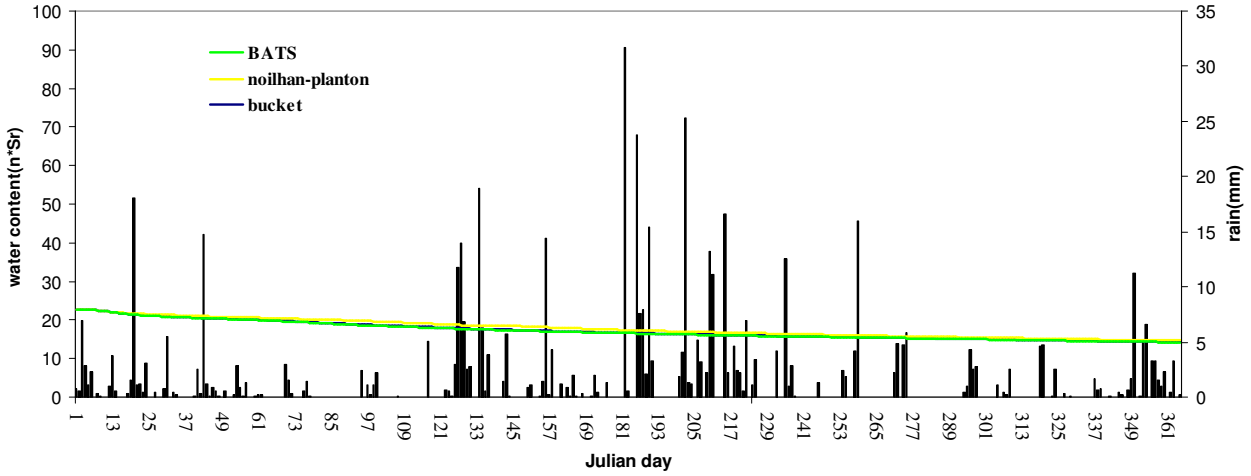

VIII layer

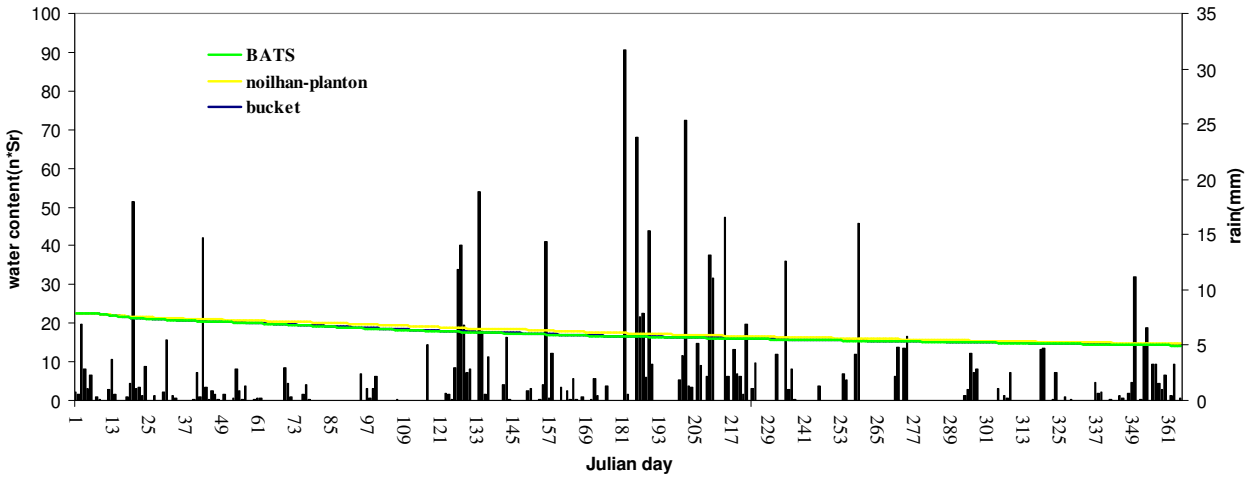

I layer

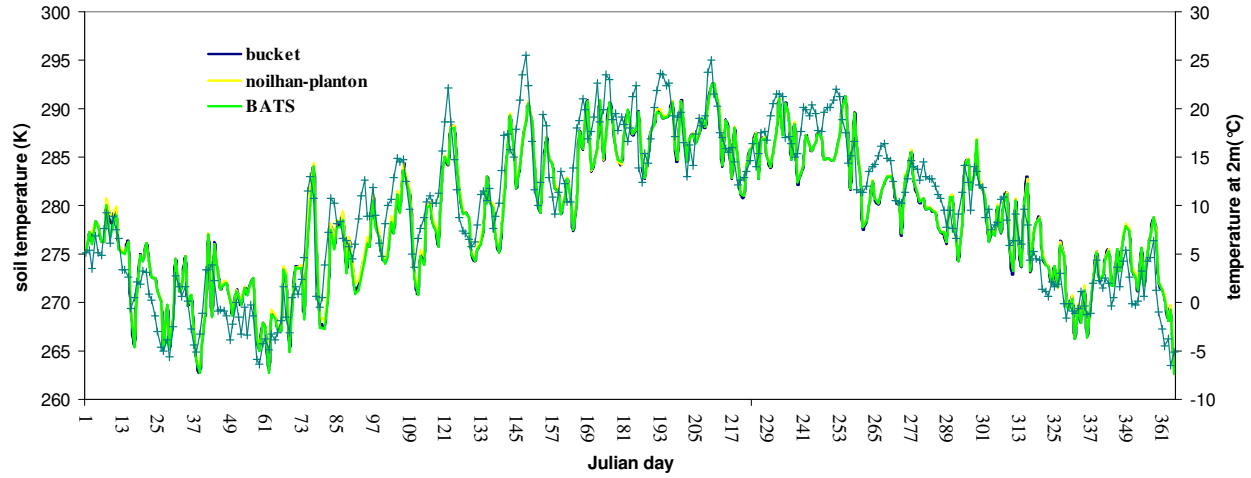

latent heat

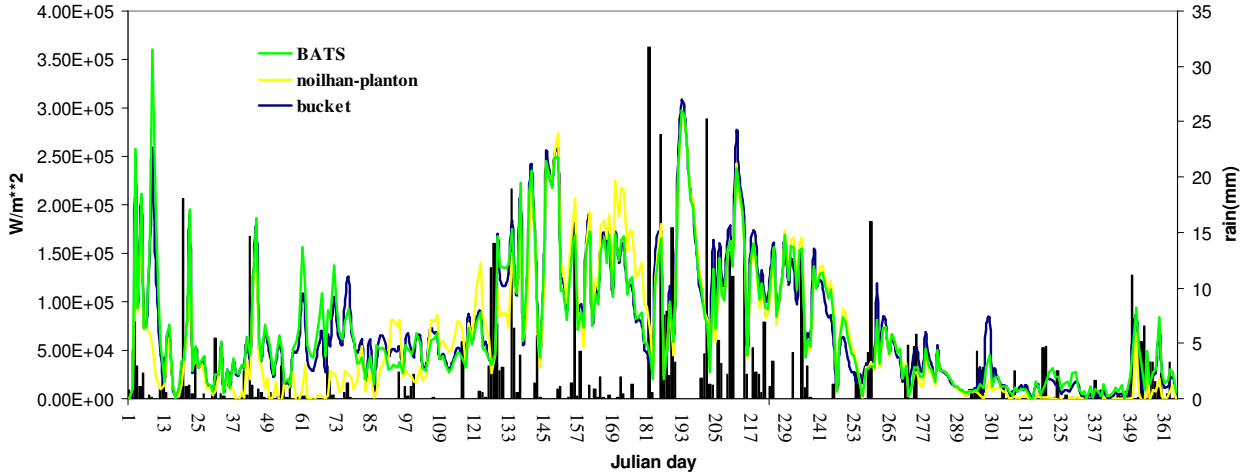

sensible heat

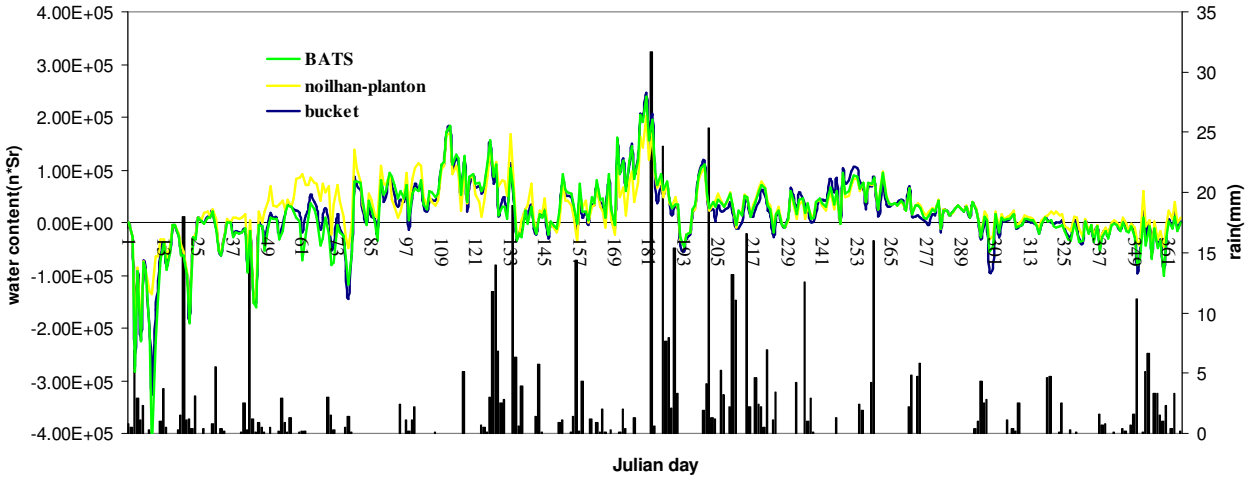

solar radiation

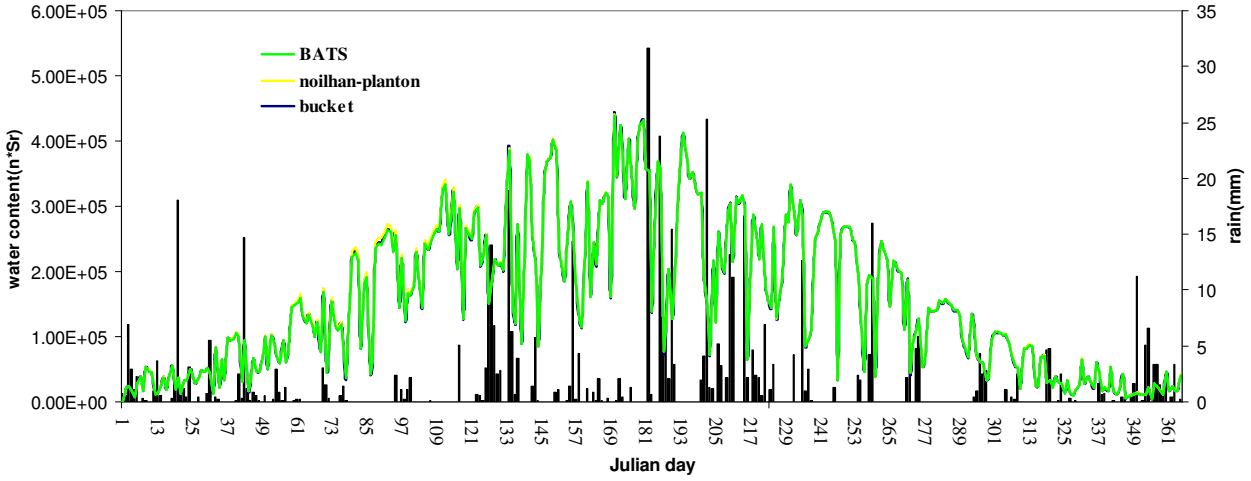

thermal radiation

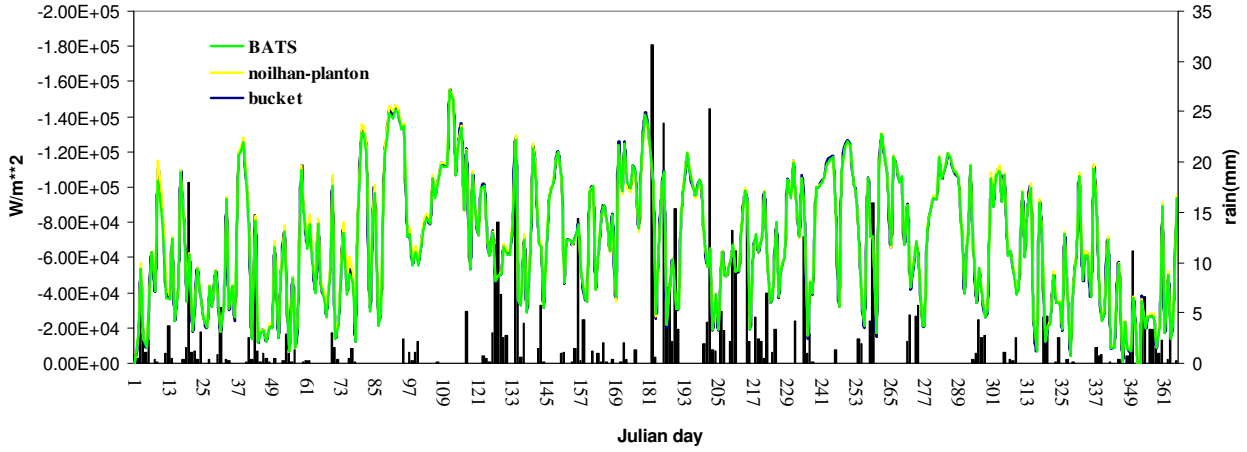

surface runoff

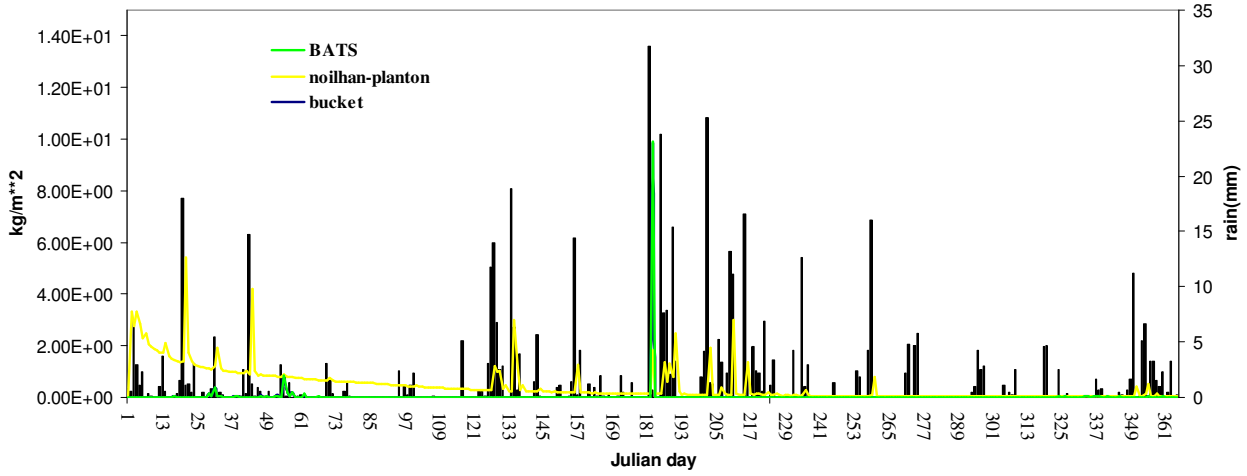

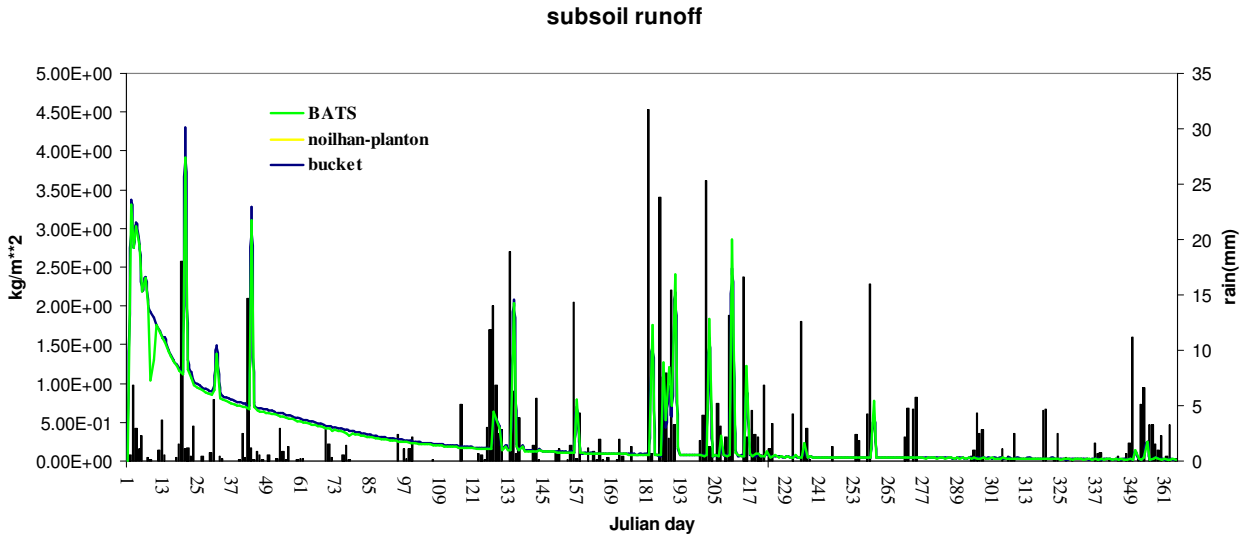
subsoil runoff
BATS
noilhan-planton
bucket
kg/m**2
rain(mm)
Julian day
5.00E+00
4.50E+00
4.00E+00
3.50E+00
3.00E+00
2.50E+00
2.00E+00
1.50E+00
1.00E+00
5.00E-01
0.00E+00
35
30
25
20
15
10
5
0
1
13
25
37
49
61
73
85
97
109
121
133
145
157
169
181
193
205
217
229
241
253
265
277
289
301
313
325
337
349
361

Lower boundary

I layer

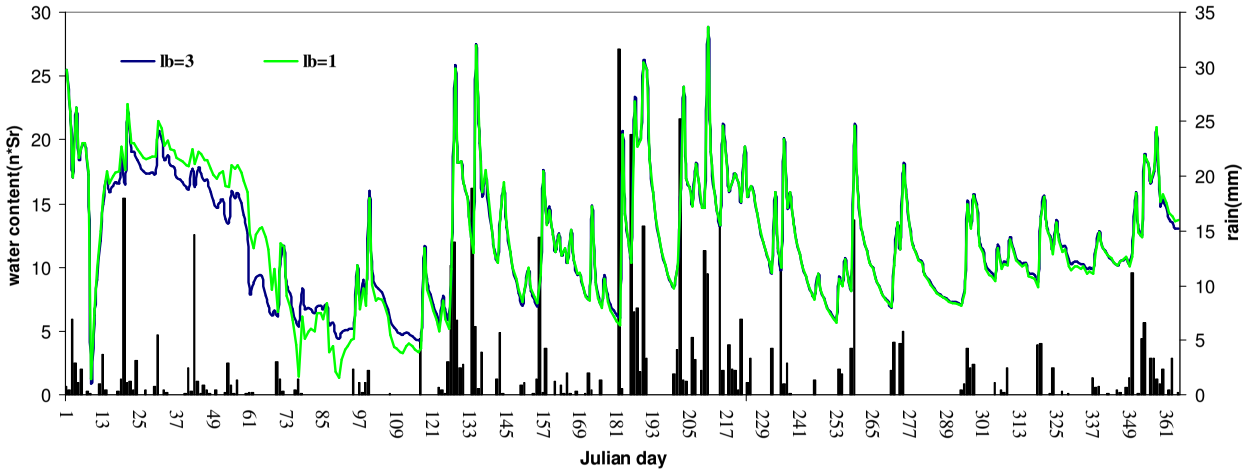

II layer

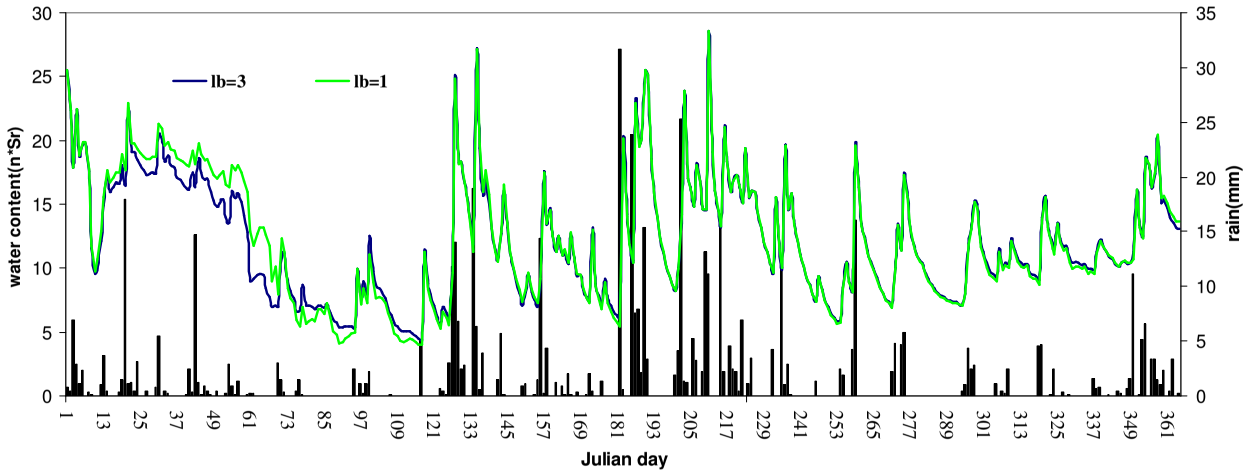

III layer

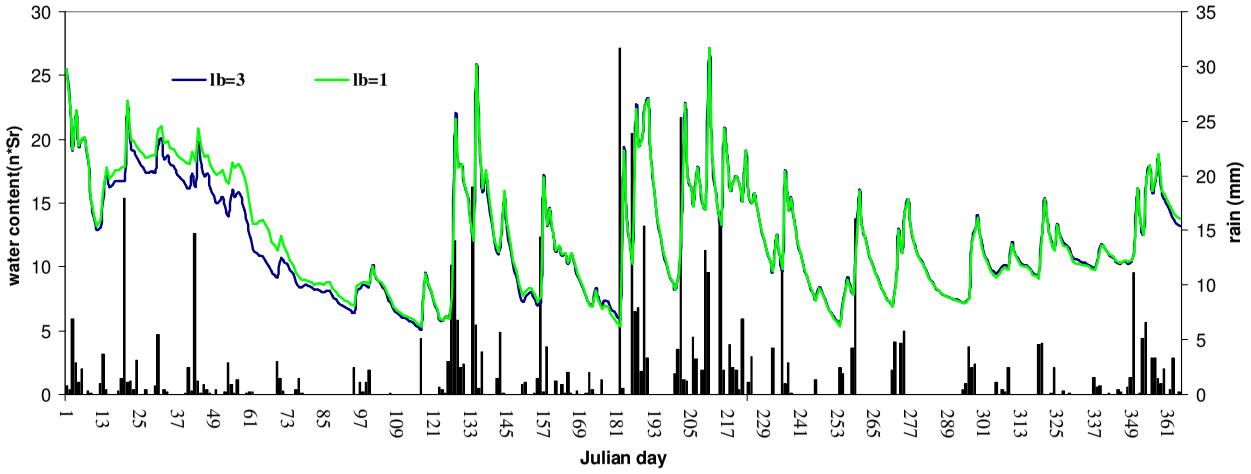

IV layer

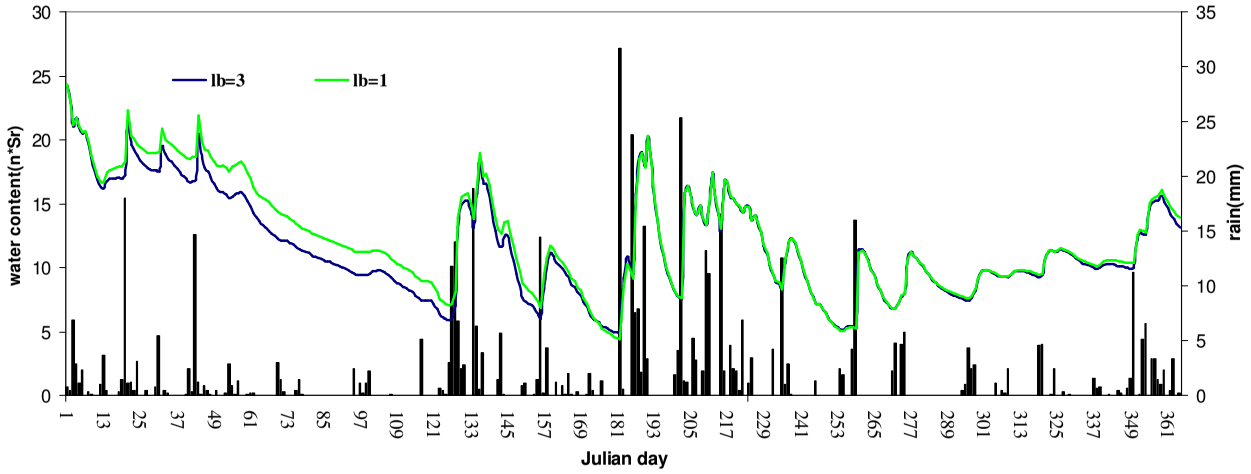

V layer

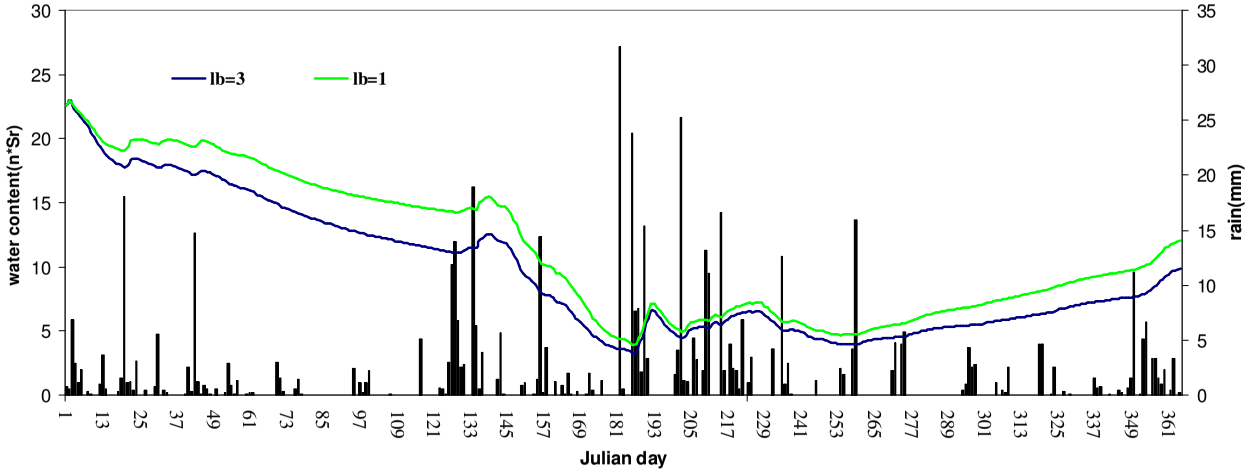

VI layer

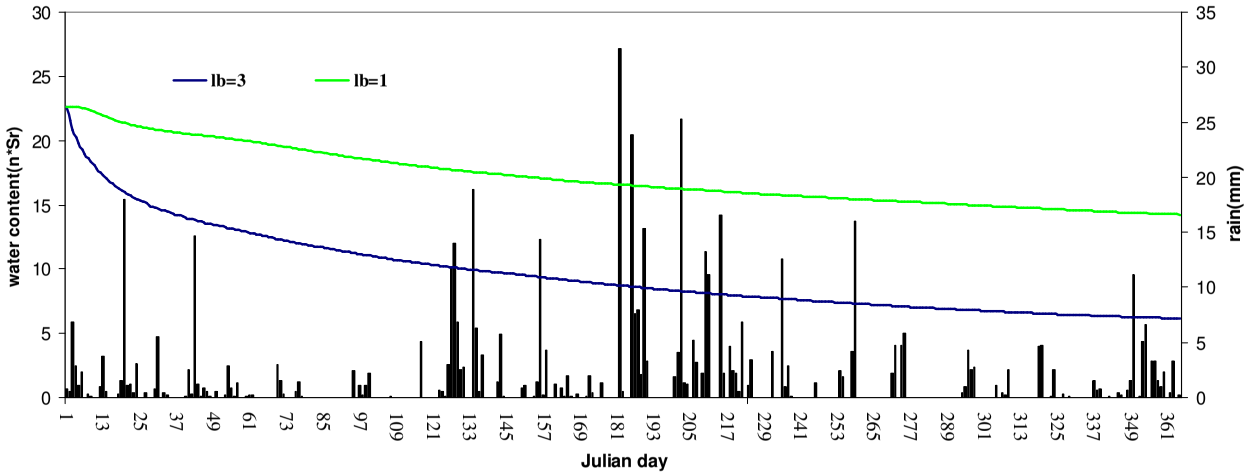

VII layer

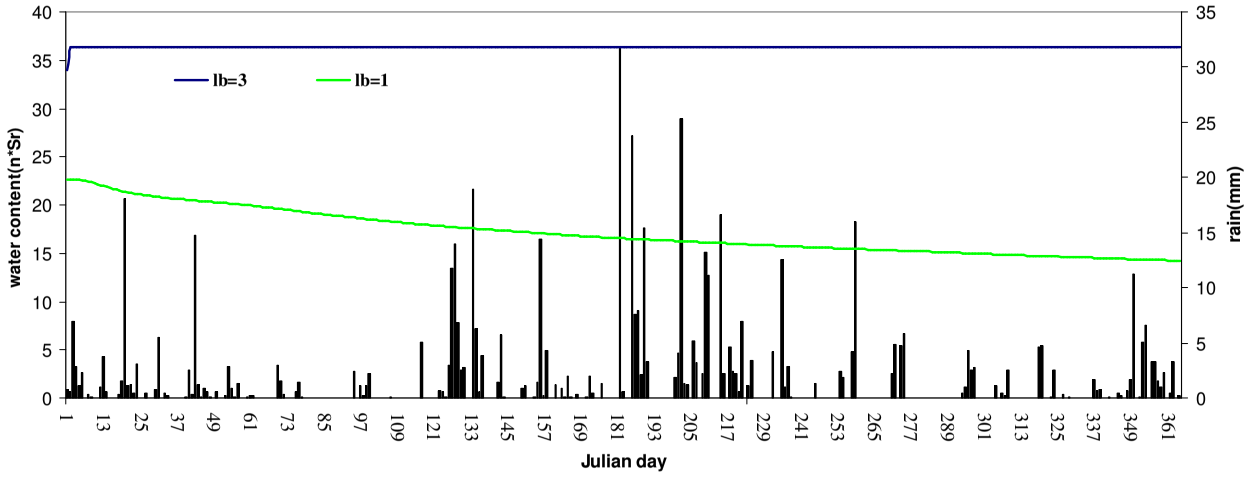

VIII layer

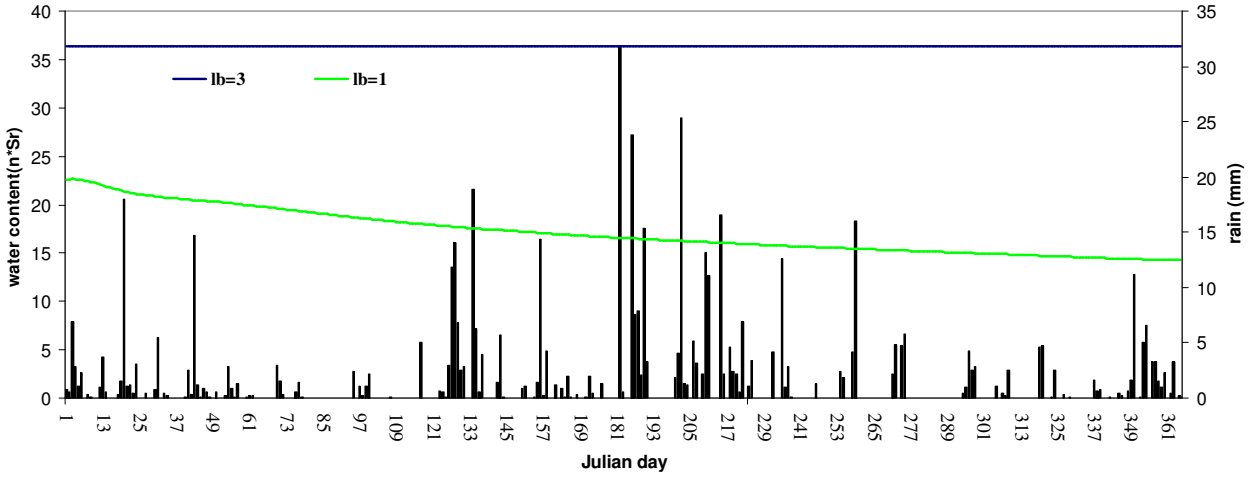

latent heat

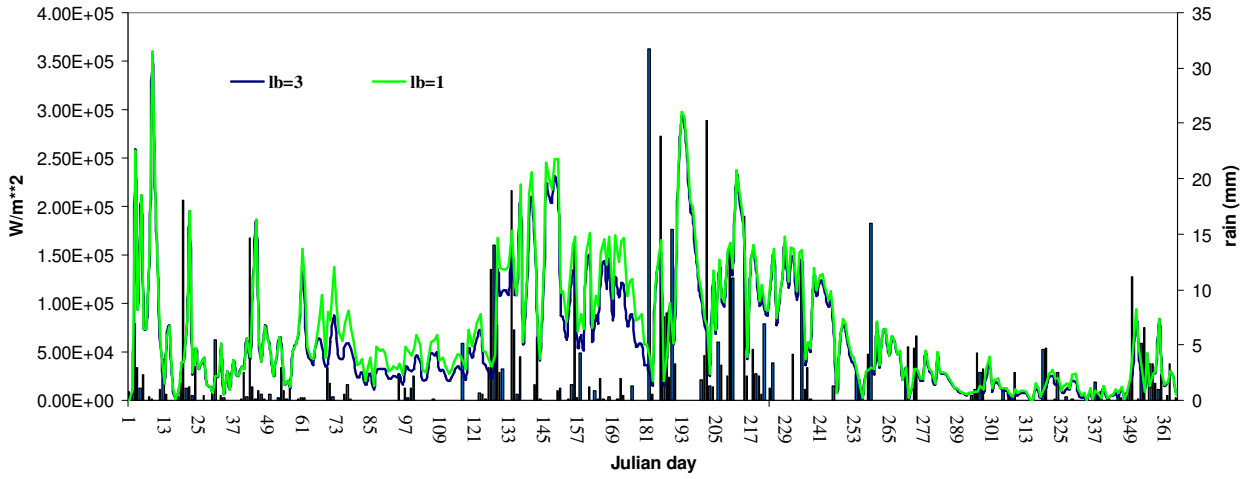

subsoil runoff

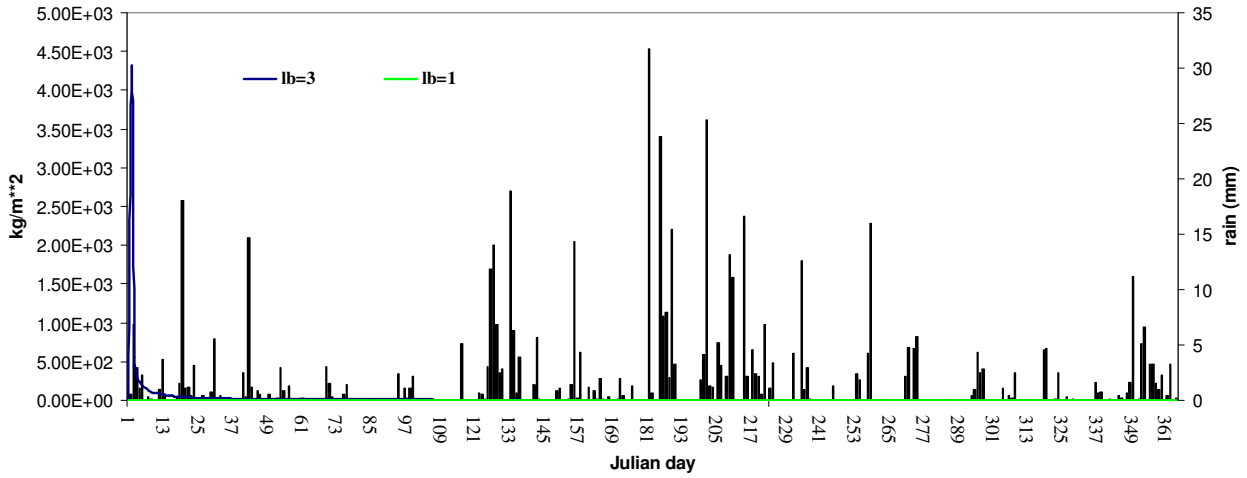

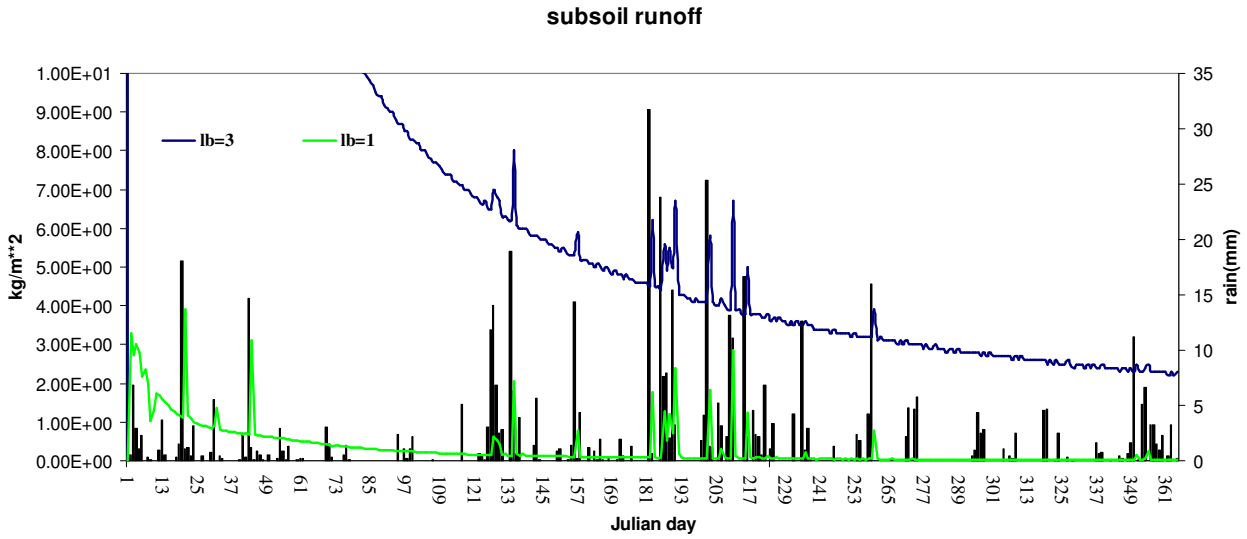
subsoil runoff
lb=3
lb=1
kg/m**2
rain(mm)
Julian day
1.00E+01
9.00E+00
8.00E+00
7.00E+00
6.00E+00
5.00E+00
4.00E+00
3.00E+00
2.00E+00
1.00E+00
0.00E+00
35
30
25
20
15
10
5
0
1
13
25
37
49
61
73
85
97
109
121
133
145
157
169
181
193
205
217
229
241
253
265
277
289
301
313
325
337
349
361